

THE USE OF REMOTE SENSING TO  
REVEAL LANDSCAPE-SCALE ECOSYSTEM  
ENGINEERING BY SHELLFISH REEFS

SIL NIEUWHOF

## Graduation Committee:

### Chairman/Secretary

Prof.dr.ir. A. Veldkamp      University of Twente, ITC

### Supervisors

Prof.dr. D. van der Wal      University of Twente, ITC  
Prof.dr. P.M.J. Herman      Technical University of Delft

### Members

Prof.dr. Z. Su      University of Twente, ITC  
Prof.dr. S.J.M.H. Hulscher      University of Twente, ET  
Em.Prof.dr. A.C. Smaal      Wageningen University  
Prof.dr. L. Barillé      University of Nantes  
Prof.dr. T. Ysebaert      Royal Netherlands Institute for Sea Research  
University of Antwerp

### Paranymphs

Josse Nieuwhof  
Tijmen Nieuwhof

The work presented in this thesis was carried out at the Estuarine & Delta Systems (EDS) department of the Royal Netherlands Institute for Sea Research (Royal NIOZ). It was financially supported by the User Support Space Research program of the NWO division for the Earth and Life Sciences (ALW) in cooperation with the Netherlands Space Office (NSO) (ALW-GO-AO/11-35).

ITC dissertation number 320  
ITC, P.O. Box 217, 7500 AE Enschede, The Netherlands

ISBN 978-90-365-4542-6  
DOI 10.3990/1.9789036545426

Cover designed by Sil Nieuwhof  
Printed by ITC Printing Department  
Copyright © 2018 by Sil Nieuwhof



UNIVERSITY OF TWENTE.

ITC

FACULTY OF GEO-INFORMATION SCIENCE AND EARTH OBSERVATION

# THE USE OF REMOTE SENSING TO REVEAL LANDSCAPE-SCALE ECOSYSTEM ENGINEERING BY SHELLFISH REEFS

## DISSERTATION

To obtain  
the degree of doctor at the University of Twente,  
on the authority of the rector magnificus,  
prof.dr. T.T.M Palstra,  
on account of the decision of the graduation committee,  
to be publicly defended  
on Thursday 19 April 2018 at 12.45 hrs

by

Sil Nieuwhof,  
Born on 21 September 1987  
in Ede, The Netherlands

**This thesis has been approved by:**

Prof.dr. D. van der Wal (supervisor)

Prof.dr. P.M.J. Herman (supervisor)



---

## Contents

|           |  |            |
|-----------|--|------------|
| CHAPTER 1 | <i>Introduction</i>  | <b>1</b>   |
| CHAPTER 2 | <i>Remote sensing of epibenthic shellfish using synthetic aperture radar satellite imagery</i>   | <b>17</b>  |
| CHAPTER 3 | <i>Niche separation and facilitation along an intertidal inundation gradient drives large scale coexistence of invasive oysters and native mussels</i> | <b>45</b>  |
| CHAPTER 4 | <i>Shellfish reefs increase water storage capacity on intertidal flats over extensive spatial scales</i>   | <b>67</b>  |
| CHAPTER 5 | <i>Satellite remote sensing reveals basin-wide boost of phytobenthos due to shellfish reefs</i>  | <b>87</b>  |
| CHAPTER 6 | <i>Synthesis</i>   | <b>103</b> |
|           | <i>References</i>  | <b>113</b> |
|           | <i>Appendix</i>  | <b>125</b> |
|           | <i>Summary</i>   | <b>137</b> |
|           | <i>Samenvatting</i>  | <b>143</b> |
|           | <i>Acknowledgements</i>  | <b>149</b> |
|           | <i>Curriculum Vitae</i>  | <b>153</b> |







### Introduction

#### Influential beyond proportion

Imagine a pond, on a clear windless summer evening. The water surface is completely flat and undisturbed and there are no ripples at all. If you were to cast a small stone into this pond the disturbance creates a radial wave that travels outwards from the impact. The impact of the stone on the water surface, although small and local, ultimately affects the surface of the entire pond. It is not uncommon for large-scale phenomena to be caused by relatively small local processes. For instance, every now and then sea surface temperatures in a narrow band of the Pacific Ocean become relatively warm. Although this body of water is a local feature in itself, the temperatures cause a shift in atmospheric pressure and sometimes cause the trade winds to weaken or reverse their direction. The effects ultimately scale up to affect global climate patterns with some countries facing severe winds and droughts. This phenomenon, commonly known as the El Niño Southern Oscillation, is perhaps the best example of how a (relatively) small scale feature has large scale effects (Trenberth 1997).

Likewise, in ecology some organisms have a disproportionate effect on the ecosystem. These so called keystone species (Paine 1969) may be relatively low in abundance, yet their removal may drastically change the entire ecosystem. Several types of keystone species are distinguished. The first group is characterized by its importance in trophic relations. For instance, a species may be a reliable food source and some predators may limit the gregarious growth of prolific prey species (Mills et al. 1993). Furthermore, there are organisms that engage in mutualistic beneficial relationships with other organisms. These relationships can be so important for ecosystems that if they were to break down, the consequences would be considerable for ecosystem functioning (Mills et al. 1993). Finally, there is a group of organisms which are called ecosystem modifiers (Mills et al. 1993), nowadays termed ecosystem engineers (Jones et al. 1994). This is a distinct group of organisms, which have a large influence on the ecosystem through non-trophic interactions. Such organisms change the physical state of their surroundings by their behavior (allogenic ecosystem engineering) or simply by being present and adding structure to the environment (autogenic ecosystem engineering) (Jones et al. 1994).

The archetypical example of an ecosystem engineer is the beaver (*Castor sp.*). This animal fells trees in the riparian zone of streams and subsequently uses the wood to build dams. This has large effects on the hydrology and geomorphology, and subsequently on the ecology of streams (Pollock et al. 2003). This is generally regarded beneficial for species richness (Wright et al. 2002). Interactions between species that transcend local habitats are other examples of how small scale processes can influence patterns at much larger scales. Typically, such interactions happen by exchange of resources (such as prey, nutrients or detritus) between habitats. Often this results in increased (primary) production of the recipient habitat (Polis et al. 1997).

In estuarine and coastal systems, physical processes highly influence the suitability of habitats for species. In systems where physical stress is high, such as coastal regions, ecosystem engineering species are essential in providing sheltered habitat, boosting population numbers, species diversity and abundance, and ecosystem functioning (Crain & Bertness 2006). In temperate systems reef building shellfish are often the dominant ecosystem engineer in the intermediate to low intertidal.

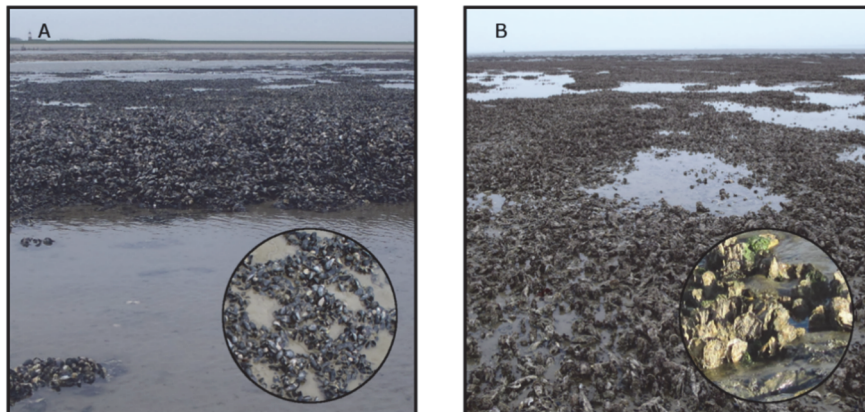


Figure 1.1 A) An example of a mussel reef on a mudflat near de Cocksdorp (Texel). B) An example of an oyster reef on the Galgenplaat (Oosterschelde).

### The blue mussel and Pacific oyster as ecosystem engineer

The blue- or common mussel (*Mytilus edulis*) and the Pacific-, Japanese- or Miyagi oyster (*Crassostrea gigas*) are (semi) sessile bivalves that inhabit estuarine intertidal zones where they attach to hard substrates such as rocks. However, in the absence of hard substrates these shellfish use conspecifics to attach to, resulting in the formation of reefs (see Figure 1.1). This allows the shellfish to better resist waves (van de Koppel et al. 2005) and predation (Bertness & Grosholz 1985; Okamura 1986) on sedimentary substrates. At larger scales,

the calcium carbonate shells not only provide habitat to many organisms (Gutiérrez et al. 2003), but the induced surface roughness further helps to reduce water flow (van Leeuwen et al. 2010) and attenuate waves (Donker et al. 2013) resulting in sedimentation in and close to the reef.

Sedimentation may result in the formation of hummocks in mussel- (Liu et al. 2012) and oyster reefs (Walles et al. 2015; Rodriguez et al. 2014). The hummocks typically consist of muddy and fine organic material and are within oyster reefs often strongly laminated due to a lack of endobenthic species (while epibenthic organisms profit from the added shell structure) (Malkin et al. 2017); See Figure 1.2. The absence of burrowing species may be explained by the lack of oxygen associated with sediments with high organic matter contents (Pearson & Rosenberg 1978; Rosenberg 2001). Furthermore, the silt fraction increases with increasing hummock height (see Figure 1.2). Such changes to the environment caused by the physical presence of the engineering organism is commonly referred to as autogenic ecosystem engineering (Jones et al. 1994).

The ability of ecosystem engineers to introduce more complex physical structure to the landscape in the form of hummocks and hollows is generally considered beneficial to organisms because it increases niche space (Kovalenko et al. 2012). Such landscapes may also increase water storage capacity, i.e. the potential to retain water in the form of tidal pools. Tidal pools are important for many species prone to desiccation that, without these ponds, would be unable to inhabit the tidal zone. Yet, not much is known about how shellfish modify the physical structure of the landscape and how this alters water storage capacity.

Ecosystem engineering by reef building shellfish is not limited to modifying bed level and changing sedimentation patterns locally. These species also have allogenic ecosystem engineering characteristics, i.e. means by which the organisms change the environment through their behavior (Jones et al. 1994). Being filter feeders, epibenthic shellfish filter huge amounts of water. As a result, suspended particles are trapped by the filter feeder and cleared from the water column, enhancing light penetration (Porter et al. 2004; Cressman et al. 2003; Newell et al. 2002). Organic matter is expelled from the shellfish bed through the production of pseudo-faeces. This organic material settles in proximity to the reef, enhancing the productivity of nearby sediment (Donadi, Westra, et al. 2013). Many benthic organisms rely on the enriched sediment, which is indicated by a higher infaunal biomass and species richness in areas influenced by shellfish reefs (Kröncke 1996). More importantly, the sheltered circumstances in combination with high nutrient (Asmus & Asmus 1991) and light input (Porter et al. 2004) close to shellfish reefs is ideal for growth of microphytobenthos (Engel et al. 2017).

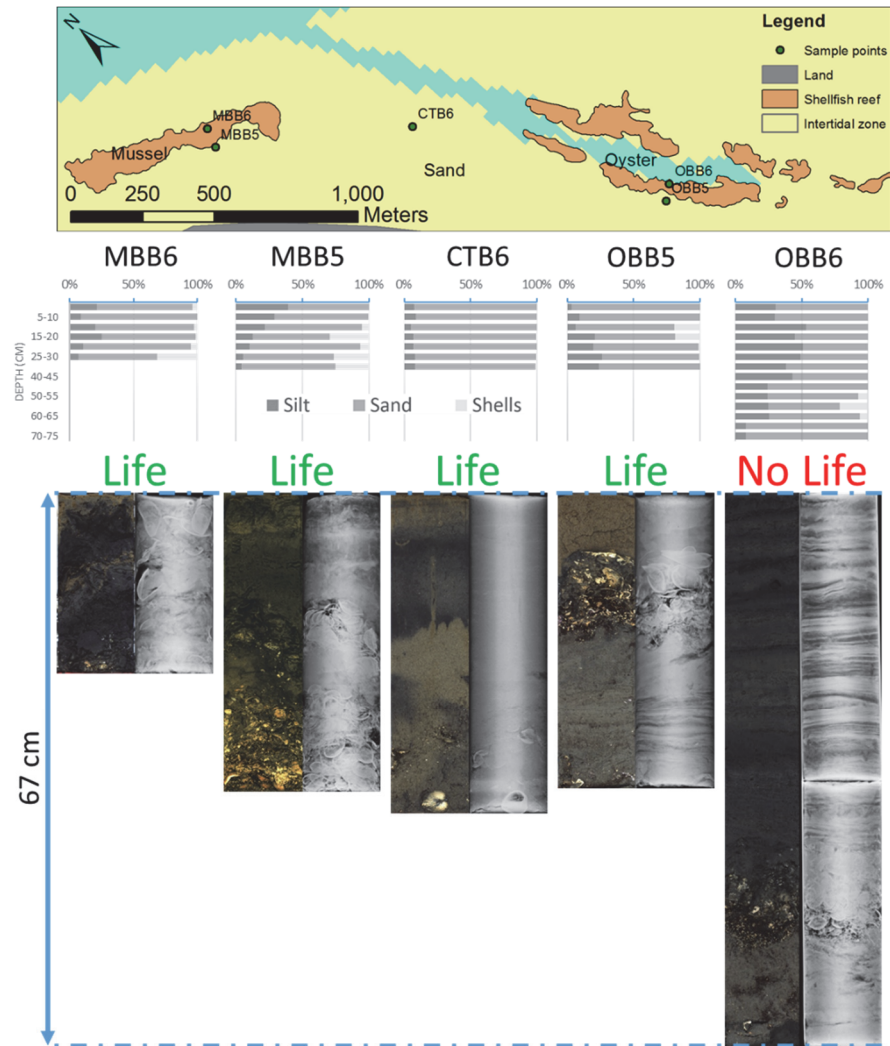


Figure 1.2 A selection of cores ( $\varnothing = 15\text{cm}$ ) from different substrates ranging in depths of  $\sim 30$  to  $\sim 70\text{cm}$ , collected near de Cocksdorp, in the Dutch Wadden Sea. The top panel shows the core locations. These cores are from a mussel reef, oyster reef and sand flat, and of sediment close to a mussel and oyster reef. The pictures show a normal photograph of the core (left) and X-Rays of the core (right). Cores from within oyster reefs and close to mussel reefs are relatively rich in silt, with increasing silt content at shallower depths. No infaunal macrobenthos was observed in oyster reef sediments. This is also evidenced by the laminated sediment layers observed in the cores, indicating absence of bioturbators.

All this is in sharp contrast to bioturbating endobenthic ecosystem engineering species, which have an antagonistic role compared to the biostabilizing reef builders. That is, these species destabilize the sediment, resuspend fine particulate

matter, reduce light penetration and push the system to a more dynamic state dominated by physical forces and allogenic ecosystem engineers (Eklöf et al. 2014) (see Figure 1.3).

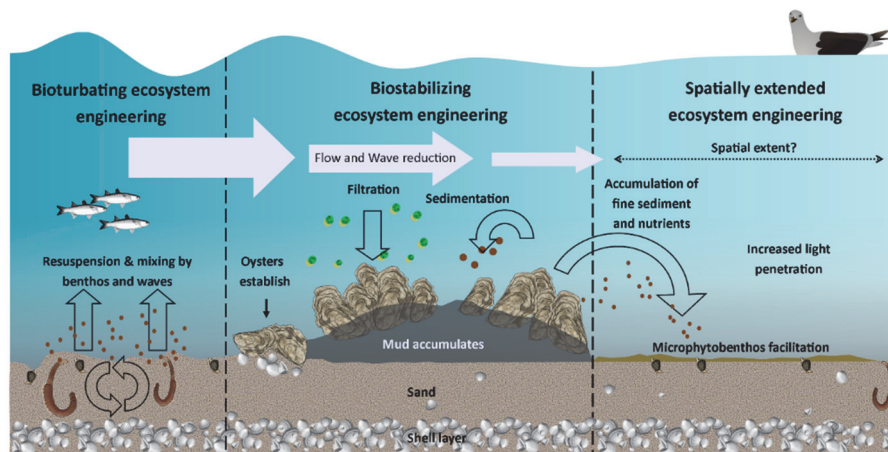


Figure 1.3 Antagonistic ecosystem engineering results in contrasting outcomes for the system. While endobenthos promotes mixing and resuspension of particulate matter, shellfish actively remove suspended material from the water column by filtering water and excreting (pseudo-) faeces. Consequently, the reduced hydrodynamic regime caused by reduction of flow and waves promotes accumulation of matter near the shellfish reef. Ultimately, this results in the formation of muddy hummocks. Such effects can extend beyond the physical boundaries of the reefs. This spatially extended ecosystem engineering has been shown to be important in ecosystem functioning, but the actual spatial extent and significance at the landscape level remains uninvestigated.

Biostabilizing ecosystem engineers are considered especially valuable as they aid in coastal protection. About 60 percent of the world's population resides in close proximity to coasts (Lindeboom 2002). Global change, more specifically sea level rise (Nicholls & Cazenave 2010), storm surge (Lin et al. 2012) and land subsidence (Syvitski et al. 2009), puts these areas at high risk of flooding. Conventional coastal protection methods (such as dikes and embankments) are becoming increasingly unsustainable due to the high costs of maintenance, as well as the adaption to increased risk of flooding (Temmerman et al. 2013). Natural ecosystem-based defense mechanisms, largely profiting of the ability of ecosystem engineers to change the physical state of the environment, is being proposed as a more sustainable solution to this problem and has already proven effective in some regions (Temmerman et al. 2013; Arkema et al. 2013). In the intertidal zone of estuaries, ecosystem engineers occur that make the estuary as a whole more resilient to such disturbance (Bouma et al. 2014; Temmerman et al. 2013). In the higher intertidal zones, several species of salt marsh plants can be found and in the lower intertidal zone seagrass and shellfish reefs may occur. All

of these ecosystem engineers trap sediment and protect the shoreline from eroding waves during storms.

### Shellfish reefs in a global perspective

Mussels and oysters have global distributions (Figure 1.4). However, despite the ecological relevance and importance to humanity, shellfish reefs are at risk worldwide (Beck et al. 2011). It has been estimated that 85% of oyster reefs have been lost globally, which exceeds global loss rates of salt-marsh, mangroves and coral (Beck et al. 2011) (this does not account for compensation of reefs of invasive species). Fisheries have played an important role in the loss of shellfish reefs worldwide. Fisheries reduce the total population of shellfish, and also damage the integral structure of reefs which, as a result, lose stability and may collapse (Beck et al. 2011). Another factor negatively affecting shellfish abundance are diseases (Beck et al. 2011). Furthermore, human induced global change indirectly negatively influences shellfish reefs by severe storm events, storm surges and sea level rise (Beck et al. 2011). Furthermore, coastal engineering activities such as land reclamation and dredging, construction of dams and increased unsustainable land used in the coastal zone affect sediment dynamics and water quality in such a way that it is detrimental to shellfish reefs (Beck et al. 2011).

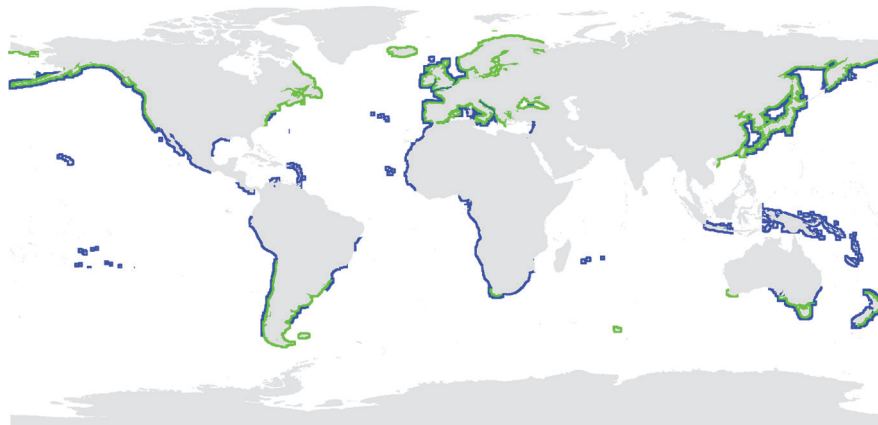


Figure 1.4 Global distribution of Pacific oyster (blue, adapted from Miossec and others 2009) and distribution of mussels in the *Mytilus* complex (green, adapted from Gaitán-Espitia and others 2016).

### Consequences of invasive ecosystem engineers

As a consequence of globalization, global transport has increased. Shipping, construction of canals, aquaculture and ornamental fish trade are important vectors for species to reach new habitats (Katsanevakis et al. 2014). A



conservative estimate indicates that 16% of marine habitats are still free from invasive species, while all other systems harbor at least one invasive species (Molnar et al. 2008). It is generally acknowledged that these invasive species mostly have an adverse effect on recipient ecosystems and the services they provide. Katsanevakis et al. (2014) report that invasive species have impacted food provision, ocean nourishment, tourism and lifecycle maintenance and that 30% of invasive species exert these effects at the scale of entire ecosystems. The Pacific oyster, while native to Asian coasts, has managed to spread worldwide (see Figure 1.4). Sometimes species invasions turn out to be beneficial, for example in case of water purification and climate mitigation (Katsanevakis et al. 2014). As far as we know, no extinctions have occurred due to the presence of oysters. In addition, the reefs built by oysters have been found to support many epibenthic organisms (Markert et al. 2010) and the reefs have great potential in providing natural shoreline protection (Wallis et al. 2014; Temmerman et al. 2013). On the other hand, oysters might influence many aspects of recipient ecosystems, such as changed flow patterns, nutrient dynamics and native ecosystem engineers, of which the cumulative impact remains poorly understood (Ruesink et al. 2005).

Mussels and oysters are quite different in terms of physiology and life history strategy (see Table 1.1). As such, it may be expected that their ecosystem engineering effects differ. In addition, their niches may not strictly overlap, potentially causing different ecosystem engineering effects, as ecosystem engineering may be conditional on the prevailing abiotic conditions (Balke et al. 2012; Bouma et al. 2009) and the engineering species (Kochmann et al. 2008).

### Introduction of the Pacific oyster into Dutch waters

The Pacific oyster was introduced into the Oosterschelde for mariculture to replace the native flat oyster in 1964 (Drinkwaard 1999). Against expectations, the oyster was highly successful in reproduction and quickly established natural populations. The invasive Pacific oyster found its way from the Oosterschelde to the intertidal flats around the Wadden island of Texel for the first time in the late 1970s (Troost 2010), and has established throughout the entire Wadden Sea since then (Fey et al. 2009). It was feared that the Pacific oyster would replace native reef building blue mussels (*Mytilus edulis*) in the intertidal zone. Pacific oysters have at least partial niche overlap with native blue mussels (Reise 1998). Researchers have attempted to investigate the impact of the Pacific oyster on both the blue mussel, but also on the ecological community, which these epibenthic ecosystem engineers support. Some studies suggest that the Pacific oyster may invade native mussel beds and replace them entirely over time (Kochmann et al. 2008), while others found that the two shellfish species can co-exist side by side

without having a big impact on one another (Fey et al. 2009). Others found that mussels may actually profit from increased surface complexity created by Pacific oysters in the Wadden Sea (Eschweiler & Christensen 2011). Co-existence of the two species within a single reef seems to be the rule rather than the exception. Still, reefs that consist predominantly of one species exhibit different reef characteristics compared to reefs consisting of the other species or of a mixture of both species. This is likely due to differences at the individual level, for example differences in attachment mode (see Table 1.1). The differences in characteristics between the species may impose limitations on shellfish performance in the natural environment. For instance, inundation may be of major importance in dictating where which species will be more successful, yet it remains largely unknown how inundation affects competition between mussels and oysters. Separation along such an abiotic gradient could allow the species to co-exist in a tidal basin.

Table 1.1. Differences in shellfish characteristics. Filtration capacity per biomass given in liter per gram dry tissue weight organism per hour. Filtration capacity per individual given in liter per hour. Abundance of organisms in grams ash free dry weight per m<sup>2</sup>.

| Organism trait:                    | <i>M. edulis</i>  | <i>C. gigas</i>   |
|------------------------------------|---|---|
| Filtration capacity per biomass    | 0.7–11.0 l/g/h <sup>(1)</sup>   | 2.0–5.9 l/g/h <sup>(1)</sup>                              |
| Filtration capacity per individual | 1.5–6.0 l/h <sup>(1)</sup>  | 1.2–12.5 l/h <sup>(1)</sup>                               |
| Density                            | 271.4 ± 67.7 g/m <sup>2</sup> <sup>(2)</sup>                          | 781.8 ± 63.9 g/m <sup>2</sup> at 80% cover <sup>(3)</sup> |
| Maturity age                       | 1 year <sup>(4)</sup>   | 2 years <sup>(1)</sup>                                    |
| Maximum average size               | 6–8 cm <sup>(5)</sup>   | 20 cm <sup>(6)</sup>                                      |
| Method of attachment               | Byssal threads <sup>(4)</sup>   | Cementation <sup>(7)</sup>                                |
| Mobility                           | Mobile as spat, semi mobile in first year then sessile <sup>(8)</sup> | Mobile as spat, sessile afterwards <sup>(1)</sup>         |
| Reef roughness                     | medium  | high  |
| Shell shape                        | Regular   | Highly variable   |
| Fecundity                          | 5–12 million eggs per spawn <sup>(9)</sup>                            | 50 million eggs per spawn <sup>(9)</sup>                  |

<sup>1</sup> (Troost 2010 and references therein), <sup>2</sup> (Markert et al. 2010), <sup>3</sup> (Green et al. 2012), <sup>4</sup> (Seed 1976), <sup>5</sup> (Seed & Suchanek 1992), <sup>6</sup> (Cardoso et al. 2007), <sup>7</sup> (Yamaguchi 1994), <sup>8</sup> (Saurel et al. 2004), <sup>9</sup> (Helm et al. 2004).

## Getting the big picture: Remote Sensing

Usually the effect of ecosystem engineering on the ecosystem is investigated by conducting small scale *in situ* experiments. In such experiments an ecosystem engineer is either introduced or excluded to investigate how sediment characteristics and faunal assemblages change locally (e.g. Ragnarsson & Raffaelli 1999; Kochmann et al. 2008). As a result, ecosystem engineering effects are only considered in direct proximity of the engineer in question. However, the spatial extent of ecosystem engineering effects may extend far beyond the local footprint of the shellfish reef. It was shown that abundance of the common cockle (*Cerastoderma edule*) was suppressed close to mussel reefs, but at about 100m from the mussel reefs cockle abundance was higher than at locations without a

mussel reef (Donadi, van der Heide, et al. 2013). Likewise, increased mud concentrations and higher numbers of foraging birds were found in zones around mussel reefs (van der Zee et al. 2012). Similarly, mussel reefs were found to boost microphytobenthos biomass over spatially extended scales (Engel et al. 2017). The mediation of sedimentation was found to be pronounced on the leeward side of oyster reefs (Wallis et al. 2014). However, the implications of the presence of shellfish reefs has not been integrated across entire estuarine systems or tidal basins. As a result, the relative importance of ecosystem engineers for entire systems remains poorly understood (Figure 1.3).

Using remote sensing, vast areas can be studied synoptically, which potentially allows assessing the spatial extent of ecosystem engineering caused by reef forming shellfish. Remote sensing is the methodology by which one acquires information about an object with data obtained by a device (sensor) which does not physically touch the studied object (Lillesand et al. 2014). Remote sensing can be used in a wide range of earth science disciplines to study processes on a variety of spatial scales. For instance, a simple camera can be used to infer information on a square meter of soil, while at the same time earth observation satellites can be used to infer information on global climate patterns. Satellites use electromagnetic radiation to infer information about the earth and can operate either passively (e.g., detecting reflected solar radiation, as in most optical imaging sensors) or actively (by emitting radiation, e.g. microwaves). In ecology the use of remote sensing is becoming more wide-spread in studies that encompass large spatial extents and cannot simply be addressed using field measurements (Kerr & Ostrovsky 2003).

Optical multispectral remote sensing (using wavelengths of 300 to about 1000nm) has been used extensively to infer information on the surface of the intertidal environment. Chlorophyll *a* levels, which are indicative for the microphytobenthos concentration on the sediment, can be predicted using spectrometers, regardless of the structure and humidity of the sediment (Carrère et al. 2004). Optical sensors have been used, for instance, to measure microphytobenthos biomass at estuary scale (Kazemipour et al. 2012), as well as temporal variations in benthic algae (Benyoucef et al. 2013; van der Wal et al. 2010). A typical drawback of optical sensors is that they are sensitive to atmospheric effects, limiting the window of opportunity to obtain useful data. Furthermore, the classification of biotopes such as mussel or oyster reefs is complicated because of fouling organisms which make shellfish cryptic (Le Bris et al. 2016a).

The application of synthetic aperture radar (SAR) satellite data to study geological and biological processes on a broad spatiotemporal scale in intertidal

areas has great potential. Unlike optical satellite data, microwaves (with wavelengths typically between 1 and 10 cm) are largely unhindered by atmospheric effects making SAR a powerful remote sensing tool which can be used in a wide range of weather conditions. This is even more so when we consider the fact that suitable satellite acquisition times are relatively rare because satellite overpass has to coincide with low tide, making missed opportunities due to adverse weather even less desirable. Initially, SAR was mainly used to study roughness and moisture of agricultural sites (e.g. Ulaby et al. 1986, Fung et al. 1992, Dubois et al. 1995, Altese and Bolognani 1996). More recently, the technique has also been applied to study sediment characteristics on intertidal mudflats (e.g. Tanck et al. 1999, van der Wal et al. 2004, van der Wal et al. 2005, Gade et al. 2008, 2014, Park et al. 2009, 2010, Lee et al. 2011). Van der Wal et al. (2005) found that on intertidal flats typically characterised by wet sediments, Synthetic Aperture Radar (SAR) systems are mostly sensitive to surface roughness. This sensitivity to surface roughness can also be applied to detect shellfish structures. Lee et al. (2006) were the first to extend the use of SAR interferometry beyond intertidal sediment characterization and used the technique to study polarimetric scattering in an oyster farm structure. Choe et al. (2012) used fully polarimetric C-band data to locate oyster reefs on the intertidal zone west of the Korean peninsula. They were able to show that oyster reefs can be detected due to their ability to depolarize the microwave signal through multiple scattering. Dehouck et al. (2011) showed that TerraSAR-X satellite imagery also has great potential for mapping different habitat types in the intertidal zone, including oyster habitat.

### Study sites: areas in transition

The Dutch Oosterschelde and Wadden Sea tidal basins were selected as study sites (see Fig. 1.5 for locations). They are model ecosystems in that they have been studied intensively for the past decades. In addition, shellfish reef builders have always had prominent roles in both systems, in both an economic and ecological sense. The Oosterschelde is a semi-enclosed sea arm in the south western delta region of the Netherlands. It is a macrotidal system, even though the tidal prism was reduced significantly due to the construction of a storm surge barrier in 1986. Because of this the tidal channels have become oversized with respect to the amount of water that they transport, and the tidal flats are eroding, while the channels are filled in (so-called sand hunger effect) (Nienhuis & Smaal 1994). In this respect, ecosystem engineers have gained interest due to their ability to trap sediment and stabilize intertidal flats (Wallis et al. 2014). The Oosterschelde is very important for shellfish culture. Although wild mussel reefs have been absent for decades, Pacific oyster reefs occupy large parts of the estuary since their introduction in 1964 (Troost 2010). Furthermore, the

Oosterschelde is a Natura 2000 site due to its unique wildlife that inhabits the mudflats and salt-marshes.

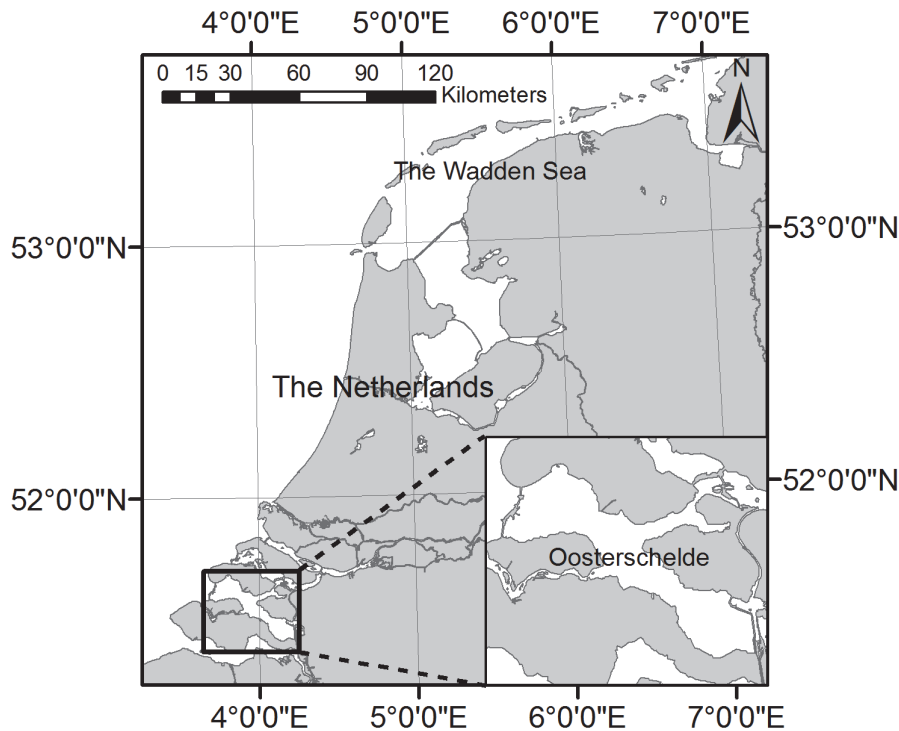


*Figure 1.5 The regions that were the focus of study in this thesis: the Dutch part of the Wadden Sea in the north of the Netherlands and the Oosterschelde estuary in the south-western part of the Netherlands.*

The Wadden Sea is a shallow sea along the north coast of the Netherlands, which is fringed by barrier islands. Its range expands on the north side of Germany and the west coast of Denmark. Due to its unique dynamics, the Wadden Sea became a UNESCO world heritage site in 2009. The vast intertidal flats, which are exposed during low water, cover 111882 ha in the Netherlands, and provide food for many species, among which large populations of migratory birds (Ens et al. 2009). Yet, human influence is pronounced in the area. Natural resources (gas and salt) and (shell)fish stocks make the Wadden sea valuable in economic sense. Mussel fisheries were unrestricted in the past which caused the mussel reefs to disappear largely from the Wadden Sea around 1990 (Nehls et al. 2009). After

restriction of mussel fisheries to the subtidal regions, the mussel stocks have largely recovered (Dankers et al. 2004).

### Thesis aims

This thesis aims to address how and to what extent ecosystem engineering shellfish (more specifically blue mussels *Mytilus edulis* and Pacific oysters *Crassostrea gigas*) influence landscape characteristics at the scale of tidal basins, by using remote sensing techniques. While we know that these ecosystem engineers potentially influence large areas, the spatial extent of potential effects has not been quantified at such scales. Remote sensing techniques may provide methods that can help to get insight in processes that take effect at such vast spatial scale that cannot be investigated by laboratory experiments and field studies alone. In addition it may allow acquiring large scale data on the distribution of shellfish reefs and on the changes in shellfish reef distribution over time. The same data may be gathered on the spatially extended ecosystem engineering effects. This is essential for impact assessments of natural or human-induced losses of such ecosystem-engineering on ecosystem services. Such large scale data can provide insight in the current state and the resilience of shellfish reefs to sustain natural production and biodiversity, but also to sustain human use and exploitation of natural resources. Two types of ecosystem engineering were investigated in this thesis; A) the creation of increased habitat structure (landscape roughness) and associated water storage capacity both inside shellfish reefs, as well as at spatially extended scales due to sedimentation of fine particulate matter. And B) the promotion of primary production ((micro)phytobenthic biomass) around shellfish reefs, and species-related differences in this promotion. The hypotheses evaluated in this thesis are:

#### Chapter 2:

- SAR remote sensing can be used to map shellfish reefs, determine species composition (mussels vs oysters) and determine densities of the shellfish.

#### Chapter 3:

- Oyster reefs are more dominant in the lower intertidal (i.e. high inundation durations), compared to mussels, which occur higher in the intertidal (i.e. low inundation durations).
- The adaptations with regard to the inundation gradient (individual size, condition and growth rate of the shellfish) are more favourable for oysters lower in the intertidal zone as compared to mussels.
- There is limited interspecific competition (and possibly even facilitation), when the species co-exist in a mixed reef.

## Chapter 4:

- Shellfish reefs create rough surfaces that increase the water storage capacity of the landscape, both within and around shellfish reefs.

## Chapter 5:

- Spatially extended microphytobenthos facilitation by shellfish reefs emerges when corrected for trends of microphytobenthos in response to elevation and hydrodynamics (currents, waves).
- Mussel-, oyster- and mixed reefs have different facilitative effects on microphytobenthos at spatially extended distances.

## Thesis outline

**Chapter 2** investigates whether SAR remote sensing can be used for shellfish reef mapping. It was expected that the shellfish reefs induce surface roughness in the right order of magnitude to be picked up by X- and C-band SAR satellites (TerraSAR-X and Radarsat 2 respectively). A statistical procedure was developed to map shellfish reefs, combining SAR images and results from an extensive ground survey in the Oosterschelde and in the Dutch Wadden Sea.

**Chapter 3** explores the interaction between the two intertidal reef building shellfish. Niche differentiation between reef building oysters and mussels was investigated. This was done by a field campaign, in which density and condition of shellfish and species composition at different elevations were assessed. Additionally, experiments were carried out with oysters, mussels and mixed shellfish at different water depth in the Oosterschelde to test for their growth potential at different elevations in the tidal frame. A GIS study of the occurrence of the different reefs along the intertidal gradient was performed to examine the colonization of the Pacific oyster through time and to assess the niche differentiation of oysters and mussels at larger scales.

**Chapter 4** examines how shellfish reefs modify physical structure of the landscape and subsequent water storage capacity. Ponding of water was identified as an important engineering effect of shellfish. Intertidal pools provide a habitat for many species which are prone to desiccation stress. We related surface structure created by shellfish to potential intertidal ponding on different scales, from the small scale (using terrestrial laser data and aerial photos) to the large scale (using satellite SAR-based maps resulting from Chapter 2 and airborne laser data).

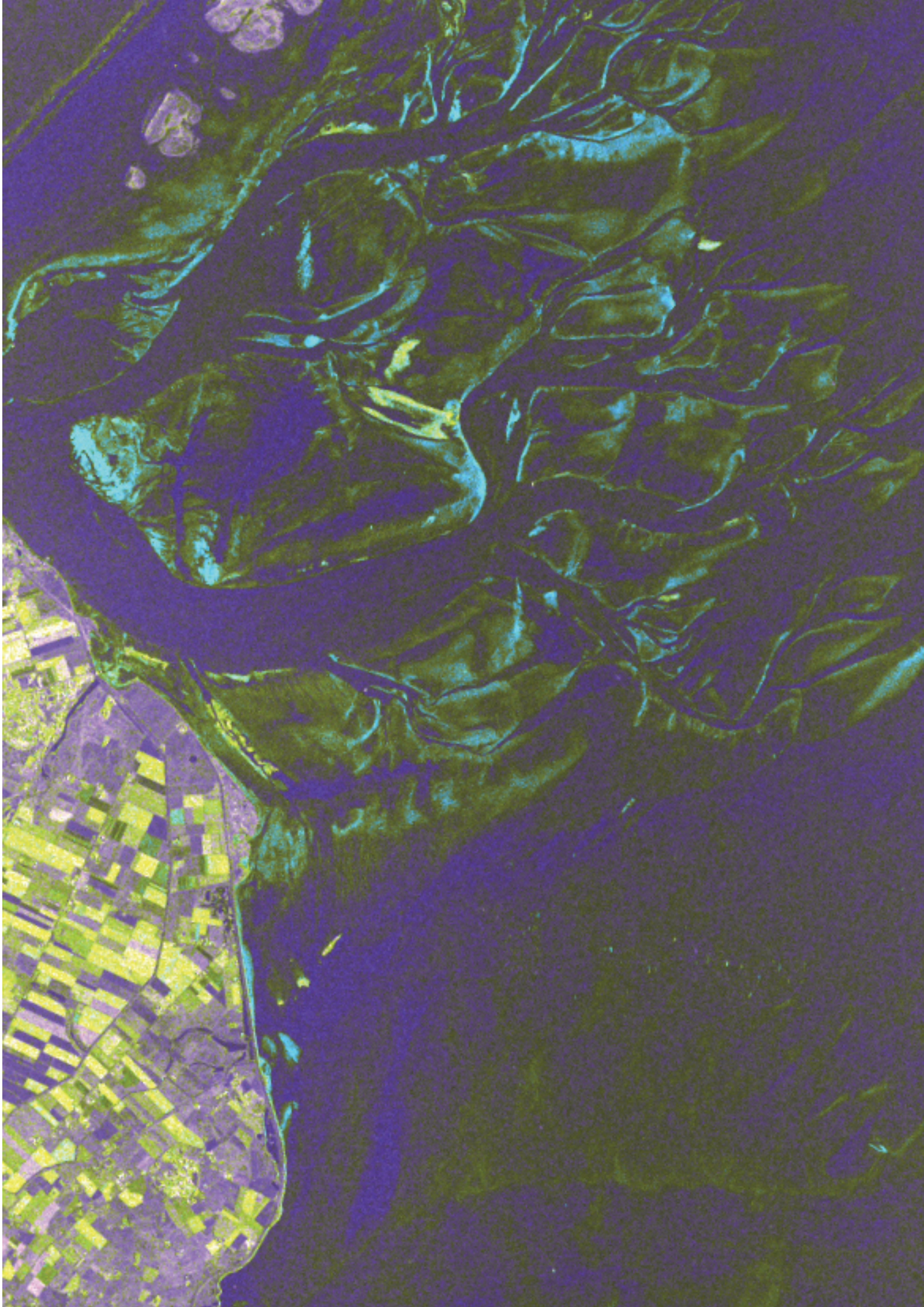
**Chapter 5** investigates the ability of shellfish reefs to create more benign environments by reducing flow and attenuating waves. We investigated up to which spatial extent shellfish are able to influence benthic algae. By using optical satellite remote sensing, we aim to unravel whether the observed differences in benthic algae occurrence can be attributed to ecosystem engineering, and whether the two shellfish species has a different effect on the distribution of benthic algae.

**Chapter 6** integrates and synthesizes the findings presented in this thesis and discusses them in a wider context of related research.











## CHAPTER 2

# Remote sensing of epibenthic shellfish using synthetic aperture radar satellite imagery

*Remote Sensing 2015*

*Sil Nieuwhof, Peter M.J. Herman, Norbert Dankers, Karin Troost and Daphne van der Wal*

### Abstract

On intertidal mudflats, reef-building shellfish, like the Pacific oyster and the blue mussel, provide a myriad of ecosystem services. Monitoring intertidal shellfish with high spatiotemporal resolution is important for fisheries, coastal management and ecosystem studies. Here, we explore the potential of X- (TerraSAR-X) and C-band (Radarsat-2) dual-polarized SAR data to map shellfish densities, species and coverage. We investigated two backscatter models (the integral equation model (IEM) and Oh's model) for inversion possibilities. Surface roughness (vertical roughness RMSz and correlation length  $L$ ) was measured of bare sediments and shellfish beds, which was then linked to shellfish density, presence and species. Oysters, mussels and bare sediments differed in RMSz, but because the backscatter saturates at relatively low RMSz values, it was not possible to retrieve shellfish density or species composition from X- and C-band SAR. Using a classification based on univariate and multivariate logistic regression of the field and SAR image data, we constructed maps of shellfish presence (Kappa statistics for calibration 0.56–0.74 for dual-polarized SAR), which were compared with independent field surveys of the contours of the beds (Kappa statistics of agreement 0.29–0.53 when using dual-polarized SAR). We conclude that spaceborne SAR allows one to monitor the contours of shellfish-beds (thus, distinguishing shellfish substrates from bare sediment and dispersed single shellfish), but not densities and species. Although spaceborne SAR cannot replace ground surveys entirely, it could very well offer a significant improvement in efficiency.

## Introduction

At the interface of land and sea, intertidal mudflats are one of the most productive and dynamic ecosystems in the world (Heip et al. 1995). Unlike endobenthic bivalves, the epibenthic species *Mytilus edulis* (blue mussel) and *Crassostrea gigas* (Pacific oyster) are able to create reefs, which provide hard substrates on otherwise entirely soft bottom sediment (Albrecht 1998; Gutiérrez et al. 2003). This autogenic ecosystem engineering makes epibenthic shellfish important species in intertidal soft bottom ecosystems, as they introduce heterogeneity and maintain habitats important for a wide variety of marine organisms, both locally and on spatially extended scales (Jones et al. 2010; van der Zee et al. 2012). In addition, both the blue mussel and the Pacific oyster are important species for mariculture.

Epibenthic shellfish communities are put under pressure by changes in their direct environment, examples of such changes include more frequent extreme weather events, global warming, sea level rise, changes in nutrient concentrations, and coastal erosion (Oliver et al. 2008). Additionally, more human induced stressors affect epibenthic shellfish reefs; such as pollution, and overfishing (Beck et al. 2009). Because of its high suitability for mariculture, the Pacific oyster has been introduced into many new waters and, facilitated by global warming, has become invasive (Troost 2010). Development of former mussel beds into hybrid beds (mixed beds of oysters and mussels) and the expansion of oyster beds has been shown to alter community composition locally (Kochmann et al. 2008; Troost 2010; Markert et al. 2013) and may also alter ecosystem functioning (Green et al. 2013). The implications of these oyster invasions still remain unclear (but see (Troost 2010)) and more research is needed to find out what the combined impacts of non-native oysters and global change will be.

In support of fisheries policy, conservation policy, and scientific study, it is important to have robust and cost efficient monitoring tools recording the evolution of shellfish coverage and extent over time. Most shellfish monitoring programs use extensive ground surveys, but these are time consuming and expensive. Currently, shellfish monitoring in the Wadden Sea is carried out on an international level following the recommendations of the Trilateral Monitoring and Assessment Program (TMAP) (Nehls et al. 2009). The monitoring protocol aims to map the boundaries of shellfish beds by walking the circumference of the beds with a GPS tracker and following a basic set of rules. Firstly, shellfish patches within 25 meters of each other are mapped as one bed by walking a convex hull; as long as the patches cover at least 5% of the total surface area. Secondly, individual patches should be at least 1 m<sup>2</sup> big if the cover of the patchy mussel bed is less than 5% to be mapped, and thirdly; dispersed shellfish (<5%)

are not included in the monitoring of the beds (de Vlas et al. 2005). See de Vlas et al. (2005) for a schematic image of the procedure.

Space borne Synthetic Aperture Radar (SAR) sensors may significantly enhance the efficiency of monitoring programs by reducing ground surveys. Unlike optical sensors, SAR can be used at night and during cloudy conditions, increasing the window of opportunity for data acquisition. SAR satellites are active systems that emit microwave signals to the surface under investigation and measure the backscattered echo. Radar backscatter depends on many parameters, which are either instrument specific (polarization, incidence angle and wavelength), or surface specific (local slope, root mean square of the height RMSz, correlation length  $L$ , and the relative permittivity  $\epsilon$ ) (van der Wal et al. 2005). However, surface roughness in terms of RMSz is found to be the most important factor in bare intertidal areas (van der Wal et al. 2005). The length scale of shellfish shells is in the right order of magnitude (centimeters) to effectively affect backscatter of C- and X-band microwave signals, and some authors have shown that both C- and X-band microwaves are sensitive to surface roughness induced by epibenthic shellfish. Choe et al. (Choe et al. 2012) showed that polarimetric descriptors (including Freeman-Durden target decomposition, cross-polarized ratio, co-polarized correlation and co-polarized phase difference) from fully polarized Radarsat-2 (C-band) and ALOS PALSAR (L-band) data can be used to pick up the roughness signatures created by oysters. In their study, the influence of the incidence angle on the backscatter in oyster reefs is small, but the difference between oyster reefs and mudflats was most pronounced at larger incidence angles (Choe et al. 2012). Dehouck et al. (2011) used TerraSAR-X data in combination with optical information to classify intertidal mudflats. Gade et al. (2014) used TerraSAR-X data to locate shellfish based on temporal statistics of multiple data acquisitions and also noted that shellfish beds were clearly visible across a range of incidence angles. However, it is unclear how accurate SAR derived shellfish maps actually are, furthermore it is not known whether SAR data can be used to distinguish between different reef forming epibenthic shellfish species (mussels vs. oysters) and whether the backscatter signal allows shellfish densities (cover) to be quantified. To develop a widely applicable method for monitoring shellfish beds, the use of single data acquisition with single or dual polarization would be preferred, as many radar sensors, including Sentinel-1, TerraSAR-X and CosmoSkyMed typically acquire single or dual polarized data.

Backscatter models like the Integral Equation Model (IEM) (Fung et al. 1992), Oh's model (Oh et al. 1992), and the Dubois model (Dubois et al. 1995), have been used to predict radar backscatter given instrument settings and substrate properties. These models can aid in the understanding of backscatter response in

intertidal environments and can potentially be used in inversion methods to predict substrate properties from backscatter imagery. A thorough evaluation is needed to ascertain that such models can be used in the environment and surface conditions under study.

The purpose of this chapter is to explore the practical potential of single acquisition dual-polarized TerraSAR-X and Radarsat-2 data for epibenthic shellfish mapping, species classification, and shellfish density estimation; and investigate how this compares to traditional field campaigns. Specifically, we investigated how shellfish cover and species composition influence surface roughness characteristics. In mussel beds, mussel cover can be described by a fractal, where the fractal dimension increases when cover increases (Commito & Rusignuolo 2000). Assuming the same is true for oysters, we hypothesized that higher shellfish densities result in rougher surfaces through lower  $L$  and higher RMSz values. Furthermore we hypothesized that morphological differences between shells of mussels and oysters also result in substrates with different roughness characteristics. Oysters are much larger compared to mussels and in soft substrates the oysters stand upright in the sediment, for this reason, we hypothesized that oyster beds are rougher compared to mussel beds, especially with regard to RMSz, resulting in higher backscatter levels. To explore the relationship between the shellfish bed properties and the backscatter properties, we evaluated a theoretical and a semi-empirical backscatter model for the range of surface conditions and sensor settings under study. Finally, it was hypothesized that SAR imagery in dual polarized setting provides a suitable means to map epibenthic shellfish in the intertidal soft bottom zones.

## Materials and methods

### Study areas

This study focused on two tidal systems in the Netherlands: the Wadden Sea and the Oosterschelde. The Wadden Sea is a mesotidal eutrophic marine system that is sheltered from the North Sea by a coastal barrier. The Wadden Sea was designated a UNESCO world natural heritage site in 2009 because of its dynamic intertidal zones, which are important foraging grounds for birds (111,882 ha of intertidal flats in the Dutch part (Ens et al. 2009)), and its diversity, which provides a suitable place for many organisms to reproduce and thrive (Lotze 2005; Reise et al. 2010). However, in the last few decades, the Wadden Sea has been subjected to different forms of human-induced stress, which caused the disappearance of mussel beds in Dutch and German parts of the Wadden Sea in the 1980s (Nehls et al. 2009; Dankers et al. 2003). After the collapse, the Dutch mussel fishery was restricted to subtidal beds in the western Wadden Sea, which resulted in recovery on the intertidal beds. Since then, mussel beds have

recovered, but not to the extent reported in the 1970s (Dankers et al. 2004). In contrast to the mussel, the Pacific oyster is an invasive species in Dutch coastal waters that found its way from Zeeland to the Wadden Sea (Texel) for the first time in the late 1970s (Troost 2010), but started increasing exponentially from the mid-1990s (Fey et al. 2009).

The Oosterschelde is a macrotidal system that is heavily influenced by human engineering; since 1986, a storm surge barrier has reduced the tidal prism in the system, resulting in a different hydrodynamic regime and changed sediment dynamics (Nienhuis & Smaal 1994). In 2001, 10,430 hectares of intertidal flat remained in the Oosterschelde estuary (van Zanten & Adriaanse 2008). Mussels are cultivated in the Oosterschelde subtidally, but wild mussel beds have been virtually absent for decades. Pacific oysters were introduced in 1964 and have expanded rapidly since the 1970s, forming dense reefs in mainly the lower intertidal zone (Troost 2010).

Two field sites were used within the Wadden Sea for this study, namely the mudflats east of the island of Texel and south of the island of Schiermonnikoog; one field site was used within the Oosterschelde (see Figure 2.1).

The flats consist of mostly sand and mud. Fragments of macroalgae can be present: their cover in the 107 sample plots of 1 m<sup>2</sup> used in this study was on average 7%. Areas with saltmarsh can also fringe some of the barrier islands and the mainland coast. Saltmarsh could potentially also be picked up with SAR satellites due to its complicated rough surfaces. However, we only focused on shellfish and did not include saltmarsh areas in this study, because saltmarsh has a more distinct optical signature, making it easier to classify using optical remote sensing.

### SAR imagery acquisition and preprocessing

Throughout 2012, three TerraSAR-X scenes were acquired through the German Aerospace Center (DLR), in strip map mode with a dual-polarization (VV and VH). In addition, three Radarsat-2 scenes were acquired (HH/HV) through the Dutch Satellietdataportaal (see Table 2.1). TerraSAR-X products were geocoded and ellipsoid corrected (GEC). Radiometric calibration of TerraSAR-X data was achieved by computing sigma naught ( $\sigma^0$ ) following product documentation (AIRBUS Defence and Space 2008). Since the studied mudflats are more or less flat, we assumed a 0° local incidence angle for all locations. Following radiometric calibration, images were filtered to reduce speckle using Lee's refined adaptive local filter ( $7 \times 7$  moving window, with an edge threshold of 5000) (Lee 1981), and pixel intensities were converted to decibels (dB).

Radarsat-2 products contained single look complex (SLC) data and were first multilooked 4 times in the azimuth direction. Radarsat-2 imagery was ellipsoid corrected, during which pixels were resampled using bilinear interpolation. The speckle filter used for Radarsat-2 imagery was similar to the one used for TerraSAR-X, and the same settings were used. Finally, pixel intensities were converted into decibels (dB). All SAR data processing was performed using the software package NEST 5.0.12. The average noise floor, noise equivalent sigma naught, was calculated for both image types, using the noise data provided with the satellite imagery.

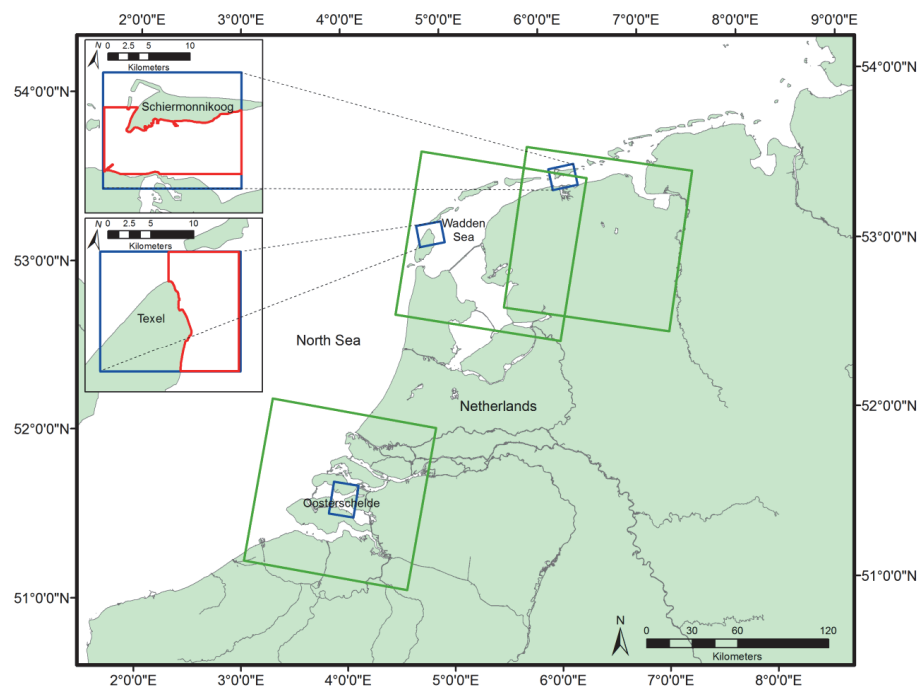


Figure 2.1 Image acquisitions by Radarsat-2 (green) and by TerraSAR-X (blue) in the Netherlands. The red lines indicate the areas used to compare remotely-sensed and Trilateral Monitoring and Assessment Program (TMAP) shellfish maps.

### *In situ* surface roughness measurements

Each image was matched with the ground campaigns in that area (Table 2.1). Ground surveys did not coincide with satellite overpass, because sufficient light was required during the ground truth campaign, while satellite overpass occurs during either the beginning or the end of the day, and both field and image data had to be acquired when the tidal flat emerged. However, caution was taken that there were no severe weather conditions, like storms, in between. To determine the location of sample stations for ground-truthing over the full range of surface



characteristics, iso cluster analysis was performed on TerraSAR-X imagery for both shellfish beds and bare mudflat surrounding the shellfish. To avoid sampling noise and to take into account positioning accuracies, the clusters were clumped and sieved in Erdas IMAGINE 2011 to retain clusters of at least 64 m<sup>2</sup>. These zones were sampled using a random sample approach, in which the samples were at least 30 m apart, and the number of samples per zone was related to the total surface area of each zone. This resulted in a total of 107 samples (see Table 2.1 for the distribution of samples over the study areas).

The sample stations were located in the field using Garmin's GPSmap 78 (average error in open sky conditions of 1.5 m; (Wing 2011)). At each station, a 1-m<sup>2</sup> frame was used to mark the sampling surface, and a single photo was taken of the frame using either a Canon D10 or D20 camera. This photograph was subsequently used for cover analysis: first, the photo of the frame was transformed in ArcGIS 10.1, so that a 0.2 × 0.2 m grid could be projected on to it; then, different cover classes were derived and quantified from this grid as cover percentage, including sediment, oyster, mussel and total epibenthic shellfish cover.

Another 60 to 100 photographs per frame were taken using Canon 10D and 20D cameras at a height of about 50 to 60 cm, making sure that the entire frame was covered with abundant overlap between the pictures. With VisualSFM (Wu 2011), these pictures were used to create a 3-dimensional representation of the frame and the surface by producing a set of data points with X, Y and Z coordinates: termed a point cloud. The point cloud was georeferenced using the corners of the frame as ground control points. A flat texture (carpet) was used to check the accuracy of the method; the planimetric and vertical root mean square error (RMSE) of this method were 0.931 cm and 0.240 cm, respectively. The vertical RMSE was largely due to a slight curvature in the measured plane, i.e., a difference with a second degree polynomial surface would result in a much lower vertical RMSE of 0.064 cm; thus, this method allows for a good comparison of roughness parameters between plots.

Table 2.1. Specification of the different SAR scenes, the local prevailing conditions and matching field campaigns. The weather conditions were acquired from the Royal Netherlands Meteorological Institute (KNMI). Information on tidal conditions was provided by Rijkswaterstaat, the Dutch agency for water management. SLC is single look complex.

| Ground Truth<br>Date and<br>Sample Size $n$ | Satellite<br>/Band | Image Date<br>and Time | Image<br>Type | Image<br>Resolution<br>(m) | Center<br>(Lat/Lon,<br>Degrees) | Incidence<br>Angle<br>(Degrees) | Polarization | Pass<br>Direction | Water<br>Height<br>(m AOD *) | Tidal<br>Stage | Wind<br>Direction<br>(Degrees) | Wind<br>Speed<br>(m/s) |
|---|--------------------|------------------------|---------------|----------------------------|---------------------------------|---------------------------------|--------------|-------------------|------------------------------|----------------|--------------------------------|------------------------|
| Schiermonnikoog                             |                    |                        |               |                            |                                 |                                 |              |                   |                              |                |                                |                        |
| 24 August 2012<br>( $n = 31$ ) and 30       | TSX/X              | 8 May 2012<br>17:18    | Strip-map     | 3                          | 53.46/6.20                      | 39.75                           | VV/VH        | Ascending         | -0.41                        | outgoing       | 328                            | 7.8                    |
| October 2012<br>( $n = 26$ )                | RS2/C              | 23 May 2012<br>5:53    | SLC           | 25                         | 53.08/6.51                      | 33.84                           | HH/HV        | Descending        | -1.34                        | low            | 56                             | 6.8                    |
| Texel                                       |                    |                        |               |                            |                                 |                                 |              |                   |                              |                |                                |                        |
| 18 September<br>2012 ( $n = 25$ ) &         | TSX/X              | 30 March 2012<br>17:27 | Strip-map     | 3                          | 53.08/4.87                      | 42.71                           | VV/VH        | Ascending         | -0.68                        | outgoing       | 310                            | 7.8                    |
| 17 October<br>2012 ( $n = 15$ )             | RS2/C              | 27 July 2012<br>5:57   | SLC           | 25                         | 53.07/5.47                      | 33.84                           | HH/HV        | Descending        | -0.69                        | outgoing       | 54                             | 5.3                    |
| Galgenplaat                                 |                    |                        |               |                            |                                 |                                 |              |                   |                              |                |                                |                        |
| 4 October 2012<br>( $n = 10$ )              | TSX/X              | 18 April 2012<br>6:00  | Strip-map     | 3                          | 51.59/3.98                      | 38.79                           | VV/VH        | Descending        | -0.42                        | outgoing       | 166                            | 7                      |
|   | RS2/C              | 2 June 2012<br>6:01    | SLC           | 25                         | 51.62/3.95                      | 33.86                           | HH/HV        | Descending        | -0.82                        | outgoing       | 57                             | 3.6                    |

\* AOD is the Amsterdam Ordnance Datum.

Commonly, in surface roughness measurements for SAR backscatter modelling, the root mean square height (RMSz) and correlation length ( $L$ ) are derived to describe the vertical and horizontal component of surface roughness, respectively (Ulaby et al. 1986). A mean plane was fitted to the height ( $Z$ ) parameter of the point cloud and subtracted from the points. Using these detrended  $Z$  values, the root mean square height (RMSz) was calculated. To compute the correlation length, the point clouds were first rasterized to a  $5 \times 5$  mm grid to calculate a 2-dimensional spatial autocorrelation function (ACF) (Petitpas et al. 2010), which, at location  $(x,y)$ , is defined by:

$$\text{ACF}(x,y) = \frac{\sum_{i=1}^{N-x} \sum_{j=1}^{N-y} (h_{i,j} - \bar{h}_{i,j}) \times (h_{i+x,j+y} - \bar{h}_{i,j})}{\sum_{i=1}^{N-x} \sum_{j=1}^{N-y} (h_{i,j} - \bar{h}_{i,j})^2}$$

In which  $N$  is the number of cells in the grid in the  $X$  and  $Y$  direction ( $N = 200$ ),  $h$  is the height grid,  $\bar{h}$  is the height grid mean and  $h_{i+x,j+y}$  is the displaced grid at a lag location defined by  $X$  and  $Y$ .

The 2D ACF grid was then transformed to a 1D ACF by calculating the mean (omnidirectional) autocorrelation over different lag distances with 1-mm increments. Horizontal surface roughness was expressed as the correlation length ( $L$ ), which is the lag distance where the 1D ACF is  $1/e$  (Ulaby et al. 1986). Thus, values for RMSz and  $L$  were obtained for all 107 field plots. The omnidirectional measurement of surface roughness measurements was used, because most plots were isotropic. Anisotropy did occur in plots where shellfish beds are patchy in appearance, but these surfaces are expected to be isotropic at sensor resolution. This is because if a single patch does not fit in the  $1\text{-m}^2$  frame, it may still fit well in a sensor pixel. In these cases, an omnidirectional estimation of the roughness parameters is expected to give a more accurate representation of surface roughness at sensor resolution, compared to a directional estimation. In addition, the surface plot methods explained here typically contain many more measurements (in the order of millions), compared to the more traditional profile measurements, which increases the accuracy of roughness derivation further. For this study, a frame length of 1 m (with a maximum distance of  $\sqrt{2}$  over which  $L$  is evaluated) was chosen to capture the roughness parameters. For longer lengths, height differences induced by mussel and oyster hummocks may affect the roughness parameters.

All spatial data were accumulated in a geographical information system (GIS). Statistical analyses described in the next paragraphs were performed using the statistical software package R (R Development Core Team 2015), using a 0.05 significance level as a rejection criterion.

## Effect of Shellfish Species and Cover on Surface Roughness and Backscatter

To test the effect of shellfish cover on surface roughness characteristics, the photos of the 1-m<sup>2</sup> frame were used to determine total shellfish cover (<1%, 1%–10%, 11%–20%, 21%–30%, >30%). In addition, five substrate types were distinguished based on Troost et al. (Troost et al. 2012), namely sediment (no shellfish present), dispersed shellfish (less than 5% cover by both mussels and oysters), mussel (less than 5% surface covered by oysters and more than 5% by mussels), mixed (both shellfish cover more than 5%) and oyster (less than 5% surface covered by mussels and more than 5% by oysters) (see Figure 2.2). After classification, 10 samples were classified as oyster, 15 as mixed, 8 as mussel, 41 as dispersed shellfish and 33 as sediment. Analysis of variance in combination with the Tukey HSD post hoc tests were used to test if differences in total shellfish cover and differences in substrate type had a significant impact on surface roughness in terms of RMSz and  $L$  and whether they had an effect on radar backscatter.

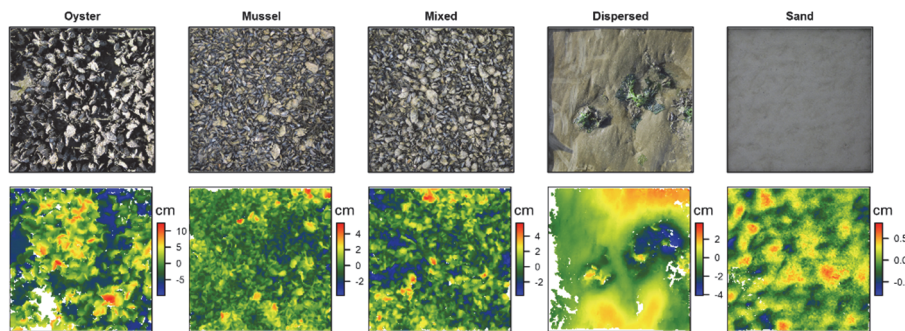


Figure 2.2 The top row shows examples of photos of the different substrate classes studied in the 1-m<sup>2</sup> plots. The bottom row shows corresponding examples of the measured height after rasterization of the point clouds at a resolution of 5 mm.

## Shellfish Backscatter Modelling and Mapping

To explore the backscatter signal in response to roughness elements in the tidal flat and to investigate the potential for surface characteristic retrieval from backscatter, we investigated the response and validity of three backscatter models over the roughness range that we observed in this study. The first two models are theoretical (the integral equation model) and semi-empirical (Oh's model), and aim to predict backscatter based on surface characteristics and sensor settings. The third model is empirical (based on logistic regression) and can only be used for mapping shellfish beds.

The integral equation model, or IEM (Fung et al. 1992), is commonly used to predict backscatter from surface parameters in intertidal environments (root mean square height, correlation length and dielectric constant) and SAR configuration (polarization of microwave signal, wavelength and angle of incidence) (van der Wal et al. 2005; Lee et al. 2011; Gade et al. 2008; Park et al. 2009). In this study, we used an extended version of the IEM that takes into account the phase effect in Green's function; as a result, this version provides much more accuracy in bistatic scattering and also includes multiple scattering (Fung et al. 2002); an elaborate description of the model can be found in Fung and Chen (2010). For this study, we used a spectrum with an exponential autocorrelation function. High moisture contents are typical for shellfish habitats due to the high amounts of silt in the sediment. We used a large number of samples ( $n = 175$ ) of the upper 3 cm of the surface from a field campaign in the Wadden Sea in 2013 to determine that the average volumetric moisture content of the sediment during low tide is  $0.45 (\pm 0.09) \text{ cm}^3/\text{cm}^3$ . Assuming this average value and taking into account the grain-size distribution of the sediment, a dielectric constant of  $\epsilon = 29.31 + 12.72i$  and  $35.67 + 9.55i$  was calculated for the X-band and C-band, respectively, following Hallikainen et al. (Hallikainen et al. 1985). The validity range of the IEM is given by  $\text{RMSz}/L < 0.4$  and  $k \times \text{RMSz} < 3$ , where  $k$  is the wavenumber ( $2 \times \pi/\lambda$ ). Using the IEM, we simulated radar backscatter over a range of RMSz and  $L$  found in the field campaign for co- and cross-polarized channels in X- and C-band.

Since the validity range of the IEM is easily exceeded (i.e.,  $k \times \text{RMSz} > 3$ , which translates to a threshold of RMSz of 1.5 cm for X-band and 2.65 cm for C-band), we also used Oh's semi-empirical model described in (Oh 2004). This semi-empirical model was fit using data from bare surfaces and was tested to be valid up to 6.98 (Oh 2004) for  $k \times \text{RMSz}$  (which translates to a threshold RMSz of 3.5 cm for the X-band and a threshold RMSz of 6.23 cm for the C-band) over incidence angles between  $10^\circ$  and  $70^\circ$ . Using this model, backscatter can be expressed as a function of RMSz, volumetric moisture content, incidence angle, wavelength and polarization. Since the simulations consequently overestimated radar backscatter based on the volumetric moisture content of 0.45, the model was also fit using nonlinear least squares based on the Gauss–Newton algorithm to determine the best fit volumetric moisture content. Based on this approach the estimated moisture contents were  $0.04$  and  $0.13 \text{ cm}^3/\text{cm}^3$  for X-band VV and VH, respectively, and  $0.06$  and  $0.15 \text{ cm}^3/\text{cm}^3$  for C-band HH and HV, respectively. This model was used to predict backscatter over the range of RMSz that was found in this study for co- and cross-polarized channels in the X- and C-band.

For mapping purposes of intertidal shellfish beds, it may be sufficient to discriminate between shellfish and bare sediment patches. We used a logistic

model to build three classifiers for both TerraSAR-X and Radarsat-2 for co- and cross-polarized channels separately. To distinguish between sediment, sediment with dispersed shellfish (where total shellfish cover  $< 5\%$ ,  $n = 70$ ), and shellfish (where total shellfish cover  $> 5\%$ ,  $n = 37$ ) classes, a multivariate logistic regression was used for a dual-polarized classification. An additional classifier based on the two single-channel thresholds was also investigated, because this will likely be less sensitive to rough rippled sediments, which were rare in the training data. The level of 5% shellfish was chosen in line with the protocol described in the TMAP procedure. The univariate logistic function  $P(x)$  can be written as:

$$P(x) = \frac{1}{1 + e^{-(\beta_0 + \beta_1 x)}}$$

This equation was used to determine at which backscatter value a pixel would have equal probabilities (i.e.,  $P = 0.5$ ) to be classified as shellfish or sediment in a single channel. The threshold value can be calculated using:

$$x(P = 0.5) = \frac{-\beta_0}{\beta_1}$$

In the dual polarized classification, we expanded the logistic function to incorporate both channels. In this case, the threshold value in the cross-polarized channel can be found for any given backscatter value in the co-polarized channel using:

$$\sigma_{crosspol}^o = \frac{-(\beta_0 + \beta_2 \sigma_{copol}^o)}{\beta_1}$$

Pixels were classified as shellfish when the threshold values were surpassed. Contingency tables were calculated to assess the performance of the three classifiers using different accuracy metrics (Fawcett 2006), which include Kappa, sensitivity, specificity, precision and accuracy.

### Comparing Shellfish Maps from SAR with Traditional Field Surveys

To determine how well the classification compares to traditional field surveys, we compared the results of the classification of Radarsat-2 and TerraSAR-X data with an extensive ground survey based on the TMAP protocol performed in 2012 in which oyster and mussel beds were mapped in the Wadden Sea (van den Ende et al. 2012). The 2012 TMAP monitoring results in a polygon feature layer covering the area under investigation in this project. The polygons were converted to raster data matching the spatial resolution of the SAR data, so that

contingency tables could be computed. In case both sediment and shellfish were present in a cell, the majority rule was used to assign the raster value. An area of interest was defined in such a way that it excluded land (and salt-marshes), yet it still occupied large parts of the Wadden Sea to the east of Texel and south of Schiermonnikoog (see Figure 2.1). From these areas, contingency tables were calculated, which were subsequently used to derive the same classification scores as described for the classifier to see how well the remotely-sensed data match with the ground survey data. Classification scores of how the SAR classification compares with the field survey campaigns were calculated separately for the eastern and western Wadden Sea, because these areas might be quite different when it comes to sediment texture and the prevalence and patchiness of shellfish beds.

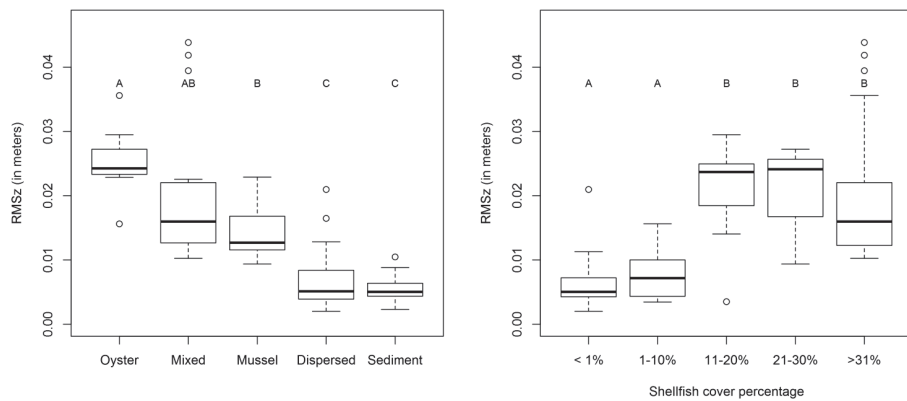


Figure 2.3 (**Left**) RMSz for oyster, mixed, mussel, dispersed and sediment plots (shellfish classes significantly different from dispersed and sediment at  $p < 0.05$ ); (**Right**) RMSz as a function of shellfish cover: RMSz in cover classes  $< 1\%$  and  $1\%–10\%$  significantly differed from that in classes  $11\%–20\%$ ,  $21\%–30\%$  and  $>21\%$  ( $p < 0.05$ ). Letters indicate homogeneous groups based on the Tukey HSD test. In the boxplots, the rectangles of the boxes show the interquartile range, the bold bar the median and the whiskers the minimum and maximum values (without outliers).

## Results and Discussion

### Effect of shellfish species and cover on surface roughness

The analysis of variance on substrate types showed that there was a significant effect of substrate class on RMSz ( $F_{4, 102} = 45.07$ ,  $p < 0.001$ ) (left graph in Figure 2.3). The Tukey HSD *post hoc* test showed that dispersed shellfish and sediment plots have lower RMSz than the shellfish-dominated plots and that oyster plots have higher RMSz than mussel plots (left graph in Figure 2.3). The ANOVA also reveals a significant effect of shellfish density on RMSz ( $F_{4, 102} = 30.74$ ,  $p < 0.001$ ); the right graph in Figure 2.3 shows that high total shellfish cover (density) is generally associated with high RMSz values and low cover with low RMSz



values, with a rather abrupt switch at lower shellfish covers. Results of the Tukey HSD *post hoc* test confirm that the lower shellfish cover classes (<1% and 1%–10%) had a significantly different RMSz than the higher cover classes (10%–20%, 20%–30%, >30%) (right graph in Figure 2.3). Figure 2.4 shows that surface roughness is mainly driven by oysters if they are present; however, the presence of mussels can actually decrease surface roughness, as these bivalves fill cracks and crevices efficiently.

Neither substrate type ( $F_{4,102} = 1.63$ ,  $p = 0.172$ ) nor shellfish cover ( $F_{4,102} = 1.804$ ,  $p = 0.134$ ) have a significant effect on correlation length. It is widely recognized that  $L$  is not scale invariant, and therefore, the values obtained are dependent on profile length and plot size (Davidson et al. 2000; Verhoest et al. 2008; Bretar et al. 2013). Zribi and Dechambre (2002) stated that neglecting  $L$  will result in large errors in estimating radar backscatter, and therefore, they proposed a new measure, called  $Z_s$ , which incorporates a slope effect. Bretar *et al.* (2013) showed that  $Z_s$  behaved more or less scale invariant. Furthermore, tortuosity and fractal dimension also appeared to be scale-invariant descriptors of surface roughness (Bretar et al. 2013). These measures were not used in this study, because it is unclear how they can be incorporated in the backscatter models used here.

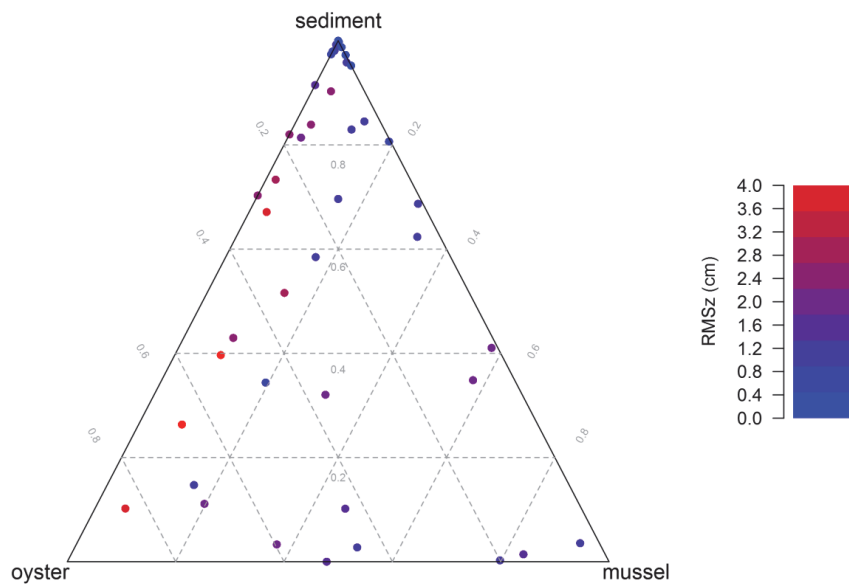


Figure 2.4 Ternary plot of RMSz between pure oyster, mussel and sediment cover fractions. RMSz values depend largely on the presence of oysters in the plot.



### Effect of surface roughness and shellfish species and cover on radar backscatter

In most backscatter channels, the shellfish substrates could clearly be distinguished from sediment and dispersed shellfish, but within shellfish beds, it was not possible to distinguish backscatter in mussel-dominated and oyster-dominated plots (Figure 2.5, Table 2.2). Backscatter saturates too quickly to distinguish species in radar imagery regardless of which wavelength was used. There was a clear trend for all backscatter channels that radar backscatter increases with increasing shellfish cover. However, due to the overlap of the different classes, as indicated by the Tukey HSD *post hoc* test, derivation of shellfish densities from radar backscatter is hard (Figure 2.6).

Table 2.2. ANOVA statistics of backscatter between different types of substrates (i.e., sediment, mussels and oysters) and ANOVA statistics of backscatter between different cover classes (densities) of shellfish.

| Satellite  | Channel | Substrate Type |             |             | Shellfish Cover |             |             |
|------------|---------|----------------|-------------|-------------|-----------------|-------------|-------------|
|            |         | D.f., N        | F Statistic | Probability | D.f., N         | F Statistic | Probability |
| TerraSAR-X | VV      | 4, 102         | 14.32       | <0.001      | 4, 102          | 17.82       | <0.001      |
| TerraSAR-X | VH      | 4, 92          | 11.46       | <0.001      | 4, 92           | 16.63       | <0.001      |
| Radarsat-2 | HH      | 4, 102         | 11.95       | <0.001      | 4, 102          | 12.56       | <0.001      |
| Radarsat-2 | HV      | 4, 102         | 15.92       | <0.001      | 4, 102          | 16.34       | <0.001      |

Both the X- and C-band SAR backscatter saturate at shellfish cover levels as low as 10%, corresponding to RMSz values as high as 1.5 cm. For future investigations, it is worth looking into data with lower incidence angles. This should decrease the strong effect of RMSz on backscatter slightly, although Choe *et al.* (2012) found that it could result in less contrast between bare sediment and shellfish. Alternatively, longer SAR wavelengths may also improve backscatter resolution within the RMSz range typically found in the shellfish class.

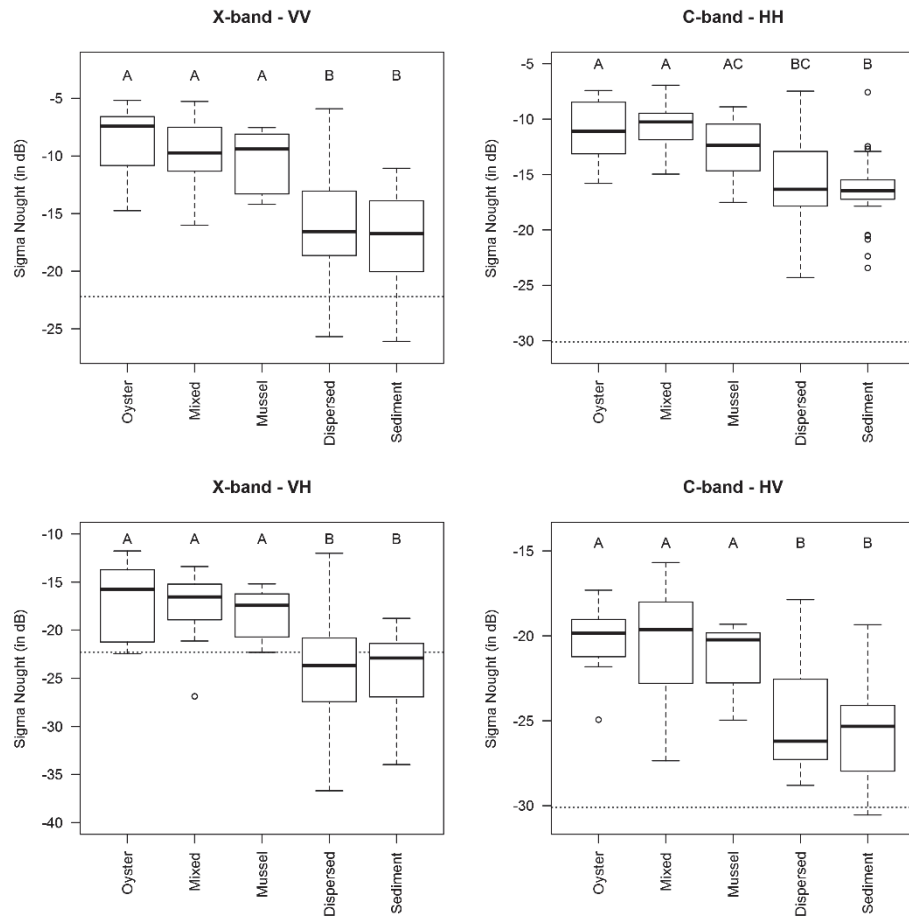


Figure 2.5 Plots with epibenthic shellfish significantly differed in backscatter from sediment and dispersed plots, but mussels, mixed and oysters do not differ significantly in backscatter. Letters indicate similar plots based on the Tukey HSD test. The dashed line indicates the average noise floor (noise equivalent sigma naught).

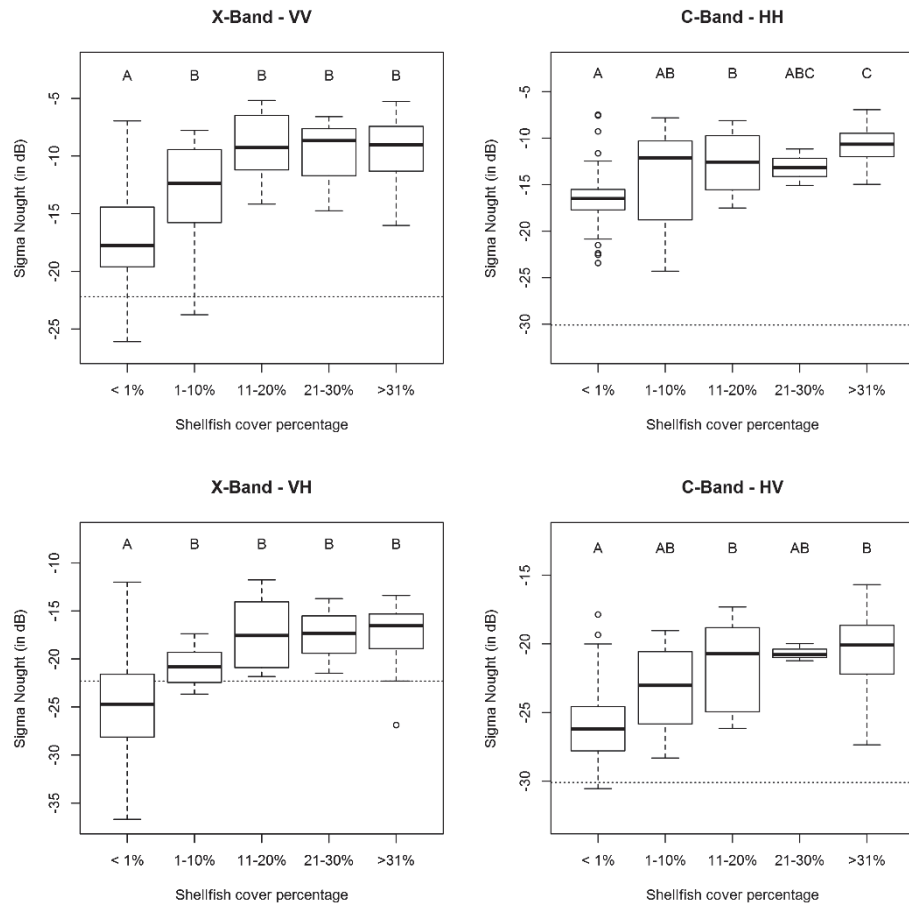


Figure 2.6 Boxplots showing the relationship between radar backscatter and shellfish cover. Letter codes indicate similarity based on the Tukey HSD test. The dashed line indicates the average noise floor (noise equivalent sigma naught).

### Theoretical and semi-empirical simulation of shellfish-induced backscatter

IEM predictions of the backscatter as a function of surface roughness RMSz and correlation length  $L$  were compared to observations at the 107 plots. First, the simulations were performed for RMSz, where we assumed correlation lengths  $L$  of 2.2, 14.4 and 32.5 cm for the IEM, which is respectively the minimum, mean and maximum  $L$  observed in this study. Our data range observed for RMSz exceeds the validity of the IEM in both the C- and X-band. We found that the IEM was rather accurate in predicting radar backscatter as a function of RMSz, especially in cross-polarized settings, given that  $L$  is assumed to be constant and provided that the model is only used within the validity range (Figure 2.7).

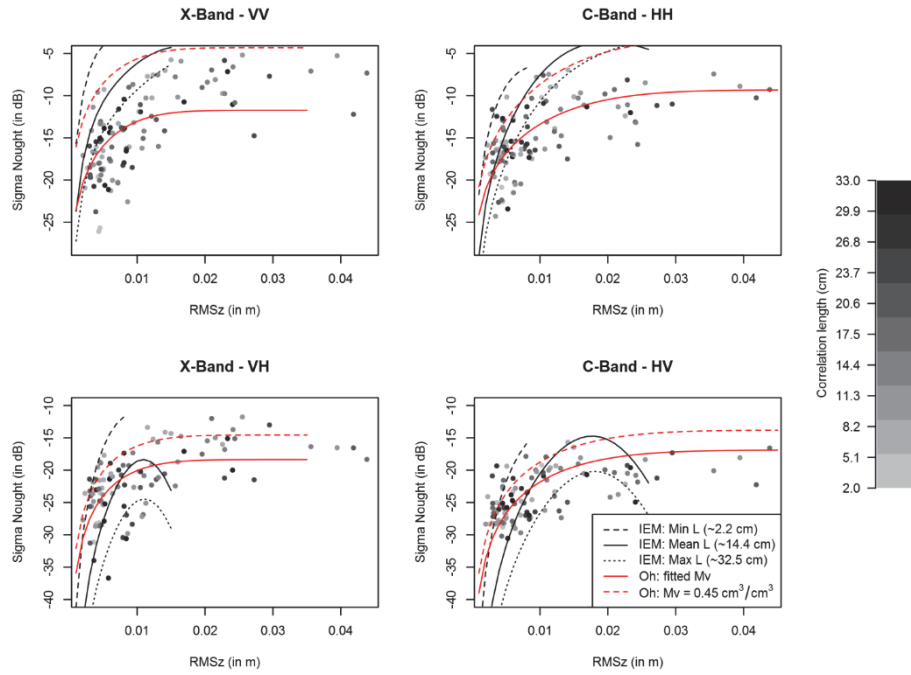


Figure 2.7 Model simulations of backscatter (sigma naught) in the X-band (VV and VH polarizations) and C-band (HH and HV polarizations) show the effect of RMSz. For the integral equation model (IEM) simulations, minimum, mean and maximum correlation lengths were used. An incidence angle of  $40^\circ$  and  $34^\circ$  was assumed for TerraSAR-X and Radarsat-2 respectively. The dots in the graphs are actual observations of surface roughness in the field and their backscatter observed in radar imagery. The grey scale in the images gives an impression of the correlation length at the measured sample points. The red lines are simulations based on Oh's model for varying moisture contents (solid red lines; see the text) and moisture content of 0.45 (dashed red lines). Lines are shown for the validity domain of the models.

In the co-polarized channel, backscatter is overestimated. The difference observed between model predictions and *in situ* roughness observations could be due to the relatively small plot size used in the ground truth campaign. This probably overestimates RMSz in relation to surface roughness estimated by the SAR sensors, which evaluate surface roughness at a much larger spatial extent dependent on sensor resolution. Shellfish beds are often patchy in nature (see, for instance, van de Koppel et al. 2005), which means that at larger spatial scales, which are used by the satellites, there is more chance of including flat mud and water in between the shellfish (Kim et al. 2011).

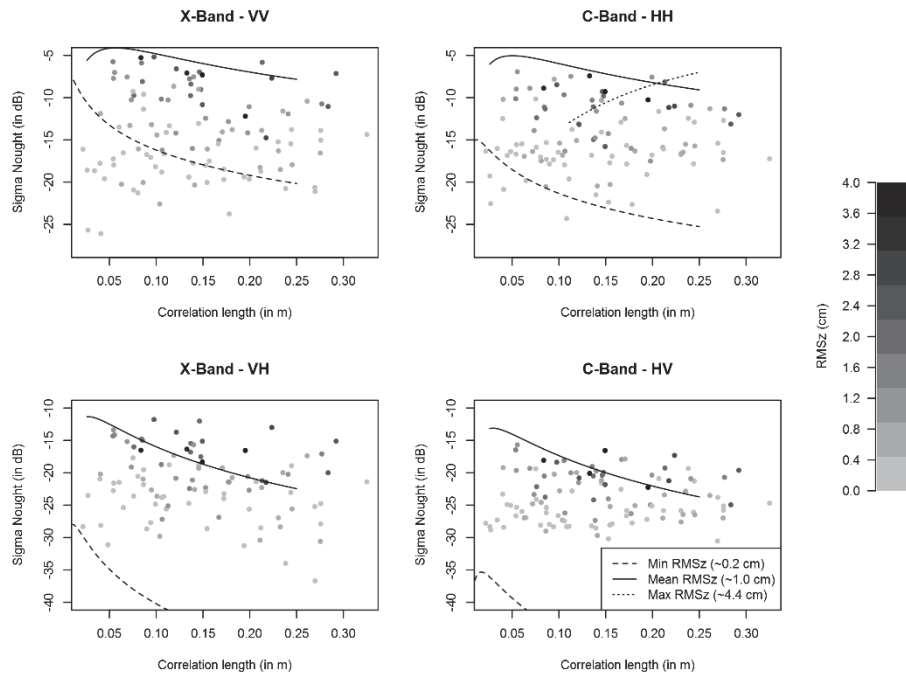


Figure 2.8 IEM simulations of backscatter ( $\sigma$  naught) in the X-band (VV and VH polarizations) and C-band (HH and HV polarizations) show the effect of  $L$ . For the IEM simulations, minimum, mean and maximum RMSz values were used. An incidence angle of  $40^\circ$  and  $34^\circ$  was assumed for TerraSAR-X and Radarsat-2, respectively. The dots in the graphs are actual observations of surface roughness in the field and their backscatter observed in radar imagery. The grey scale in the images gives an impression of RMSz at the measured sample points. Lines are shown for the validity domain of the models.

For all wavelengths and polarizations, and for all parameterizations of  $L$ , small variations in RMSz have large effects on the backscatter signal for relatively low values of RMSz, which is both predicted by the IEM model and observed. At higher RMSz levels, the IEM predicts a decreasing trend in radar backscatter. This effect is attributed to the fact that the angular curve becomes more isotropic

at larger values of RMSz at these values of incidence angles (Fung & Chen 2010). Our data, however, show a saturating response at high RMSz values; we did not observe a decrease of backscatter, but a consistent high level associated with high RMSz (up to 4 cm), even outside of the validity range. Simulations of  $L$  using the IEM were calculated at minimum, mean and maximum values for RMSz (see Figure 2.8) and show that the observed values are within the range predicted by IEM. It also shows that there is hardly any variation in  $L$  with increasing backscatter, while it is clear that high backscatter values are associated with high RMSz values. Thus, the effect of  $L$ , as measured in the field, appears subordinate to the effect of RMSz.

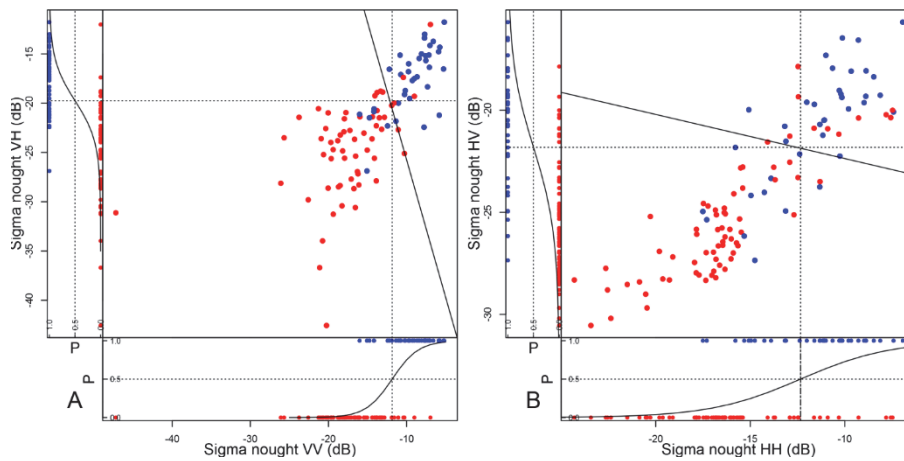


Figure 2.9 Plot showing the classification method based on the training set. (a) TerraSAR-X data and (b) Radarsat-2 data. The red points represent the class with <5% shellfish and the blue points the class with >5% shellfish. The marginal plots show the logistic regression that was used to find the threshold values (dotted lines) at the intersection, where the probability is 50% for single-polarized classifications. The solid line is the threshold value for the multivariate logistic regression for dual-polarized data. See Table 2.3 for the statistics.

The Oh (2004) semi-empirical model does not include  $L$ , both because the cross-polarized ratio is relatively insensitive to changes in  $L$  and because of the problems of estimating  $L$  properly in the field (Oh 2004). Oh's model did not predict a decrease in backscatter for higher RMSz values and performed well across the entire range of RMSz associated with both bare sediments and shellfish beds. The shape of the model matches quite well with the observations (Figure 2.7); however, model parameterization with observed moisture content largely overestimates the observed backscatter, whereas the best fit uses extremely low values for moisture content. It is therefore worth investigating the dielectric properties of the substrate in intertidal environments, including its constituents saline water and shells (calcium carbonate material). In addition, other factors,

such as the fraction of surface water influencing roughness and the spatial extent of the roughness measurements in relation to that detected by the sensor, could have played a role.

### Shellfish mapping using SAR

Shellfish presence in major Dutch intertidal regions was mapped using an empirical classification approach. The classification revealed that a threshold on dual-polarized data calculated by class separation using logistic regression is a good method to map shellfish presence (Figure 2.9).

*Table 2.3. Training statistics for the shellfish classifiers used. Thresholds (in dB) and statistics were calculated using logistic regression for co-polarized data (VV or HH), cross-polarized data (VH or HV), dual-polarized (DUAL) data and a combination of both single-band thresholds (VV + VH or HH + HV).*

|                 | TerraSAR-X |      |      |         | Radarsat-2 |      |      |         |
|-----------------|------------|------|------|---------|------------|------|------|---------|
|                 | VV         | VH   | DUAL | VV + VH | HH         | HV   | DUAL | HH + HV |
| Missing values  | 0          | 10   | 10   | 10      | 0          | 0    | 0    | 0       |
| True Positives  | 29         | 26   | 31   | 25      | 24         | 25   | 26   | 22      |
| True Negatives  | 64         | 53   | 54   | 57      | 62         | 59   | 60   | 63      |
| False Positives | 6          | 7    | 6    | 3       | 8          | 11   | 10   | 7       |
| False Negatives | 8          | 11   | 6    | 12      | 13         | 12   | 11   | 15      |
| Sensitivity     | 0.78       | 0.70 | 0.84 | 0.68    | 0.65       | 0.68 | 0.70 | 0.59    |
| Specificity     | 0.91       | 0.88 | 0.90 | 0.95    | 0.89       | 0.84 | 0.86 | 0.9     |
| Precision       | 0.83       | 0.79 | 0.84 | 0.89    | 0.75       | 0.69 | 0.72 | 0.76    |
| Accuracy        | 0.87       | 0.81 | 0.88 | 0.85    | 0.80       | 0.79 | 0.80 | 0.79    |
| Kappa           | 0.71       | 0.60 | 0.74 | 0.66    | 0.55       | 0.52 | 0.56 | 0.52    |

The performance of the classification training is given in Table 2.3. Generally, the specificity of SAR classification is slightly higher than the sensitivity, meaning that it is easier to classify bare sediments correctly, but this effect is affected by the overrepresentation of bare sediment. Kappa values, which take into account the probability of representation of bare sediment and shellfish pixels, show that all classifiers separate data with moderate to substantial performance according to Landis and Koch (1977). In general, the maps based on the dual-polarized multivariate classification, as well as the classifier that uses both single-band thresholds, perform better than single-band classifiers. TerraSAR-X performs better than Radarsat-2, e.g., Kappa = 0.74 for TerraSAR-X and Kappa = 0.56 for Radarsat-2, using the dual-polarized multivariate

classification. For an overview of the threshold parameters, please refer to Table 2.4.

*Table 2.4. Pixel thresholds to qualify as shellfish for the different classifiers for TerraSAR-X and Radarsat-2.*

|                   | Classifier | Thresholds (in dB)   |
|-------------------|------------|--|
| <b>TerraSAR-X</b> | VV         | $\sigma_{VV}^{\circ} > -11.85$   |
|                   | VH         | $\sigma_{VH}^{\circ} > -19.75$   |
|                   | DUAL       | $\sigma_{VH}^{\circ} > \frac{-(8.42 + 0.44\sigma_{VV}^{\circ})}{0.16}$ |
|                   | VV + VH    | $(\sigma_{VV}^{\circ} > -11.85) \& (\sigma_{VH}^{\circ} > -19.75)$     |
| <b>Radarsat-2</b> | HH         | $\sigma_{HH}^{\circ} > -12.34$   |
|                   | HV         | $\sigma_{HV}^{\circ} > -21.82$   |
|                   | DUAL       | $\sigma_{HV}^{\circ} > \frac{-(9.94 + 0.09\sigma_{HH}^{\circ})}{0.41}$ |
|                   | HH + HV    | $(\sigma_{HH}^{\circ} > -12.34) \& (\sigma_{HV}^{\circ} > -21.82)$     |

Table 2.5 displays how the SAR and TMAP shellfish maps compare to each other for the test areas in the Wadden Sea (Figure 2.1). Details of the classification results of dual polarized data along with TMAP shellfish outlines are depicted in Figure 2.10. The results show that SAR classification compares best to TMAP data if the classification is based on multivariate logistic regression incorporating information from both backscatter channels. Although X-band sensitivity seems most suitable for mapping shellfish as highlighted by Figures 2.6 and 2.9, it appears that X-band is sensitive to strongly-rippled sediments and steep slopes (at the edges of gullies), which do cause strong backscatter, but do not depolarize the microwave signal. This causes many false positives in the dual-polarized classification scheme, because strongly-rippled sediments and slopes were not included in our field campaign. Because of this, the dual-polarized classifier causes misclassifications of sediments, which are high in VV, but low in VH. In fact, Table 5 shows that X-band classification can be improved if a double threshold is used (VV + VH). The dual-polarization classifier obtained from Radarsat-2's C-band appears less sensitive to this.



Table 2.5. Agreement between the SAR shellfish classification and the TMAP monitoring survey, for the two sensors at Texel and Schiermonnikoog (see the text and Table 2.3 for an explanation).

|                        | Texel      |            |            |            |         |         | Schiermonnikoog |            |            |            |         |         |
|------------------------|------------|------------|------------|------------|---------|---------|-----------------|------------|------------|------------|---------|---------|
|                        | TerraSAR-X |            |            | Radarsat-2 |         |         | TerraSAR-X      |            |            | Radarsat-2 |         |         |
|                        | VV         | VH         | DUAL       | VV + VH    | HH      | HH + HV | VV              | VH         | DUAL       | VV + VH    | HH      | HH + HV |
| <b>True Positives</b>  | 64,873     | 77,090     | 68,992     | 60,275     | 962     | 1,115   | 125,729         | 105,155    | 122,806    | 80,792     | 1,709   | 1,567   |
| <b>True Negatives</b>  | 12,644,700 | 12,098,222 | 12,690,954 | 12,761,094 | 214,337 | 216,287 | 13,833,734      | 14,387,332 | 14,218,344 | 14,491,808 | 242,406 | 245,820 |
| <b>False Positives</b> | 136,044    | 682,522    | 89,790     | 19,650     | 2694    | 744     | 696,931         | 143,333    | 312,321    | 38,857     | 4003    | 589     |
| <b>False Negatives</b> | 70,167     | 57,950     | 66,048     | 74,765     | 1339    | 1186    | 232,542         | 253,116    | 235,465    | 277,479    | 4371    | 4513    |
| <b>Sensitivity</b>     | 0.48       | 0.57       | 0.51       | 0.45       | 0.42    | 0.48    | 0.35            | 0.29       | 0.34       | 0.23       | 0.28    | 0.26    |
| <b>Specificity</b>     | 0.99       | 0.95       | 0.99       | 1.00       | 0.99    | 1.00    | 0.95            | 0.99       | 0.98       | 1.00       | 0.98    | 1.00    |
| <b>Precision</b>       | 0.32       | 0.10       | 0.43       | 0.75       | 0.26    | 0.60    | 0.15            | 0.42       | 0.28       | 0.68       | 0.30    | 0.73    |
| <b>Accuracy</b>        | 0.98       | 0.94       | 0.99       | 0.99       | 0.98    | 0.99    | 0.94            | 0.97       | 0.96       | 0.98       | 0.97    | 0.98    |
| <b>Kappa</b>           | 0.38       | 0.16       | 0.46       | 0.56       | 0.31    | 0.53    | 0.19            | 0.33       | 0.29       | 0.33       | 0.27    | 0.37    |

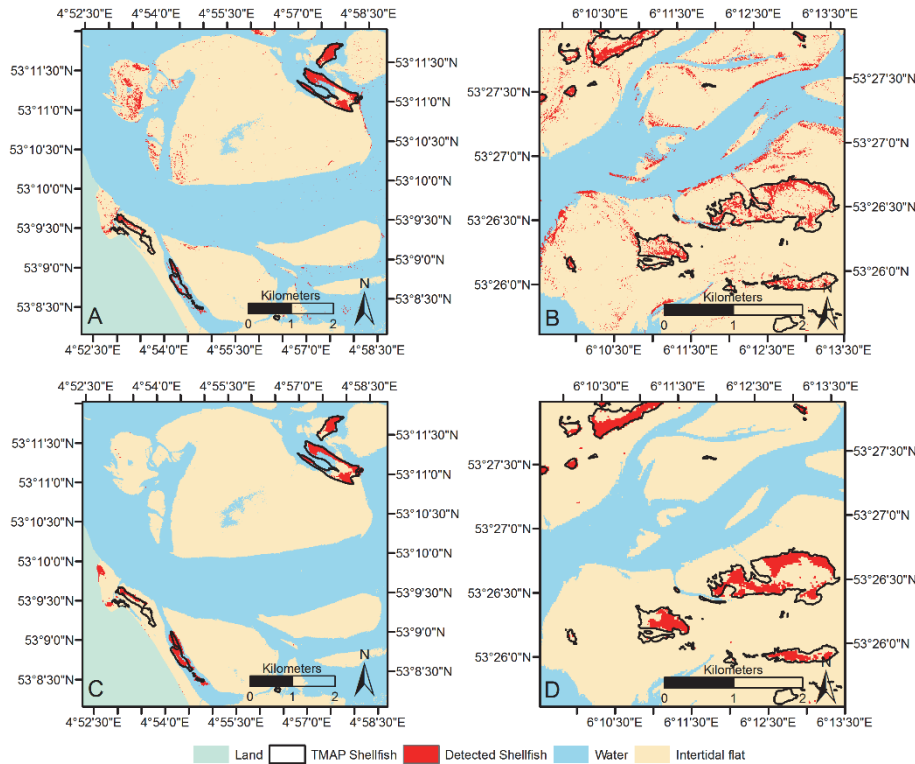


Figure 2.10 Details of the shellfish maps based on the TerraSAR-X classification for dual-polarization (brown) compared to the TMAP monitoring program (red). (a) TerraSAR-X classification of the western Wadden Sea (near Texel); (b) TerraSAR-X classification of the eastern Wadden Sea (near Schiermonnikoog); (c) Radarsat-2 classification of the western Wadden Sea; (d) Radarsat-2 classification of the eastern Wadden Sea.

Furthermore, the classification results show that mapping using Radarsat-2's C-band provides the most consistent agreement across sites, but clear differences in agreement between sites can be seen for TerraSAR-X, which agrees significantly more with the TMAP results in the western Wadden Sea (Texel) than in the eastern Wadden Sea (Schiermonnikoog). This could be explained by observations from the field that shellfish beds in the western part of the Wadden Sea are generally more strongly defined with clear boundaries, whereas in the eastern Wadden Sea, which is more shallow and sheltered, shellfish beds appear more dispersed with less clear boundaries. This would influence both the TMAP mapping and the SAR mapping, because the boundaries are harder to track *in situ* and the differences in backscatter between classes are less pronounced. The TMAP protocol also allows for misclassifications, and depending on the sensor resolution, this could result in worse performance of the mapping method. For instance, open patches can be mapped as shellfish beds, as long as they are less

than 25 m wide. Furthermore, the monitoring is very time consuming, which means that it is impossible to map all of the beds each year; as a result, the data of some beds is copied from one year to the next if the bed appears to be unchanged after determination by an aerial survey. However, even small changes in bed size and shellfish densities could result in mismatches between the SAR and the TMAP data.

To further enhance shellfish mapping based on SAR data, we propose to use a texture method that uses the spatial information in the images. The signal generated by shellfish may not be stronger than the noise, which may cause elimination of parts of the shellfish beds during speckle filtering. Spatial information retrieved by methods, such as spatial autocorrelation or Haralick's texture features, could help to enhance pixel-based image analysis (Haralick et al. 1973). Furthermore, since shellfish beds can be patchy in nature, this may have consequences for the classification of beds using high-resolution data. Methods that take into account the variation within classes in combination with the non-Gaussian behavior of SAR information prior to classification (Krylov et al. 2011) may be beneficial to further enhance shellfish mapping using SAR.

## Conclusions

Using data from a high number of ground stations, we were able to establish that dual-polarized X- and C-band SAR data can be used to distinguish between substrates with bare sediments with up to 5% shellfish cover (dispersed) and shellfish substrates (>5% cover). This observation was supported by the IEM and Oh's model and highlights that SAR remote sensing is a valuable tool for shellfish monitoring. However, because the backscatter intensity saturates with relatively low RMSz values in shellfish beds, it is not possible to derive information on shellfish density or species composition. Mussels and oysters both increase RMSz of intertidal soft bottom substrates, with the largest RMSz values being found in oyster beds with high cover. Mussels, on the other hand, also increase RMSz, but at higher densities, the surfaces become smoother, as the mussels efficiently fill all available spots. No significant effects were found of the surface classes on correlation length.

Tide, weather and light conditions typically limit the window of opportunity to acquire data for optical remote sensing. SAR, on the other hand, only depends on suitable tidal conditions and much less on light and weather. Furthermore, SAR is less influenced by epibionts, which camouflage the shellfish in optical data. Furthermore, the application of single-acquisition SAR in epibenthic shellfish classification rather than multitemporal classification is particularly useful, because multitemporal data can now be used in change detection studies to monitor shellfish beds. These results highlight that by using SAR, monitoring

## | Chapter 2

surveys can be performed much more cost effectively and complement current field surveys. The current Radarsat-2, TerraSAR-X, CosmoSkyMed and Sentinel-1 missions provide suitable SAR data for such monitoring.





# Niche separation and facilitation along an intertidal inundation gradient drives large scale coexistence of invasive oysters and native mussels

*Ready to submit*

*Sil Nieuwhof, Hélène de Paoli, Jim van Belzen, Karin Troost,  
Peter M.J. Herman and Daphne van der Wal*

### Abstract

Zonation of species along environmental gradients are typically the result of an interplay between stress tolerance and competition. Invasive ecosystem engineers are often considered a threat because of their competitive strength. We investigated the invasion of the reef building Pacific oyster (*Crassostrea gigas*) into the Dutch Wadden Sea and its effects on the distribution of reefs of blue mussels (*Mytilus edulis*) along the inundation gradient. We investigated occurrence, condition and competition of the two species along this gradient. A spatiotemporal GIS analysis of in situ intertidal shellfish surveys, spanning a period from 2001 to 2014, combined with inundation data, shows that before the introduction of the Pacific oyster, mussel reefs were found in the intertidal zone with inundation times of 50-100%. Oysters gradually invaded the deeper zones of the intertidal zone (70-100% inundation). More recently, oyster reefs have become colonized by mussels and vice versa resulting in mixed reefs. The niches of oysters and mussels now largely overlap although the optima of occurrence along the inundation gradient for mussels is shallower than that of oysters. Field and experimental results revealed that oysters had a higher condition index when inundation time was longer, while mussels had an optimum condition index at intermediate inundation durations. Interference competition between the two species was significant, but only affected shell size negatively, suggesting this did not influence species performance locally. Conversely, a growth experiment showed that mussels attained larger shell area and ash free dry weight of the flesh along the inundation gradient in a mixed setting, suggesting a slight advantage for mussels. Overall, our study points to the potential for coexistence of both shellfish species. We expect that the majority of intertidal shellfish reefs in the Wadden Sea will become mixed reefs in the future. Within the intertidal zone, pure mussel reefs are likely limited to the higher areas and might become temporarily more numerous after a successful spatfall, while pure oyster reefs may become increasingly rare.



## Introduction

Ecological zonation is the segregation of species (or communities of species) along a physical gradient, which often results in conspicuous banding (Chappuis et al. 2014). Zonation can be found in a number of systems. For example, on mountains, altitudinal zonation in vegetation is driven by differences in temperature, humidity and solar radiation (Daubenmire 1943). In freshwater ponds, water depth plays an important role in structuring species distributions (Grace & Wetzel 1981). While potential species distributions are determined by their physiological limitations (Somero 2002), biological interactions are of significant importance too (Connell 1972). In the intertidal zone, saltmarshes (e.g. Bertness 1991) and rocky shores (Connell 1972) exhibit zonation of plants and animals along the inundation gradient, which are mediated by the competitive ability of organisms at the expense of the ability to cope with stress (Grime 1977). More specifically, more competitive species occupy benign zones displacing less competitive species into more stressful areas (Pennings et al. 2005; Pennings & Callaway 1992; Bertness 1991).

While zonation is visually apparent on rocky shores and saltmarshes in the high intertidal, it is less apparent on the soft-bottom (i.e. sandy and muddy) flats of the lower intertidal with higher inundation regimes, even though it may be expected that the same structuring mechanisms apply (Peterson 1991). While strong competition over space on rocky shores drives mutual exclusion of species and results in sharp delineation between the different zones, this is not typically a driving force on soft-bottom tidal environments (Peterson 1991). Competition over a mobile food source (i.e. phytoplankton), which is more prevalent in waters of intertidal flats, results in segregation of species over much larger spatial scales and zonation patterns are not necessarily clearly delineated (Peterson 1991). Still, emersion duration limits feeding time of suspension feeders, such as shellfish, and it has been identified as one of the driving factors determining the distribution of benthic species (e.g. Compton et al. 2013). Yet, how the inundation in combination with competition shapes benthic shellfish community structure of soft-bottom environments is still largely unclear.

Shellfish are key species on many marine soft-bottom environments. The blue mussel (*Mytilus edulis*) and the Pacific oyster (*Crassostrea gigas*) occur on intertidal sand- and mudflats where they form extensive reefs. The creation of these reefs is often referred to as autogenic ecosystem engineering (sensu Jones et al. 1994) because they modify the habitat both locally and at extensive spatial scales due to their presence (Donadi, Westra, et al. 2013; van der Zee et al. 2012 and Chapters 4 and 5). In many soft-bottom estuaries, reef building shellfish are the dominant ecosystem engineering species in the lower intertidal providing

otherwise absent biogenic hard substrate, which has important implications for the ecosystem at large. For example, shellfish reefs have been shown to alter benthic assemblages (Norling et al. 2015; Kochmann et al. 2008; Markert et al. 2010), promote primary production (Engel et al. 2017) and to retain water during low tide in pools (see Chapter 4) because of the biogenic structure they add to the intertidal soft-bottom environment.

The Pacific oyster is an invasive species along European coastal waters (Troost 2010) and is still, partly driven by global warming, expanding its distribution range (Thomas et al. 2016). In the Wadden Sea, the oyster invasion received considerable attention (Troost 2010). Since mussels and oysters have similar strategies and are thought to share the same niche (Reise 1998), it was feared that oysters would expand at the cost of native mussels (Diederich 2006). Oysters compete for food and space with native shellfish species which could result in species shifts (for an overview see Troost (2010)). Hence, it has been suggested that typical native mussel reefs would be fully transformed into oyster reefs (Diederich 2006), or at least mixed reefs (Fey et al. 2009).

Currently three reef types can be distinguished in the Dutch Wadden Sea as a result of the invasion by the Pacific oyster: 1) mussel-dominated, 2) mixed- and 3) oyster dominated (see for definition: Nehls and others 2009). The relative contribution of each of these three types to the total surface of shellfish reefs has been continuously changing over the past decades, and the fate of the native mussel reefs in the face of the invasion by Pacific oysters is still unclear. Here we review these trends and relate them to underlying physiological limitations and competitive processes, in order to better understand the patterns and predict how they will likely develop in the future.

Differences in species-specific traits and performance between Pacific oysters and blue mussels might result in niche separation with optima at different inundation levels. Generally, inundation has been identified as an important factor in defining population dynamics within mussel- (McGrorty & Goss-Custard 1993) and oyster reefs (Walles, Fodrie, et al. 2016). Oyster reefs are more robust than mussel reefs because *C. gigas* is larger and uses a stronger attachment technique based on cementation (Yamaguchi 1994), compared to the smaller *M. edulis* which attach using byssal threads (Wa Kangeri et al. 2014). In addition, recruitment and growth of oysters increase towards areas with higher inundation values (Walles, Troost, et al. 2016; Walles, Smaal, et al. 2016; Walles, Fodrie, et al. 2016). The same is generally true for mussels (Buschbaum & Saier 2001), but they may be able to persist with less inundation as they are smaller and need less feeding time to meet their energetic demands. Individuals of the blue mussel may survive inundation times of just a few hours (Brinkman et al. 2002). Bird

predation may affect mussel abundance on the higher intertidal zones (Brinkman et al. 2002), but this may be sustainable on stable reefs which receive enough spatfall allowing production to match consumption (Nehls et al. 1997). Trait differences between the species might result in segregation along the inundation gradient, with oyster reefs being more successful in the deeper intertidal where currents are stronger and benthic predation higher (and more limiting to mussels). Holm et al. (2016) therefore hypothesized that there should be niche separation between mussels and oysters because the two species seem to be able to co-exist in this manner. However, within a single mixed reef, they found no evidence for separated niche space in shellfish condition over a depth gradient, nor in species distribution. We argue, based on Herman and others (1990) and Peterson (1991), that the nature of competition between patches of filter feeding species happens on larger spatial scales (landscape scale). As a result, the spatial separation between the oysters and mussels along the inundation gradient might be more clearly observed by investigating distributions at the scale of an entire coastal system consisting of multiple shellfish reefs.

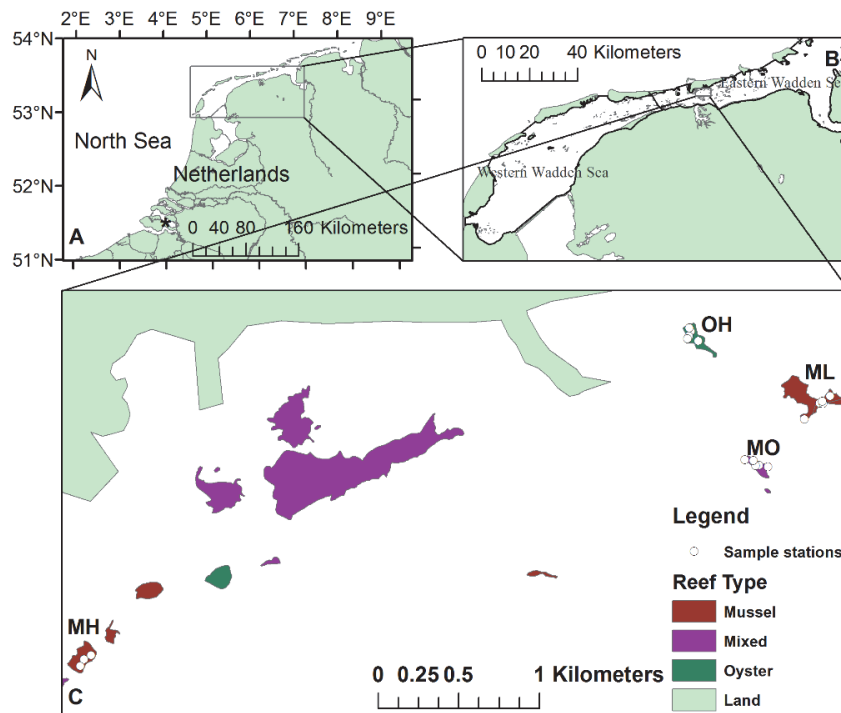


Figure 3.1 A. Oosterschelde (location of field experiment is indicated by the \*) and Wadden Sea in the Netherlands, with B. shellfish reefs in the western and eastern part of the Wadden sea and C. detail of the investigated shellfish reefs (MH = mussel reef high, ML = mussel reef low, OH = Oyster reef high and MO = mixed reef) and sample locations.

In this study, we explore whether reefs of the invasive Pacific oyster, the blue mussel and of both species mixed exhibit niche separation along the inundation gradient, using shellfish survey data combined with inundation data in a Geographical Information System (GIS). From time-series of the shellfish reef distributions, we investigate the stability of this spatial segregation, to address interspecific competition. We hypothesize that oyster reefs are more dominant in the lower intertidal (i.e. high inundation durations), compared to mussels, which occur higher in the intertidal (i.e. low inundation durations).

Furthermore, we also investigate whether spatial segregation of shellfish reefs is driven by differences in adaptation (i.e. scope for growth) with regard to inundation at the individual level and by interspecific competition, by performing a survey in the field, and a growth experiment. We hypothesize that the adaptations with regard to the inundation gradient (individual size, condition and growth rate of the shellfish) are more favorable for oysters lower in the intertidal zone as compared to mussels. We further hypothesize there is limited interspecific competition (and possibly even facilitation), when the species co-exist in a mixed reef. The latter was tested in the observational field survey by comparing shell size and condition of a species in presence of the other species, and experimentally by comparing (shell and flesh) growth of both species in isolation and in mixed setting at different inundation levels.

## Materials and Methods

### Study sites

The study focused on two tidal basins in the Netherlands (Figure 3.1A), the Wadden Sea for the GIS analysis and observational field survey (south of Wadden island of Schiermonnikoog, Figure 3.1C), and the Oosterschelde for the growth experiment (harbor of Yerseke). The Wadden Sea is a mesotidal shallow basin. In the Dutch Wadden Sea, reef building shellfish are the dominant autogenic ecosystem engineer in the lower intertidal. In the absence of hard substrate the blue mussel (*Mytilus edulis*), native in the Wadden Sea, forms extensive shellfish reefs by forming dense aggregates in a process referred to as self-organisation (Liu et al. 2012; van de Koppel et al. 2005). Due to a combination of subsequent years of poor recruitment and extensive fishing the mussel populations collapsed around 1990 (Nehls et al. 2009; Dankers et al. 2003), after which mussel fishing was restricted to the subtidal zones in the western part of the Dutch Wadden Sea (Dankers et al. 2004). Meanwhile, the Pacific oyster (*Crassostrea gigas*) was introduced in the Wadden Sea (Texel) in the late 1970s (Troost 2010), after which it started becoming abundant in the 1990s (Fey et al. 2009). The Oosterschelde is an oligotrophic macrotidal sea-arm that has been heavily influenced by human engineering, i.e. a large storm surge

barrier was constructed in 1986 which decreased the tidal prism (Nienhuis & Smaal 1994). The Pacific oyster was introduced in the Oosterschelde (south-west Netherlands) in 1964, to replace the native edible oyster (*Ostrea edulis*) which disappeared due to disease and a cold winter, and *C. gigas* were spread throughout the entire basin by the end of the 1970s (Troost 2010). In the Oosterschelde, large aggregates of blue mussels (*Mytilus edulis*) are largely confined to subtidal culture lots (Troost 2010).

### GIS analysis

To study the differences and changes in inundation duration between the three types of bed, shellfish reef distribution data in the Dutch Wadden Sea (see Figure 3.1) from the annual WOT Fisheries program were used. In this program, that is commissioned by the Dutch ministry of economic affairs and carried out by Wageningen Marine Research, shellfish stock sizes are assessed annually since the early 1990s (Troost et al. 2012; Folmer et al. 2014). Intertidal mussel and Pacific oyster beds are mapped according to TMAP protocol (TMAG—Trilateral Monitoring and Assessment Group 1997). We used reef contours from the period 2001 to 2014, which were made available for this project as a polygon file in a Geographical Information System (GIS). During mapping of the beds, a visual assessment was made whether the bed qualified as a pure mussel bed (more than 5% of the bed area occupied by mussels and less than 5% by oysters), a pure oyster reef (>5% oyster cover and <5% mussel cover) or a mixed reef (both species individually occupy more than 5% of the available area) (Troost et al. 2012). Emergence duration data of the Dutch Wadden Sea was acquired from Rijkswaterstaat (the Dutch agency for water management) as a raster file with a resolution of 20 m and converted to inundation time (%). The shellfish distribution data was imported into ArcGIS 10.1, converted to raster data, imported in R and variation in inundation duration was investigated within the different shellfish reef types for each year. In addition, the basin in which each of the reef polygons were situated was recorded so that differences could be investigated for different regions of the Dutch Wadden Sea (i.e. east versus west, see Figure 3.1B). Using this GIS we investigated changes in area occupied by the reefs, changes in composition and changes in reef distribution along the inundation gradient for all years between 2001 and 2014.

### Field Survey

A field survey was conducted south of the island of Schiermonnikoog in the Dutch Wadden Sea to investigate condition and interspecific competition of the two different shellfish species along the intertidal gradient. In the week of 1 to 7 October 2014, 18 sample locations were investigated located on four shellfish reefs (5 on a high oyster reef (OH), 5 on a low mussel reef (ML), 5 on a low



mixed reef (MO) and 3 on a high mussel reef (MH); See Figure 3.1 for the sample locations and Figure 3.2 for a field impression). At each of the sample locations cover, density, average shellfish condition and size class structure was studied per species. The exact location and elevation of each sample location was measured using a differential Global Positioning System (dGPS). To estimate size class structure, all shellfish within a small surface area (to save time, see Table 3.1) were detached and thoroughly cleaned. The cleaned shellfish were placed on a whiteboard (60\*72 cm<sup>2</sup>) with marks for a perspective correction and photographed for further analysis (see section Image Analysis). Finally, up to 10 mussels and 10 oysters were collected from each sample location at random to estimate their condition (see section Laboratory analysis).

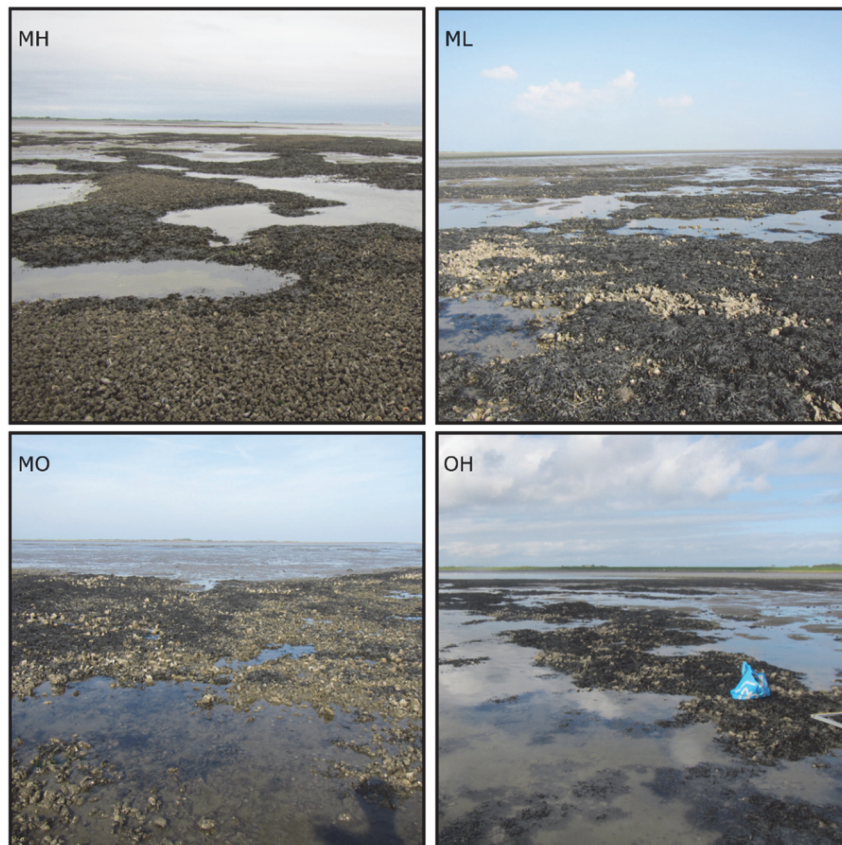


Figure 3.2 Photographs of the investigated shellfish reefs (MH = mussel reef high, ML = mussel reef low, OH = Oyster reef high and MO = mixed reef)

### Growth experiment

To investigate growth and competition along the intertidal gradient, a growth experiment was conducted in the field in the harbor of Yerseke in the Oosterschelde, the Netherlands (Figure 3.1A). We installed three lines consisting of a cable with bags with shellfish attached at different elevations: one line with oysters, one with mussels and one with mussels and oysters. Given the size of the animals in the experiment we estimated that the filtration capacity of oysters was 2 times as large as that of mussels, therefore we used twice the amount of mussels compared to oysters (for adult animals, the filtration capacity of oysters may be three times as large compared to mussels (Troost et al. 2008)). At fixed heights, on each line, three bags were placed, each containing 16 mussels in the mussel treatment, 4 oysters and 8 mussels in the mixed treatment and 8 oysters in the oyster treatment. The bags had a mesh size of approximately 0.5 cm to allow ample amounts of water circulation in the bags. The mussels were acquired from an intertidal location in Vlissingen (51°27'36.5"N 3°31'49.2"E, mouth of the Westerschelde) and the oysters were obtained from an intertidal location in Yerseke (51°29'21.4"N 4°03'26.7"E, Oosterschelde). An extra batch of 50 specimens of both species was stored in the freezer to compare initial size and condition (T0) to the individuals that were used in the experiment. The lines had five height treatments. The heights were fixed at five inundation values: 98.5%, 97%, 82%, 64% and 48%. For the tidal range in Yerseke, this results in treatments at -1.7m, -1.6m, -1.2m, -0.6m and 0m (this conversion was calculated using a tidal model from Rijkswaterstaat: <http://getij.rws.nl>). The experiment started the 21<sup>st</sup> of May 2014. The experiment was revisited to clean and inspect shells on the 20<sup>th</sup> of June, the 29<sup>th</sup> of July, the 1<sup>st</sup> of September and the 1<sup>st</sup> of October that same year. In order to track individual growth, each shell was tagged using 8 \* 4 mm oval polyethylene glue-on shellfish tags (FPN 8x4, [www.hallprint.com](http://www.hallprint.com)) attached using cyanoacrylate glue. In case of mortality the shellfish was replaced with a new individual. Unfortunately, all shellfish of the upper three exposures of the oyster treatment were lost in July and had to be replaced with new individuals. Therefore, caution should be taken when these shellfish are compared with the initial batch (T0) batch of shellfish.

Table 3.1. Characteristics of the sampling stations; reef classification, elevation with regard to mean sea level and inundation time. Furthermore, shellfish densities, shell areas and lengths (major) were investigated within a section of the 1 m<sup>2</sup> frame (the section size is indicated by Inspected surface area).

| Station | Reef Classification (species and elevation) | Elevation (in m NAP) | Inundation time (%) | Mussel                  |                                     |                                   | Oyster                |                                     |                                   |                       |
|---------|---|----------------------|---------------------|-------------------------|-------------------------------------|-----------------------------------|-----------------------|-------------------------------------|-----------------------------------|-----------------------|
|         |   |                      |                     | Inspected surface area* | Shell Density (nr m <sup>-2</sup> ) | Shell Area (cm <sup>2</sup> ± sd) | Shell Major (cm ± sd) | Shell Density (nr m <sup>-2</sup> ) | Shell Area (cm <sup>2</sup> ± sd) | Shell Major (cm ± sd) |
| MH1     | Mussel High                                 | 0.007                | 56                  | 0.0625                  | 3152                                | 4.64(±2.98)                       | 3.23(±1.18)           | 48                                  | 24.86(±19.48)                     | 6.81(±3.99)           |
| MH2     | Mussel High                                 | 0.053                | 54                  | 0.0625                  | 2016                                | 4.71(±4.02)                       | 3.1(±1.67)            | 192                                 | 19.86(±13.9)                      | 6.03(±2.26)           |
| MH3     | Mussel High                                 | 0.012                | 56                  | 0.0625                  | 3808                                | 4.43(±3.17)                       | 3.12(±1.22)           | 176                                 | 42.79(±13.81)                     | 10.09(±2.48)          |
| ML1     | Mussel Low                                  | -0.403               | 67                  | 0.25                    | 620                                 | 5.08(±3.55)                       | 3.27(±1.33)           | 20                                  | 63.2(±31.53)                      | 10.81(±3.56)          |
| ML2     | Mussel Low                                  | -0.56                | 71                  | 0.25                    | 444                                 | 7.06(±4.85)                       | 3.93(±1.6)            | 128                                 | 102.42(±29.67)                    | 16.24(±3.55)          |
| ML3     | Mussel Low                                  | -0.295               | 64                  | 0.0625                  | 1984                                | 3.08(±2.8)                        | 2.43(±1.04)           | 48                                  | 59.64(±25.26)                     | 10(±2.42)             |
| ML4     | Mussel Low                                  | -0.599               | 72                  | 0.25                    | 908                                 | 8.87(±4.04)                       | 4.54(±1.25)           | 36                                  | 87.82(±28.12)                     | 13.36(±2.67)          |
| ML5     | Mussel Low                                  | -0.299               | 64                  | 0.0625                  | 2832                                | 3.63(±3.17)                       | 2.7(±1.35)            | 208                                 | 44.14(±24.13)                     | 8.89(±2.87)           |
| MO1     | Mixed Low                                   | -0.193               | 61                  | 0.0625                  | 2976                                | 3.79(±2.51)                       | 2.86(±1.09)           | 16                                  | 36.41(±11/a)                      | 7.62(±1/a)            |
| MO2     | Mixed Low                                   | -0.284               | 64                  | 0.25                    | 852                                 | 6.78(±3.95)                       | 3.98(±1.25)           | 32                                  | 48.88(±15.09)                     | 9.53(±1.68)           |
| MO3     | Mixed Low                                   | -0.356               | 66                  | 0.0625                  | 928                                 | 5.68(±4.78)                       | 3.48(±1.66)           | 96                                  | 62.33(±35.12)                     | 11.57(±5.54)          |
| MO4     | Mixed Low                                   | -0.191               | 61                  | 0.0625                  | 2480                                | 5.53(±2.59)                       | 3.6(±0.96)            | 48                                  | 74.56(±4.69)                      | 11.59(±0.92)          |
| MO5     | Mixed Low                                   | -0.244               | 63                  | 0.0625                  | 1696                                | 4.96(±2.62)                       | 3.39(±1.04)           | 0                                   | n/a                               | n/a                   |
| OH1     | Oyster High                                 | 0.109                | 53                  | 0.25                    | 368                                 | 6.57(±2.92)                       | 3.9(±1.01)            | 32                                  | 50.34(±26.79)                     | 10.3(±3.73)           |
| OH2     | Oyster High                                 | -0.002               | 56                  | 0.25                    | 172                                 | 4.84(±2.4)                        | 3.28(±0.85)           | 28                                  | 69.3(±38.44)                      | 12.07(±3.78)          |
| OH3     | Oyster High                                 | 0.064                | 54                  | 0.25                    | 532                                 | 4.78(±2.92)                       | 3.23(±0.96)           | 92                                  | 69.13(±31.27)                     | 11.83(±3.64)          |
| OH4     | Oyster High                                 | -0.048               | 57                  | 0.25                    | 960                                 | 1.69(±1.44)                       | 1.77(±0.76)           | 48                                  | 61.38(±24.83)                     | 11.42(±2.81)          |
| OH5     | Oyster High                                 | -0.007               | 56                  | 0.25                    | 256                                 | 6.23(±3.26)                       | 3.81(±1.14)           | 48                                  | 59.93(±21.26)                     | 11.25(±2.79)          |

\* The surface area used to investigate shellfish characteristics (shell densities, shell areas and shell lengths), Reef roughness was obtained from the full 1 m<sup>2</sup> frame.

### Laboratory analysis

The shellfish in the growth experiment were re-measured on the revisit days. Photos were made of the shells on a 15\*15 cm<sup>2</sup> reference square, using Canon's D20 digital photo camera, which were used in Fiji (Schindelin et al. 2012) to calculate the surface area of the shell (see Image Analysis section). Length, width and thickness (the pair of clams combined) of the mussels were measured using digital calipers to the closest 10<sup>th</sup> of a millimeter. For oysters, only shell thickness was measured, as length and width were irregular in shape. The shellfish harvested at the end of the growth experiment, the T0 shellfish from the start of the growth experiment and the shellfish from the field survey were dissected to obtain Ash Free Dry Weights (AFDW). The shellfish were frozen prior to analysis so that they could be opened easily. First, the fresh weight was determined. After that the shellfish were opened and shell and flesh wet weight were determined separately. After that flesh and shells were dried for four days at 70 °C and weighed again for dry flesh- and shell weight (g). Finally, the flesh was incinerated at 540 °C for four hours to determine AFDW (g). Condition index (CI) was calculated for the shellfish retrieved from the field using  $CI = \text{Ash free Dry weight(g)} / (\text{Length (mm)}^{2.8})$  for mussels following Troost et al (2009). This method is not appropriate for oysters because of their irregular shell shape. For that reason, we expressed condition index for the oyster as  $AFDW \text{ (g)} / \text{age (yr)}$ . The age of the oysters from the field was estimated using growth marks within the hinge of the shells following (Harding & Mann 2006).

### Image Analysis

All photographs for shellfish measurements from the lab and from the field were imported into Fiji (Schindelin et al. 2012) for further analysis. A perspective correction was applied by using an artificial template image and using the landmark correspondences tool. The contrast differences were sufficiently large for most images to use the magic wand tool to automatically delineate the shellfish. In some cases, minor manual corrections had to be made to these selections in case shadows were included. Area and the major and minor axis of a fitted ellipse were determined for all shellfish in centimeters.

### Statistical Analysis

All data was imported into the statistical software package R (R Development Core Team 2015) for statistical analysis and visualization of data. We set the rejection criterion at a probability P of under 5% ( $P < 0.05$ ) to test whether differences were statistically significant. For the GIS-analysis, we computed and visualized proportional probability density functions to investigate the occurrence of the three different reef types along the inundation gradient. In order to investigate the relationship of shellfish performance as a function of inundation,

as well as competition (as measured by the number of the other reef building shellfish) we fitted linear models where inundation was included as a second order polynomial. Finally, to test whether observed differences were statistically different in the experimental work, analysis of covariance (ANCOVA) was used. Here inundation was a covariate and time (as month) and treatment (mixed or monospecific) were entered as factors. The significance of the entire linear model was computed by means of an ANOVA and the significance of each of the entered variables was computed.

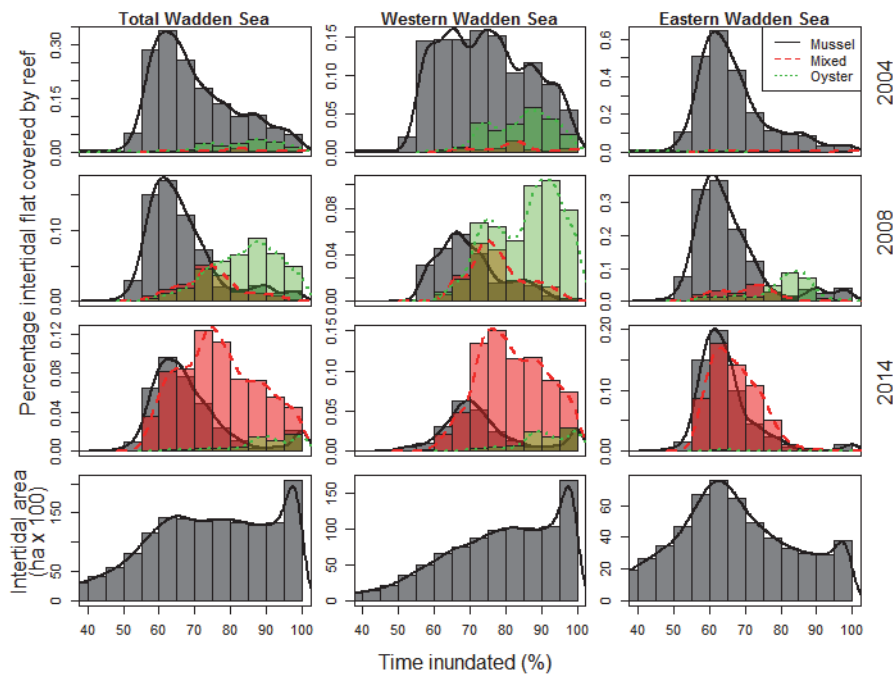


Figure 3.3 Percentage reef cover of total intertidal for mussel-, oyster- and mixed reefs along the inundation gradient for the years 2004, 2008 and 2014. The bottom row shows the distribution of intertidal flat available for different inundation values.

## Results

### GIS analysis

For the period 2001 to 2014, oyster reefs occur at higher inundation values (85% of the time inundated on average), mussel reefs at low inundation values (68%) and mixed reefs in between (76%) in the Dutch Wadden Sea. It was observed that in the absence of oysters at the start of the observation period in 2001, mussels occupied the entire inundation gradient between 50 and 100%. In later years, oysters started colonizing the low intertidal. Pure oyster reefs formed mainly in the western Wadden Sea, where the intertidal flats are relatively deeper compared



to the eastern Wadden Sea (Figure 3.3). In the eastern Wadden Sea most mussel reefs occur at 60-65% inundation, which is also the most common inundation level found across the intertidal in this region. In the eastern Wadden Sea, oysters started colonizing the system mostly by invading mussel reefs, creating mixed reefs. Mussels invaded the oyster reefs in the western Wadden Sea in later stages, resulting in even more mixed reefs. In 2014, mixed reefs were the dominant reef structures in the Wadden Sea, occurring along the entire inundation gradient occupied by both mussel and oyster reefs (see Figure 3.3).

Figure 3.4 A and B reveal that oyster reefs achieved their maximal coverage in 2008, but declined steadily onwards in favor of mixed reefs. In addition, it can be observed that pure oyster reefs were further limited to the low intertidal by invading mussels in the oyster reefs (Figure 3.4B).

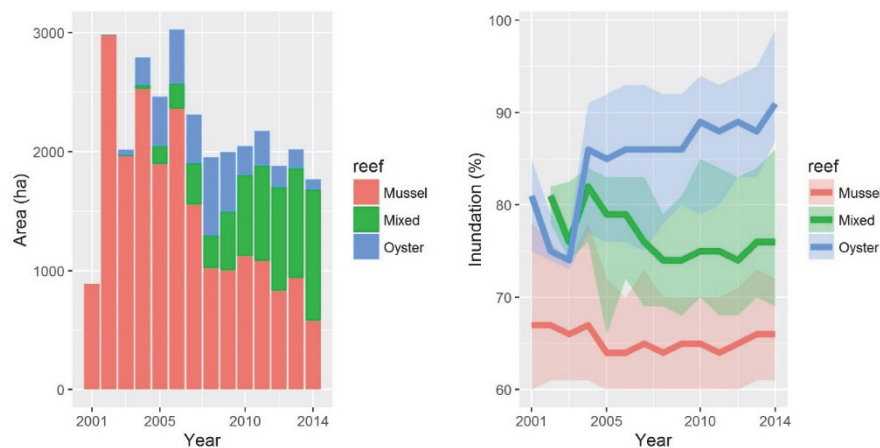


Figure 3.4 A) The area occupied by the different shellfish reef types and their relative proportion (Total, mussel-, mixed- and oyster reefs). B) Median inundation of the reef types over the years (bands indicate 25% and 75% quantiles)

### Field Survey

Pronounced differences in shellfish density and individual size were observed (Table 3.1 provides information on the 18 sampling stations visited in the field (elevation in the intertidal frame, inundation period, surface roughness and reef classification) as well as information on the shellfish specimen at that specific station). As expected, an exploratory scatterplot revealed no relationship between inundation and mussel density, nor between inundation and oyster density, in the limited range of inundation times surveyed. At the same time, the relationship between the number of oysters and mussels was not significant ( $R^2=0.14$ ,  $F_{1,16}=2.57$ ,  $p = 0.13$ ), yet also indicated that space occupation by one species did not exclude the other locally. Linear models of shellfish condition of one species,

with a second order polynomial term for inundation and a first order term for shellfish density of the other species as explanatory variables, showed that inundation and competition (density of other species) significantly explain average size attributes (shell length and mean shell area), as well as condition index of both mussels and oysters (see Table 3.2 for significant terms). Mussels were largest in the low intertidal, both in terms of average shell length ( $R^2=0.11$ ,  $F_{3,2641}=111.7$ ,  $p < 0.05$ ) and shell area ( $R^2=0.14$ ,  $F_{3,2641}=138.1$ ,  $p < 0.05$ ) while at inundation values of around 60% there was a minimum in size attributes. Additionally, the model indicated a small negative effect of the number of oysters on mussel shell length and area. Oyster shell length ( $R^2=0.32$ ,  $F_{3,164}=26.19$ ,  $p < 0.05$ ) and area ( $R^2=0.36$ ,  $F_{3,164}=31.17$ ,  $p < 0.05$ ) showed a similar trend with inundation (see Figure 3.5) and a small negative effect of mussels was observed (Table 3.2). Condition index for mussels ( $R^2=0.15$ ,  $F_{3,168}=10.15$ ,  $p < 0.05$ ) and for oysters ( $R^2=0.46$ ,  $F_{3,139}=39.4$ ,  $p < 0.05$ ) was only influenced by elevation and not by presence of the other species (see Table 3.2).

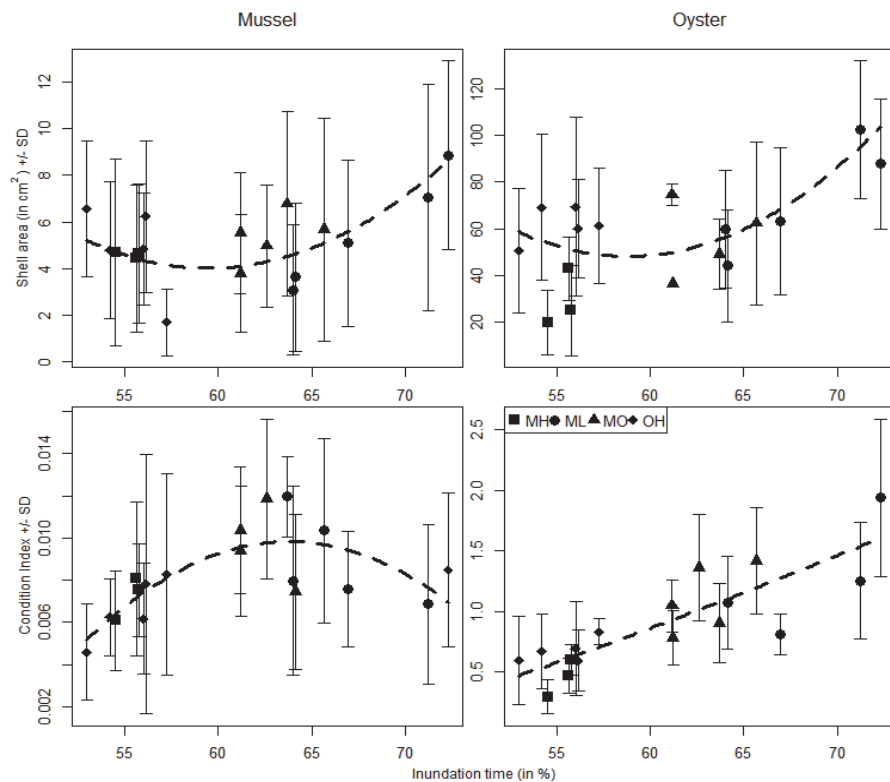


Figure 3.5 Relationship between inundation time (in %) and shell area (as derived in Fiji), condition index for mussels ( $AFDW (g) / Length (mm)^{2.8}$ ) and oyster ( $AFDW (g) yr^{-1}$ ). The values are averages at the different stations and the error bars indicate standard deviations. The curve is a second order fit between inundation time and the dependent variables without taking into account the competition effects (i.e. the amount of the other shellfish species).

### Growth experiment

In figure 3.6 the effect of inundation, as well as competition effects on shell size (area in  $\text{cm}^2$ ) and ash free dry weight of the T0 batch with the mussels and oysters at the end of the experiment were summarized. ANCOVA revealed similar patterns as observed in the field campaign. Mussel length ( $R^2=0.16$ ,  $F_{6,1369}=44.57$ ,  $p < 0.05$ ) and area ( $R^2=0.18$ ,  $F_{6,1369}=49.6$ ,  $p < 0.05$ ) depended on inundation, time (month) within the growing season and the presence of the other species (Treatment in Table 3.3). The presence of oysters had a positive effect on shell growth of mussels, whereas in the field survey the inverse was observed. Oyster length ( $R^2=0.16$ ,  $F_{6,589}=18.44$ ,  $p < 0.05$ ) and area ( $R^2=0.16$ ,  $F_{6,589}=18.62$ ,  $p < 0.05$ ) were dependent on inundation and timing, but no effect of the presence of mussels was observed. Condition index was not determined each month, because condition determination requires sacrificing the specimen. Ash free dry weights at the end of the experiment revealed no treatment effect for oysters ( $R^2=0.07$ ,  $F_{3,162}=4.133$ ,  $p = 0.07$ ), but for mussels the treatment effect was significant ( $R^2=0.17$ ,  $F_{3,350}=24.23$ ,  $p < 0.05$ , see Table 3.3).

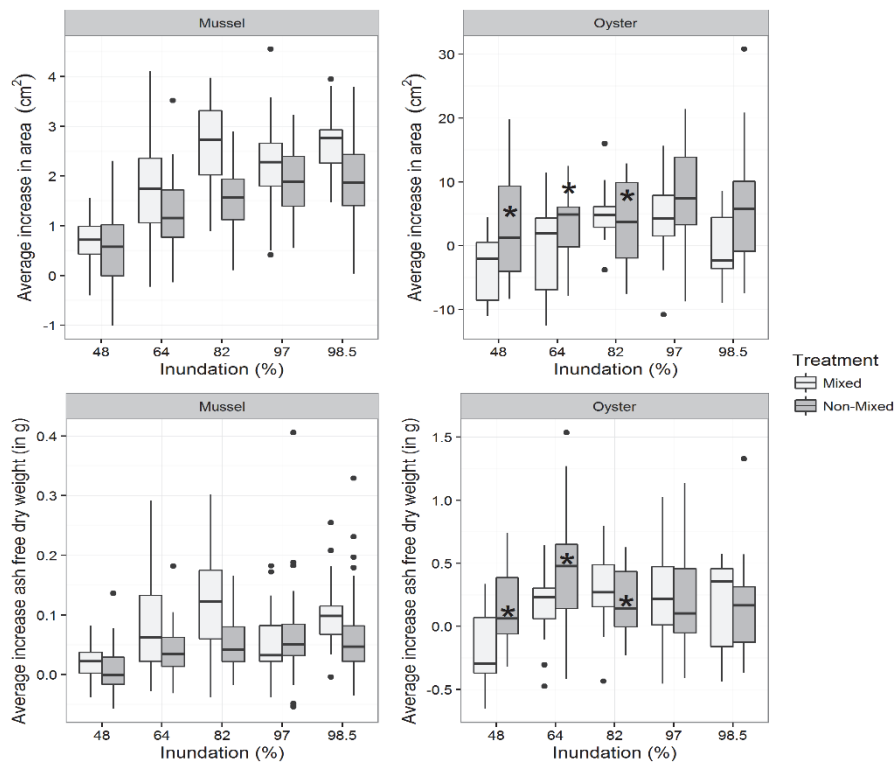


Figure 3.6 Average differences in shell area ( $\text{cm}^2$ ) and AFDW (g) between the T0 group and the animals at the end of the experiment. Note that some oysters in the non-mixed treatment (indicated with an \*) were lost and replaced with a completely new batch.

Table 3.2. Average shellfish size (length and area as measured using Fiji) and condition index modelled as a function of inundation (second order polynomial) and competition (i.e. the amount of the other shellfish species).

| Species | Variable      | Shellfish length (cm) |            |         |              | Shellfish area (cm <sup>2</sup> ) |            |         |              | Shellfish condition index |            |         |              |
|---------|---------------|-----------------------|------------|---------|--------------|-----------------------------------|------------|---------|--------------|---------------------------|------------|---------|--------------|
|         |               | Estimate              | Std. Error | t value | P value*     | Estimate                          | Std. Error | t value | P value*     | Estimate                  | Std. Error | t value | P value*     |
| Oyster  | Intercept     | 12.724                | 0.420      | 30.302  | <b>0.000</b> | 75.432                            | 3.375      | 22.352  | <b>0.000</b> | 0.942                     | 0.056      | 16.933  | <b>0.000</b> |
|         | Inundation    | 21.591                | 3.546      | 6.088   | <b>0.037</b> | 191.544                           | 28.502     | 6.720   | <b>0.000</b> | 4.097                     | 0.388      | 10.557  | <b>0.000</b> |
|         | Inundation^2  | 9.443                 | 3.777      | 2.500   | <b>0.013</b> | 70.185                            | 30.354     | 2.312   | <b>0.022</b> | -0.057                    | 0.415      | -0.138  | 0.891        |
|         | Nr of Mussels | -0.001                | 0.000      | -3.600  | <b>0.000</b> | -0.009                            | 0.002      | -4.115  | <b>0.000</b> | 0.000                     | 0.000      | -0.961  | 0.338        |
| Mussel  | Intercept     | 3.391                 | 0.040      | 85.495  | <b>0.000</b> | 5.344                             | 0.105      | 50.794  | <b>0.000</b> | 0.009                     | 0.000      | 20.200  | <b>0.000</b> |
|         | Inundation    | 15.627                | 1.335      | 11.702  | <b>0.000</b> | 47.844                            | 3.541      | 13.510  | <b>0.000</b> | 0.010                     | 0.004      | 2.699   | <b>0.008</b> |
|         | Inundation^2  | 16.879                | 1.321      | 12.776  | <b>0.021</b> | 49.037                            | 3.504      | 13.996  | <b>0.000</b> | -0.015                    | 0.004      | -4.257  | <b>0.000</b> |
|         | Nr of Oysters | -0.002                | 0.000      | -4.345  | <b>0.000</b> | -0.004                            | 0.001      | -3.984  | <b>0.000</b> | 0.000                     | 0.000      | -1.258  | 0.210        |

\***Bold values** are significant at  $p < 0.05$

Table 3.3 Statistics for the growth experiment. Shellfish length and shell area were both determined using Image analysis. "Month" indicates the month over which growth (change in shell length and area) was assessed (June, July, August and September respectively). Since determination ash free dry weight required scarification of the animal, these parameters are only measured at the end of the experiment. Therefore, time is not included there.

| Species | Variable     | Shellfish length (cm) |        |         |         |              | Shellfish area (cm <sup>2</sup> ) |        |         |         |              | Ash free dry weight (g) |        |         |         |                 |
|---------|--------------|-----------------------|--------|---------|---------|--------------|-----------------------------------|--------|---------|---------|--------------|-------------------------|--------|---------|---------|-----------------|
|         |              | Df                    | Sum Sq | Mean Sq | F value | P value      | Df                                | Sum Sq | Mean Sq | F value | P value      | Df                      | Sum Sq | Mean Sq | F value | P value         |
| Oyster  | Inundation   | 1                     | 0.170  | 0.170   | 55.820  | <b>0.000</b> | 1                                 | 0.625  | 0.625   | 57.189  | <b>0.000</b> | 1                       | 0.098  | 0.098   | 0.739   | 0.391           |
|         | Inundation*2 | 1                     | 0.005  | 0.005   | 1.599   | 0.207        | 1                                 | 0.014  | 0.014   | 1.265   | 0.261        | 1                       | 1.172  | 1.172   | 8.797   | <b>0.003</b>    |
|         | Treatment    | 1                     | 0.000  | 0.000   | 0.008   | 0.930        | 1                                 | 0.005  | 0.005   | 0.480   | 0.489        | 1                       | 0.381  | 0.381   | 2.863   | 0.093           |
|         | Month        | 3                     | 0.162  | 0.054   | 17.744  | <b>0.000</b> | 3                                 | 0.577  | 0.192   | 17.602  | <b>0.000</b> |                         |        |         |         |                 |
|         | Residuals    | 589                   | 1.789  | 0.003   |         |              | 589                               | 6.438  | 0.011   |         |              | 162                     | 21.574 | 0.133   |         |                 |
| Mussel  | Inundation   | 1                     | 0.321  | 0.321   | 71.848  | <b>0.000</b> | 1                                 | 1.657  | 1.657   | 82.506  | <b>0.000</b> | 1                       | 0.127  | 0.127   | 35.020  | <b>7.78E-09</b> |
|         | Inundation*2 | 1                     | 0.056  | 0.056   | 12.627  | <b>0.000</b> | 1                                 | 0.243  | 0.243   | 12.076  | <b>0.000</b> | 1                       | 0.045  | 0.045   | 12.420  | <b>0.000</b>    |
|         | Treatment    | 1                     | 0.006  | 0.006   | 1.435   | 0.231        | 1                                 | 0.164  | 0.164   | 8.148   | <b>0.004</b> | 1                       | 0.091  | 0.091   | 25.260  | <b>8.03E-07</b> |
|         | Month        | 3                     | 0.811  | 0.270   | 60.504  | <b>0.000</b> | 3                                 | 3.914  | 1.305   | 64.953  | <b>0.000</b> |                         |        |         |         |                 |
|         | Residuals    | 1369                  | 6.119  | 0.005   |         |              | 1369                              | 27.496 | 0.020   |         |              | 350                     | 1.264  | 0.004   |         |                 |

\*Significant values (at  $P < 0.05$ ) are bold. Where treatment effects are significant Tukey-HSD posthoc test reveals that the mussels in mixed treatment performed better.

## Discussion

In this paper, we studied the distribution of mussel-, oyster- and mixed reefs along an inundation gradient at large spatial scales (distribution of shellfish reefs in the Wadden Sea) and individual performance at smaller spatial scales (in a field survey and in a field experiment) to investigate competition and facilitation between the species. The different shellfish reef types had different optima in occurrence along the inundation gradient; i.e. mussel reefs occur in areas with relatively low inundation duration (high elevations in the intertidal), oyster reefs in areas with relatively high inundation duration (low elevations in the intertidal) and the mixed reefs at intermediate inundation duration. The mixed reefs occur along the entire inundation gradient encompassing both pure mussel and oyster reef distributions. Optima in condition index were also different for the two species; while oysters had the highest condition index in the low intertidal, the optimum condition index for mussels was at intermediate inundation values. Only small effects of competition were observed in the field with regard to shell size, but not condition index. Finally, oysters seemed to facilitate mussel growth in a mixed experimental setting.

The patterns of distribution of oysters and mussels are influenced by the availability of areas with specific inundation durations. For example, average inundation duration is lower in the eastern Wadden Sea as compared to the western Wadden Sea. Upon the introduction of the oyster, oyster reefs became dominant in the lower intertidal of the western Wadden Sea in 2008, to be invaded by mussels afterwards (Figure 3.3). It should be noted that both mussels and oysters occur in the subtidal zones of the Wadden Sea as well (Troost 2010; Folmer et al. 2014), but these were not included in this investigation. Based on the different height distributions of tidal flats in the western and eastern Wadden Sea, the eastern Wadden Sea seems to be better suited for mussels and the western Wadden Sea for oysters.

The experiment and the field survey indicate that physiological preference is another important aspect in defining distribution patterns along the inundation gradient. The experiment revealed that higher inundation is generally better for growth of both species. Correspondingly, oysters have a higher condition index with increasing inundation in the field. However, mussels have an optimal condition index around 60-65% inundation in the field. Apart from height distribution of tidal flats and physiological preference, variables such as hydrodynamic conditions at landscape scale, recruitment patterns, predation, competition and facilitation, are important for the distribution patterns of mussels and oysters along the inundation gradient as well.



Hydrodynamic conditions caused by waves and currents, although not elaborated on in the current study, may affect the distribution of mussels and oysters at landscape scale. These conditions are very important in regulating settlement, reef establishment and reef survival (Folmer et al. 2014; Donker et al. 2013). Strong shellfish cementation (Yamaguchi 1994) and the use of dead shell material in the reef core (Waldbusser et al. 2013; Walles et al. 2015) as anchorage in highly cohesive muddy sediments help oysters to resist strong physical forces (currents and waves) in the deeper parts of the intertidal. Mussels on the other hand use byssal threads to adhere to conspecifics or shell debris (Wa Kangeri et al. 2014), but do not make such a strong anchorage with endobenthic structures. This makes mussel beds more prone to destruction by storms, restricting their distribution to sheltered areas (e.g. Nehls & Thiel 1993).

Recruitment dynamics play an essential role in determining niche space and community structure of mussels and oysters (Petraitis 1990; Diederich 2005; Walles, Smaal, et al. 2016). Oysters hardly recruit at all in the higher reaches of the intertidal zone and recruits are mostly found from the subtidal to regions which are inundated around 60% of the time (Walles, Smaal, et al. 2016). This is in line with the spatial distribution of the oysters we observed in the Wadden Sea. Therefore, it may be concluded that the oysters' upper limit in the intertidal is set by limitations of oyster spat to settle high in the intertidal. Mussels require cold winters for reproduction (e.g. Nehls et al. 2006), whereas oysters require warm summers for reproduction (Troost 2010). Oysters prefer to settle on conspecifics, whereas no such preference is present in mussels (Kochmann et al. 2008). However, while mussel spat survival may depend on the amount of mussels adults present (Mcgrorty et al. 1993), in good years mussels may form many seed beds (Nehls et al. 2009). The implication is that, given a favorable cold winter, new mussel seedbeds can suddenly occupy large areas independent of the present distribution of shellfish, but depending on favorable hydrodynamic conditions for settling. Oysters expand existing reefs and form new reefs in years with warm summers, on stretches of shell rubble or old cockle beds that may be associated with high energy hydrodynamic conditions, as mentioned above (Lenihan 1999).

Predation may limit the distribution of shellfish reefs, in the subtidal mainly by benthic predators such as starfish, crabs and shrimps, and in the intertidal by birds during low tide and by benthic predators when submerged (Johnson & Smee 2014; Weerman et al. 2014; Van Der Veer et al. 1998; Waser et al. 2016). Although predation has been shown to be important for oyster distribution (Fodrie et al. 2014; Johnson & Smee 2014; Weerman et al. 2014), many predators still have a preference for mussels over Pacific oysters. This may be partly due to potential predators not having learned yet how to handle Pacific oysters (enemy

release hypothesis (Troost 2010)), and partly due to the fact that the relatively large and irregularly shaped Pacific oysters and their spat are more difficult to detach from the substrate and to handle. Mussels have a number of avian predators that may push them to higher inundation regimes (Seed & Suchanek 1992; Waser et al. 2016), even if their potential physiological growth rate might allow them to persist at lower inundations. It is unclear, however, how shellfish reefs are affected in their spatial distribution by both avian and/or benthic predators. Because oysters do not have many predators yet, we argue that oysters are largely unaffected in their distribution by predation in Dutch waters. Mussels, on the other hand, may suffer large losses due to avian predation intertidally (Nehls et al. 1997) and due to predators such as starfish (Saier 2001; Agüera et al. 2012) subtidally. Predation is especially an important factor during spatfall of mussels; for mussels to achieve successful reef establishment important predators (mostly shrimp) need to be suppressed by means of a cold winter (Beukema et al. 2015). Such winters are becoming increasingly rare, and might explain part of the decline in pure mussel reefs (Beukema et al. 2015) relative to mixed reefs. However, whether predation is a determining factor in the distribution of mussel beds in the intertidal, is yet unclear and was not addressed in the present study.

Two remaining factors affecting distribution of mussels and oysters along the inundation gradient are facilitation and competition. Overall, we found no strong support for interference competition between the two reef builders within reefs. Reduced shell growth in presence of the other reef building bivalve species is probably of minor importance in the performance of species at large. The data from the growth experiment suggest that the presence of oysters may actually be beneficial for mussels. This facilitative effect may have been (partly) caused by an experimental artifact. Large oyster shells in the bags push aside the mesh, thereby creating more moving space that allows mussels to better orient themselves with respect to the flow. In the field other facilitative and competitive effects may be effective between the two species. Mussel spat may be able to escape predation by utilizing existing reefs as refuge. It may be speculated that the rough surface of oysters provides such protection. As some of the oyster reefs turned into mixed reefs, it might be that oysters facilitate mussels in this way. Earlier studies already indicated mussels do well in oyster reefs (Markert et al. 2010) and mussels actively migrate in between the larger oyster shells to gauge between feeding ability and reduction of predation by shore crabs (Eschweiler & Christensen 2011). This might imply that the competition with the filter feeding oysters is offset by the higher feeding times in deeper waters and the benefits of protection from predators and high flow rates. This might have its limits, as it should be noted that increased filter feeding activity in the system due to the oyster invasion might result in decreased phytoplankton availability (Ruesink et

al. 2005 and references therein). As a result, the facilitative effects may only be sustainable for mussels if the carrying capacity of the ecosystem is not reached, since food limitation results in decreased condition index and reproductive success (Vismann et al. 2016). The implication would be that mussels slightly expand their distribution in the mixed reefs, but still have reduced stocks at the scale of the entire system. This could be an issue in the Oosterschelde estuary (Smaal et al. 2013), however the Wadden Sea is generally not regarded as a food-limited system for bivalves (Beukema & Dekker 2015). Competition by species other than mussels and oysters might affect distribution at different intertidal depths as well. Buschbaum and Saier (2001) remark that fouling by epibionts (overgrowth by barnacles) can prevent high growth rates in the low intertidal. This has also been observed intertidally for the Suminoe oyster (*C. ariakensis*) (Bishop & Peterson 2006). Conversely, mussels that take refuge within the biogenic structure of oyster reefs have reduced barnacle overgrowth which is detrimental to their growth (Buschbaum et al. 2016). This might be another facilitative effect of oysters on mussels explaining the expanding distribution of mixed reefs. Although the effect of fouling was minimized in the experiment presented in this work, it could be that oysters deal better with epigrowth when compared to mussels due to their larger size. This, in addition to a larger resistance to predation pressure, may explain why on average oyster reefs, compared to mussel reefs, occur lower in the intertidal where they profit from increased feeding times and decreased desiccation stress (Byers et al. 2015).

The distribution of oysters and mussels in the Wadden Sea does not seem to have stabilized yet (cf. Figure 3.4). Based on our results, it is expected that most shellfish reefs will become mixed reefs in the Wadden Sea in the future. The occurrence of different types of shellfish reefs segregated along the inundation gradient within an estuarine system could be beneficial because each reef type has specific ecosystem engineering traits (Bouma et al. 2009), with distinct consequences for sediment (grain size and organic matter) and associated fauna (Kochmann et al. 2008). While some bird species are hampered by the presence of oysters, others profit from them (Markert et al. 2013; Waser et al. 2016). In addition, shellfish reefs have been found to modify their environments at spatially extended scales (e.g. van der Zee et al. 2012; Donadi, van der Heide, et al. 2013; Walles et al. 2014 and Chapter 4 and 5). If their long distance effects have different consequences for the intertidal habitat, then diverse reef structures created by these reef types might result in a more heterogeneous littoral seascape at larger spatial scales (Eklöf et al. 2014). Mixed reefs, which seem to become the more dominant reef type, appear to have the largest potential to facilitate primary production over extended distances (see Chapter 5). Overall we show that, while the expansion of the Pacific oyster in the Wadden Sea likely affects

many trophic levels in either a supporting or depressing way, the effect of the Pacific oyster on mussels might be predominantly facilitative and thus result in a diversification in intertidal shellfish reefs.



## CHAPTER 4

---

### Shellfish reefs increase water storage capacity on intertidal flats over extensive spatial scales

*Ecosystems 2017*

*Sil Nieuwhof, Jim van Belzen, Bas Oteman, Johan van de Koppel,  
Peter M.J. Herman and Daphne van der Wal*

#### Abstract

Ecosystem engineering species can affect their environment at multiple spatial scales, from the local scale up to a significant distance, by indirectly affecting the surrounding habitats. Structural changes in the landscape can have important consequences for ecosystem functioning, for example, by increasing retention of limiting resources in the system. Yet, it remains poorly understood how extensive the footprint of ecosystem engineers on the landscape is. Using remote sensing techniques, we reveal that depression storage capacity on intertidal flats is greatly enhanced by engineering by shellfish resulting in intertidal pools. Many organisms use such pools to bridge low water events. This storage capacity was significantly higher both locally within the shellfish reef, but also at extensive spatial scales up to 115 m beyond the physical reef borders. Therefore, the footprint of these ecosystem engineers on the landscape was more than 5 times larger than their actual coverage; the shellfish cover approximately 2% of the total intertidal zone, whereas they influence up to approximately 11% of the area by enhancing water storage capacity. We postulate that increased residence time of water due to higher water storage capacity within engineered landscapes is an important determinant of ecosystem functioning that may extend well beyond the case of shellfish reefs provided here.



## Introduction

Since the introduction of the concept of ecosystem engineering by Jones and others (1994), the notion that certain species may drive ecosystem structuring and functioning through habitat modification has largely been accepted by the scientific community. Ecosystem engineering organisms are able to influence abiotic conditions and resource availability, thereby creating specific niches within the landscape that change community composition (Bruno et al. 2003; Crain & Bertness 2006) and boost biodiversity at larger spatial scales (Jones et al. 1997; Wright & Jones 2004; Bouma et al. 2009). These bioengineered systems are often characterized by feedbacks that increase stability (Gurney & Lawton 1996; Jones et al. 1997; Hastings et al. 2007) and resilience (Eriksson et al. 2010). Although more recently it became evident that ecosystem engineering also affects ecosystem structure and functioning over long distances, well beyond the boundaries of the physical engineered structures (van de Koppel et al. 2015), less is known about what determines the extent of ecosystem engineering.

A key feature of ecosystem engineering is that species can introduce or remove physical structure, altering the overall topography of the landscape (Wright & Jones 2004; Jones et al. 2010). Habitat complexity, which is often used interchangeably with the notion of topographical complexity, is regularly used to explain dynamics in species distributions because it explains the amount of refuge space or food available through either increased niche space or increased surface area (Kovalenko et al. 2012). Although structural complexity mainly increases niche space in benign systems, the interaction between biogenic structure and the abiotic environment results in additional effects that structure the landscape and boost heterogeneity. For example, structural changes due to ecosystem engineering can modify grain size distribution (Gutiérrez et al. 2003; Bos et al. 2007; Yang et al. 2008; van Katwijk et al. 2010; Meadows et al. 2012), organic matter content (Jones et al. 1994; van Katwijk et al. 2010; van der Zee et al. 2012) and moisture in sediments (Crain & Bertness 2006; Meadows et al. 2012).

The interplay of the physical environment and added structure through ecosystem engineering is clearly exemplified by the beaver (*Castor* spp.), the archetypal example of an ecosystem engineer (Wright et al. 2002; Wright et al. 2003). The beaver builds dams, which impound water upstream. The size of the water reservoir depends on the size of the dam, but also on the underlying landscape topography; in a steep canyon valley the reservoir can only extend to a moderate surface area before the dam overflows, but on flat wetlands the reservoir can be much larger (Johnston & Naiman 1987). The effects of these reservoirs on fish communities are generally beneficial because they provide extreme flow refuge, breeding sites and habitats (Kemp et al. 2012). In addition, the retention in beaver

ponds may improve water quality as particulate matter can settle (Correll et al. 2000). Yet, so far the beaver example is as idiosyncratic as it is iconic. Little is known about pond formation by other ecosystem engineering species, thereby limiting the generality of this example.



Figure 4.1 A) Tidal pools between patches of mussels studied in this paper south of the island of Schiermonnikoog. B) Tidal pools on and around an oyster reef south of the island of Schiermonnikoog. C) Tidal pools observed in the Oyster reef at Neeltje Jans location. All of these pools have been verified to persist during low water events.

In this study, we investigated how bioengineering shellfish, in particular the blue mussel (*Mytilus edulis*) and the Pacific oyster (*Crassostrea gigas*), increase storage capacity (that is, depression storage capacity) within an estuarine landscape resulting in tidal pools. In a process referred to as self-organization, engineering by shellfish can lead to the formation of a regular or semi-regular mosaic of raised hummocks and depressions (van de Koppel et al. 2005; Liu et al. 2012). Raised hummocks are formed by trapping fine particulate sediment and organic matter locally causing variations in the elevation within reefs (ten Brinke et al. 1995; Rodriguez et al. 2014; Walles et al. 2014). This increases the structural complexity of the landscape and increases water storage capacity (Gutiérrez et al. 2011). Trapped water in depressions forms tidal pools which are typical features within shellfish reefs (see Figure 4.1). Increased storage capacity at spatially extended scales (surrounding the reefs) is likely the result of the influence shellfish reefs has on the hydrodynamic regime (waves and tidal flow) beyond the physical borders of the engineered structures (van Leeuwen et al. 2010). This results in sedimentation of fine particulate matter around these reefs (van Leeuwen et al. 2010; van der Zee et al. 2012; Donadi, van der Heide, et al. 2013; Walles et al. 2014). This, in turn, leads to the typical surface topography with high storage capacity associated with cohesive sediments, which may also trap water (Whitehouse et al. 2000).

We investigated whether intertidal flats with shellfish reefs have a greater depression storage capacity, both within and around reef areas compared to non-

engineered intertidal flats. First, we investigated local effects of shellfish on depression storage capacity and compared this to the reefs immediate surroundings by using high-resolution terrestrial laser scan data. Secondly, we used remotely sensed (airborne LiDAR for elevation measurement and space borne synthetic aperture radar for shellfish mapping specifically) data to compare storage capacity within reefs with that of the intertidal flat at increasing distances from the reefs to see to what spatially extended scales storage capacity is still significantly enhanced. Finally, to provide general understanding of how water storage capacity depends on landscape roughness, we ran simulations of different landscape structures to reveal how storage capacity depends on landscape structure and topography (more specifically the vertical and horizontal roughness elements, and slope).

## Methods

In this study, we estimate the depression storage capacity as a proxy for the potential for the amount of water that can be retained in a landscape, following the definition and methodology of Knecht et al. (2012) and Schrenk et al. (2014). We used standard GIS routines to fill depressions in elevation maps (more specifically MATLAB's imfill routine and ArcGIS 10.1's fill routine were used depending on the data type analyzed). The depression storage capacity map is calculated by subtracting the original elevation map from the filled elevation map. Statistical software R was used for statistics (R Development Core Team 2015).

It should be noted that in this study we use depression storage capacity to indicate the potential for tidal pool formation, yet depressions in an elevation map do not necessarily result in water accumulation. In reality, water may infiltrate or seep away in small-scale structures, too small to be captured by the resolution of the elevation map. However, field observations indicate that the majority of depressions on shellfish reefs and their surroundings do contain water throughout an entire low tide event. This is supported by the fact that low infiltration rates (in the order of 1–60 mm per day) caused by fine particulate matter and water saturated sediments are typical for the intertidal zone (for example Harvey et al. 1987; Nuttle & Harvey 1995; Hughes et al. 1998). This was confirmed by water level measurements with pressure loggers placed in tidal pools within and around an oyster reef, which revealed limited drainage during low tide (see Appendix A.1). In addition, reef structures slow down runoff and increase the residence time of water in the landscape. In the case of mussel and oyster reefs, this will likely result in hydrodynamically benign environments, which usually result in higher deposition or decreased erosion of fine particulate and organic matter (Rodriguez et al. 2014). These associated differences in sediment characteristics will further emphasize the differentiation in water retention between shellfish

influenced areas and bare intertidal flats, as the latter are usually sandier. Although such differences are not accounted for in the methodology used here, the concept of depression storage capacity is widely used in hydrological studies (for example Mitchell & Jones 1978; Hansen et al. 1999).

### Study sites

This study was carried out on two spatial scales. To study storage capacity at reef scale, three shellfish reefs, with their neighboring mudflats, were used to study the difference in ponding between reef surfaces and sandy surfaces. The small-scale sites included an oyster reef and a mussel reef on the tidal flats south of the island of Schiermonnikoog in the Dutch Wadden Sea. The Wadden Sea is a mesotidal eutrophic system, which was designated as an UNESCO world heritage site in 2009 because of diverse seascapes and the wildlife (particularly birds) that it supports. In addition, an oyster reef on the tidal flats bordering the island of Neeltje Jans was studied. Neeltje Jans is a mudflat in the Oosterschelde, a macrotidal sea arm located in the southwest delta region of the Netherlands. Pacific oysters were introduced for mariculture into this estuary in 1964, after the collapse of the indigenous oyster species, and pacific oyster populations have gradually expanded throughout the system since the 1970s, building extensive reefs (Troost 2010). Sediment samples were taken in and around the reefs from the top 2 cm of the sediment bed, and particle size distributions were characterized using a Malvern 2600 particle sizer. See Table 4.1 for more general information about the shellfish reefs.

To study the effects of shellfish on storage capacity at basin scale, a part of the Wadden Sea south of the barrier island of Schiermonnikoog was investigated. In this part of the Wadden Sea both blue mussel beds, Pacific oyster beds and mixed beds are present (Figure 4.1).

Table 4.1. Locations, areas, tidal characteristics and average sediment fractions (clay < 2  $\mu\text{m}$ , silt 2 – 50  $\mu\text{m}$  and sand > 50  $\mu\text{m}$ ) of the reefs studied. The tide values are with regard to NAP (Normaal Amsterdams Peil, which is the Dutch ordnance system and is approximately similar to mean sea level).

| Basin                 | Location        | Species | Coordinates             | Mean elevation (m NAP) | Area inside reef (m <sup>2</sup> ) | Area outside reef (m <sup>2</sup> ) | Average Tidal Range (cm)* | Spring Tidal Range (cm)* | Inundation time reef structure | N soil sample | % Clay ( $\pm$ SD) | % Silt ( $\pm$ SD) | % Sand ( $\pm$ SD) | Median grainsize, D50 ( $\mu\text{m}$ ) |
|-----------------------|-----------------|---------|-------------------------|------------------------|------------------------------------|-------------------------------------|---------------------------|--------------------------|--------------------------------|---------------|--------------------|--------------------|--------------------|---|
| Wadden Sea            | Schiermonnikoog | Mussel  | 53°28'42"N<br>6°13'29"E | -0.61                  | 8782                               | 17552                               | -124,104                  | -138,119                 | 0.72                           | 7             | 4.31<br>(0.80)     | 60.38<br>(12.94)   | 35.50<br>(13.63)   | 30.33<br>(28.46)                        |
| Wadden Sea            | Schiermonnikoog | Oyster  | 53°28'16"N<br>6°12'42"E | -0.06                  | 21537                              | 13557                               | -124,104                  | -138,119                 | 0.61                           | 7             | 3.65<br>(0.56)     | 47.04<br>(9.11)    | 49.49<br>(9.58)    | 54.03<br>(23.93)                        |
| Oosterschelde Estuary | Neeltje Jans    | Oyster  | 51°37'35"N<br>3°43'32"E | -0.48                  | 9079                               | 8570                                | -121,133                  | -123,152                 | 0.63                           | 6             | 3.28<br>(1.91)     | 40.63<br>(19.69)   | 56.11<br>(21.56)   | 139.69<br>(104.67)                      |

\* Tidal conditions from (Rijkswaterstaat 2012). Schiermonnikoog tidal data was obtained at the Schiermonnikoog station, Neeltje Jans tidal data was acquired at the Roompot binnen station.

## Water storage capacity in and around individual shellfish reefs

### *Retrieval of surface topography using Terrestrial Laser Scanning at the reef scale*

During low tide (when the reefs were fully exposed) A RIEGL VZ-400 terrestrial laser scanner (TLS) was used to obtain laser scans from four sides of the selected reefs to avoid gaps in the data due to shadowing (accuracy of 5 mm). The scans were made on June 20, February 21 and March 22, 2012, for the mussel reef and oyster reef at Schiermonnikoog and the oyster reef at Neeltje Jans, respectively. The data were georeferenced using white reflectors, which were geolocated using a differential global positioning system (dGPS). Thereafter, the scans were merged and cleaned to provide coherent xyz-point-cloud data of each location using the software package RiScan Pro (v1.7.2). The scan of the oyster reef at Neeltje Jans, the oyster reef at Schiermonnikoog and the mussel reef at Schiermonnikoog contained 54, 46 and 42 million xyz-points, respectively. The point clouds were rasterized to grids with 0.25 m cell size by calculating mean height of the xyz-points within each cell using the R package “raster” (Hijmans 2015).

Because the terrestrial laser scanner used in this study operates in the near-infrared part of the spectrum, measuring the bathymetry underneath the water surface in tidal pools is problematic, due to high absorbance of water at these wavelengths and diffraction of the laser beam. In fact, 12.9, 41.8, and 18.3% of the grids of, respectively, the oyster reef at Neeltje Jans, the oyster reef and mussel reef at Schiermonnikoog, contains no data (Figure 4.2 second row). Because the storage capacity analysis requires a raster without missing cells, we filled these gaps using inverse distance weighting interpolation to produce coherent elevation maps (Figure 4.2 third row). We expected that this interpolation would result in an underestimation of depression depth. Next, storage capacity was determined using MATLAB's imfill routine. In order to test whether our acquisition and rasterization procedure yields reasonable results, we compared the final raster to field measurements acquired using a dGPS for the Neeltje Jans site. A total of 117 wet points were compared revealing that there was a relatively good correspondence ( $R^2 = 0.63$ ) between the dGPS and the rasterized and interpolated TLS data. Only 7 out of 117 interpolated points turned out to be slightly deeper than dGPS values and the average underestimation of depression values was about 11 cm. Although these measurements are just a snapshot and do not say anything about pool stability (and hence ecological function), measurements of water depth development in and around the oyster reef reveal that water is retained during an entire low tide event and water loss due to drainage is limited within pools (see Appendix A.1 for methods and results).



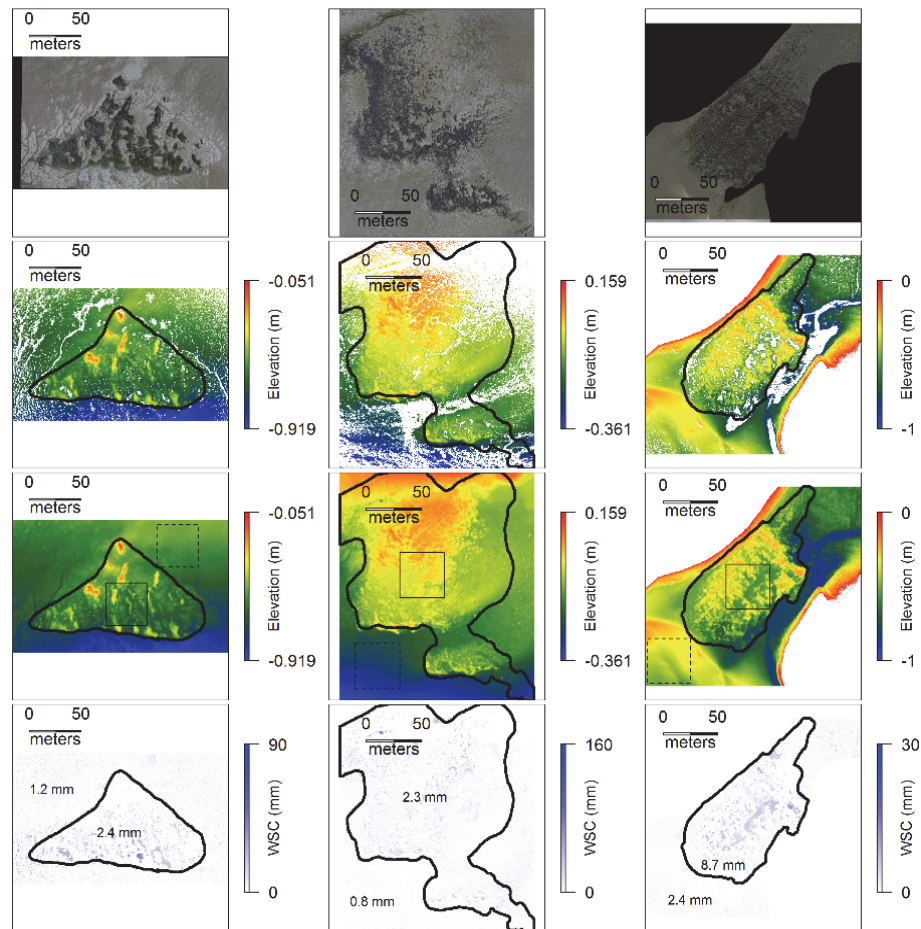


Figure 4.2 Elevation differences and water storage capacity across three shellfish reefs. Elevation maps before inverse distance weighting interpolation (top row, pixels with no value are white), IDW interpolated elevation maps (middle row) and water storage capacity (WSC) maps (lower row, with average ponding per zone) of the mussel reef at Schiermonnikoog (left column), oyster reef at Schiermonnikoog (middle column) the oyster reef at Neeltje Jans (right column). The black line indicates the outline of the shellfish reef. The squares (in the third row) indicate the regions used for landscape characterization (see supplementary material).

#### Comparing water storage capacity between reef and tidal flat area

To delineate reef area in the study site, aerial photographs (Figure 4.2 top row) were used to outline the convex hull of the shellfish reefs. Using these outlines, one part of the data was qualified as shellfish reef, while the other was qualified as bare mudflat without shellfish. MATLAB's `imfill` routine was used for estimating the storage capacity. The storage capacity within shellfish areas was compared with storage capacity outside of the reefs by calculating average storage capacity (in mm) (see Figure 4.2 bottom row).

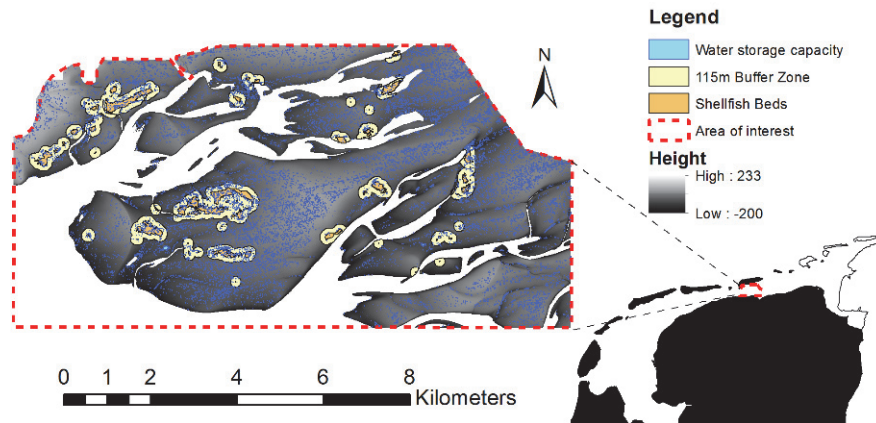


Figure 4.3 Bathymetry map within the region of interest south of the island of Schiermonnikoog as detected by LiDAR (dark-grey values represent low elevations, whereas light-grey values represent higher elevations). SAR detected shellfish reefs are indicated in orange and the 115-m buffer zones in green. The water storage capacity is depicted in blue.

### Water storage capacity at basin scale

#### *Retrieval of surface topography using airborne laser altimetry data at the basin scale*

To study how shellfish reefs influence water retention by influencing depression storage capacity at extensive spatial scales (basin scale), we used high-resolution laser altimetry (LiDAR) data of the intertidal regions in the Wadden Sea. We acquired 5-m resolution LiDAR data (2009) of the mudflats south of Schiermonnikoog from Rijkswaterstaat (the Dutch agency for water management) for this purpose (see Figure 4.3). Gaps in the data on the intertidal flats due to the scanning method and the presence of water were filled using inverse distance weighting, while the subtidal region was excluded from the analysis. A 3\*3 median filter was used to remove noise from the bathymetry data. Unrealistic ponding in small-scale channels was removed using a mask that was created in the regions where depressions were deeper than a standard deviation from the mean in a 7\*7 moving window. Afterward, the fill algorithm of ArcMap 10.0 was used to fill all depressions and the original bathymetry map was subtracted from this data. The resulting map is the water storage capacity map, from which volumes and areas were determined for all intertidal pools. It should be noted that resolution differences between TLS and large-scale LiDAR affect the estimated amount of water retention in depressions, that is, overall retention is underestimated slightly with LiDAR, but the ratios of retention between the different classes are about the same (see Appendix A.2).

### ***Shellfish reef delineation using SAR satellite remote sensing***

Shellfish reefs were mapped using Synthetic Aperture Radar (SAR) satellite imagery. Dual polarized (HH and HV) C-band (5.3 GHz) images from Radarsat2 were downloaded through the Dutch Satellite Data Portal website (Netherlands Space Office). Image acquisition was at 5:53 AM on 5/23/2012, and the satellite was in descending orbit. Water level was 1.34 m below sea level and wind direction was 56° at 6.8 m/s. NEST 5.0.12 was used to (1) calibrate the image following product specifications to sigma naught, (2) filter noise using Lee's refined adaptive local filter, (3) perform ellipsoid correction (resampling using bilinear interpolation), and (4) convert pixel intensities to decibels. To map shellfish, we used a multivariate logistic regression method incorporating both cross- and co-polarized channels following Chapter 2. SAR data resolution was approximately 12 m; but to match the LiDAR data, the resulting presence/absence map was interpolated to 5-m resolution using nearest neighbor interpolation and converted into polygons using the standard procedure available in ArcGIS 10.0.

### ***Determination of the spatial extent of increased storage capacity around shellfish reefs***

A spatial analysis was performed to find how the storage capacity differed at increasing distances from the shellfish reefs. ArcGIS 10.0 (buffer tool) was used to find the storage capacity at the different distance intervals from the shellfish reefs using the ponding map. Storage capacity values of individual pixels were then binned (by calculating average storage capacity) to raster resolution (5 m) in the statistical software package R (the minimum amount of observation for a bin was 5280 pixels). A cumulative sum control chart (CUSUM) (Page 1954) was used to investigate at which distance the storage capacity was significantly different from background (mudflat) storage capacity. Background storage capacity was defined as the storage capacity between 900 and 1000 m from the reef. Based on the CUSUM analysis, the data were subsequently divided into three groups: (1) reef (0-m distance), (2) buffer (elevated storage capacity on the intertidal flat surrounding shellfish reefs) and (3) intertidal flat (distances at which storage capacity was not elevated). These groups were used to investigate differences in total storage capacity within these groups (average amount of mm per pixel). In addition, the area and volume of each pool (connected by pixels which together make up a depression) was determined to investigate differences in pool size distributions between the three different zones.

### **Effect of surface topography on water storage capacity from simulated landscapes**

Semivariogram statistics (range, sill and nugget) were used to describe the spatial correlation structures of intertidal landscapes (Legendre & Legendre 2012) using

the gstat package in R (Pebesma 2004). The range parameter indicates the maximum lag distance over which there is still spatial correlation (see Appendix A.3), whereas the sill parameter describes the maximum amount of vertical variation found in a surface (similar to the total variance, see Appendix A.3). Different range (1–10 m, with steps of a meter) and sill (1–10 mm, with steps of a millimeter) parameters were simulated with exponential correlation structures. To show that the used simulation settings are realistic, semivariogram statistics (sill and range) were determined for parts of the TLS data of the individual reefs and mudflats studied (see boxes in Figure 4.2 third row). For further details on the methods and results of this characterization, we refer the reader to Appendix A.3. The simulated landscapes were 512\*512 cells large (with 0.25 m cell sizes) and replicated 50 times. Finally, the simulations were also performed with a 5% slope (on intertidal flats that is about the maximum slope one would expect), to assess the impact of slope on the water storage capacity.

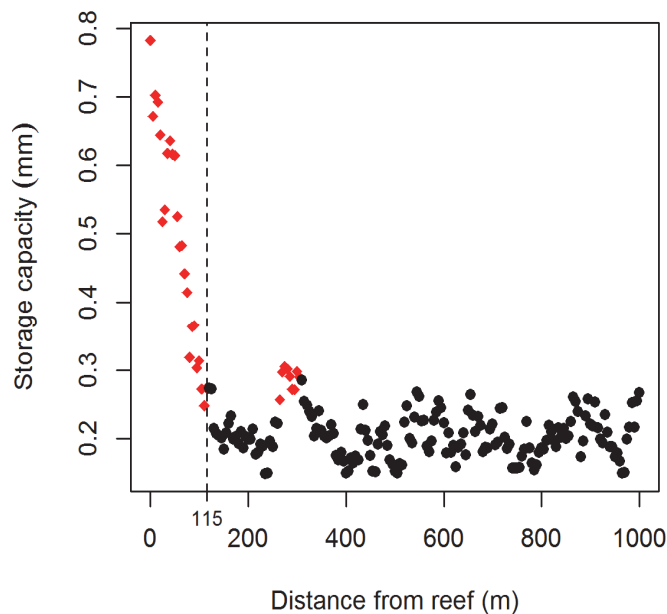


Figure 4.4 Average storage capacity values for different distances from the reef edges. 0 meters indicates ponding within the reef. The values are binned to 5 meter classes. The red triangles indicate significant changes from background ponding (last 20 points in this graph). The dotted line indicates the 115-meter zone used in the buffer analysis.

## Results

### Water storage capacity in and around individual shellfish reefs

We found clear local effects of the presence of ecosystem engineering shellfish on water storage capacity in the three individual reefs (Figure 4.2). Visual inspection of the elevation maps reveals that complex surface structures occur within the boundaries of the shellfish reefs (see Figure 4.2, 2nd and 3rd row). These structures are characterized by spatially alternating hummocks and depressions, in which water can be trapped (see Figure 4.2 bottom row). Although there were large differences between the three study sites, there was a consistent difference between the two different substrate types (shellfish and bare mud). Storage capacity inside the reefs is consistently higher than outside the reef: at Schiermonnikoog 2.4 mm (that is,  $2.4 \text{ L m}^{-2}$ ) in the mussel reef, and 2.3 mm in the oyster reef, and at Neeltje Jans 8.7 mm at the oyster reef, as opposed to 1.2, 0.8 and 2.4 mm outside the reefs, respectively.

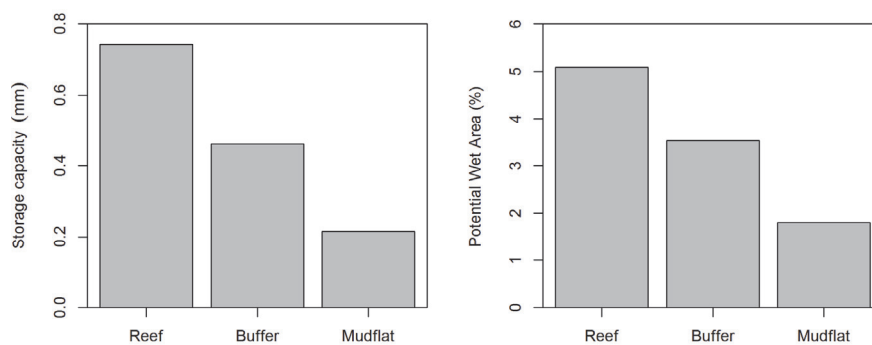


Figure 4.5 Left: Differences in water storage capacity in mm between the Reef, Buffer (115-meter zone) and Mudflat zone calculated from the LIDAR data. Right: Differences in percentage of potential wet area between the Reef, Buffer and Mudflat zone.

### Water storage capacity at basin scale

The combination of airborne laser altimetry (LiDAR) and satellite SAR data of the Wadden Sea area, allowed us to analyze 5,508 ha of intertidal flat, of which 105 ha was occupied by shellfish (approximately 2%). The storage capacity analysis revealed a total of 14,097 depressions that are potentially tidal pools, of which 488 were located in shellfish occupied areas. We found that oyster and mussel reefs increased storage capacity in the area directly surrounding the reef up to 115 m from the reef edge, that is, the storage capacity at distances between 0 and 115 m from the reef is significantly different from the background retention (see Figure 4.4). Within this zone of 115 m, there is a steady decrease in storage capacity with increasing distance from the shellfish reefs. Water storage capacity was largest within the shellfish reefs (at 0 m distance). Note that the CUSUM

analysis also reveals a small but significant peak at around 300 m, probably associated with periodic topographic features intrinsic to mudflat morphology. The periodic pattern was not caused by a lack of observations (the minimum amount of observations in a distance class was 5280).

The buffer zone that we have identified significantly extends the zone of influence of the shellfish reefs (see Figure 4.3). Within this buffer zone around the shellfish reefs, which is 495 ha large, 1472 tidal pools are located. Although the effects on water storage capacity in terms of total pool volume and surface area is strongest locally within the reefs, at extensive spatial scale up to 115-m storage capacity is still elevated compared to surrounding unaffected intertidal flats (Figure 4.5). Moreover, despite the fact that shellfish reefs only occupy a little less than 2% of the total area, up to 11% of the intertidal zone is influenced by shellfish by changing surface topography and influencing water retention by modifying the depression storage capacity (Figure 4.3). This implies that the footprint of the shellfish reefs is increased by more than 5 times, because of this long-range influence of the reefs on their surrounding habitat. In addition, while the highest storage capacity values are found within the reefs, the largest pools, both in terms of area and volume, are on average found in the buffer zone, followed by the reef pools and the smallest on uninfluenced mudflat (see Figure 4.6).

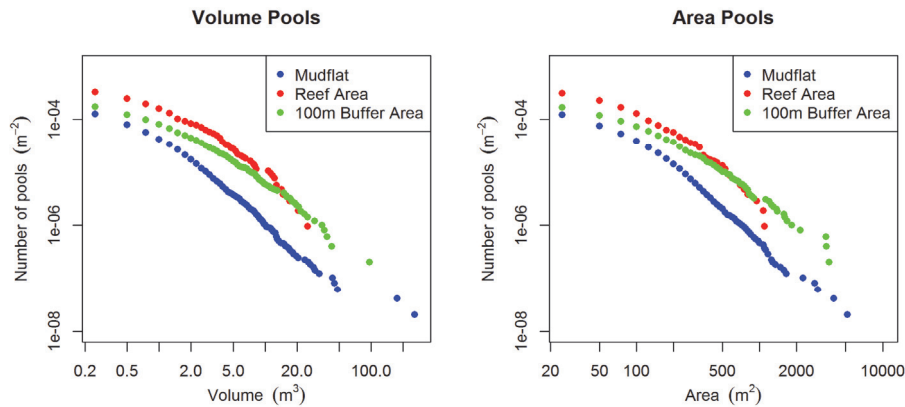


Figure 4.6 Water storage capacity in the three different classes (mudflat, reef area and 115m Buffer Area) results in pools with different sizes in terms of volume and area. The log-log plot reveals that the buffer-zone has the largest pools and the mudflat the smallest both in terms of area and volume.



### Effect of surface topography on water storage capacity from simulated landscapes

Water storage capacity was found to depend on landscape characteristics (vertical and horizontal complexity, and slope). Using a geostatistical analysis on the TLS data, the vertical surface complexity could be expressed by the sill and the horizontal surface complexity by the range of a semivariogram (Appendix A.3). Indeed, the shellfish reefs scanned using the TLS have a high vertical complexity and short range, as compared to the surrounding mudflat (see the Table in Appendix A.3).

The simulations reveal that the combined effect of vertical (as measured by the sill) and horizontal (range) complexity regulates the water storage capacity on simulated landscapes with different roughness characteristics (Figure 4.7). Storage capacity is positively influenced by the vertical component of the surface, whereas the horizontal component has a negative impact on the capacity to retain water. The 5% slope as opposed to a flat surface decreases water storage capacity overall and mainly affects landscapes with high range values (highly autocorrelated landscapes). This likely explains the apparent discrepancies between the empirically obtained storage capacity (with slope of intertidal flat) and those in the simulated landscape with similar landscape characteristics (without slopes). It also highlights that flat surfaces are influenced most by induced surface complexity with regard to capacity for water storage.

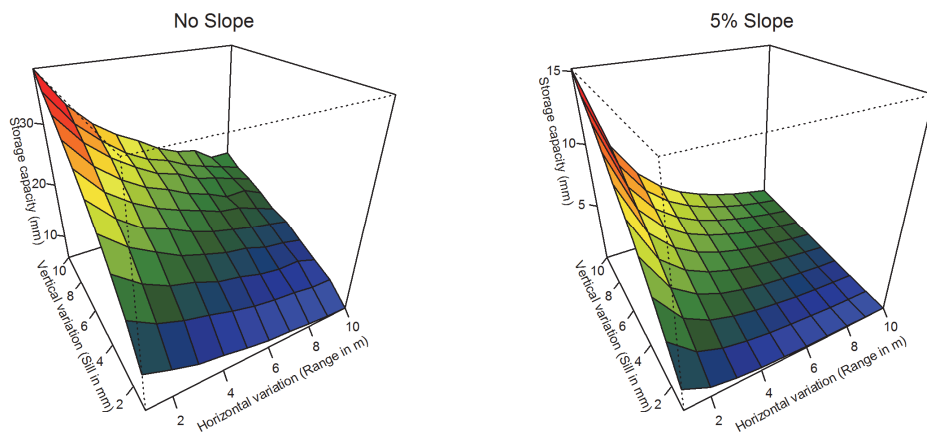


Figure 4.7 Mean predicted water storage capacity based on landscapes without a slope effect and one with a 5% slope. Different range and sill parameters (each combination is replicated 50 times) indicates a positive effect of sill and a negative effect of range on water storage capacity.

## Discussion

Ecosystem engineering has been recognized as an important structuring mechanism in ecological systems, affecting its functioning and stability both at local and extensive spatial scales (Jones et al. 1994; Jones et al. 1997; Hastings et al. 2007). The driving mechanisms have been mostly attributed to resource mediation (Lawton 1994; Wright & Jones 2006) and stress amelioration (Stachowicz 2001; Bruno et al. 2003). Here, we show for intertidal ecosystems how ecosystem engineering, that is, the addition of biogenic structure to the landscape, affects the capacity to retain water (and thereby possibly other vital resources) through the formation of tidal pools, thereby alleviating desiccation stress for many marine organisms. Within shellfish reefs, mussels and oyster reefs create vertical surface complexity through the formation of hummocks and hollows ((Gutiérrez et al. 2003; van de Koppel et al. 2005; Liu et al. 2012; Rodriguez et al. 2014), which has been suggested to be the result of spatial self-organization processes (van de Koppel et al. 2005; Liu et al. 2012). Locally, these hollows form tidal pools retaining significant amounts of water. Most strikingly, the effects were found to extend well beyond the physical borders of the shellfish reefs with significantly higher storage capacity values up to 115 m away from shellfish reefs. The size of these ponds close to the beds was found to be larger, as opposed to the ponds in and further away from the bed. This implies that, in the study area considered, the footprint of shellfish determined by increased storage capacity on the intertidal flats is more than 5 times their actual coverage, affecting up to about 11% of the intertidal area. Hence, ecosystem engineering shellfish can modify the functioning of the ecosystems to significant parts of the entire estuary due to local and spatially extended modifications of the surface structure.

Intertidal rock pools play a major role in determining ecosystem structure and functioning (Firth et al. 2014 and references therein), but much less is known about the importance and dynamics of soft-bottom pools and their relation to ecosystem engineering bivalves. Intertidal pools provide an extension of the vertical distribution of many species into areas which normally would be unsuitable for them because of desiccation stress (Metaxas & Scheibling 1993; Firth et al. 2013); they provide refuges from predators to a wide variety of intertidal organisms (White et al. 2014); they form a temporary shelter for migratory fish during low water, thereby effectively linking marine systems to freshwater systems upstream (Davis et al. 2014); they are used by many fish species as nurseries (Chargulaf et al. 2011). Different pool characteristics suit different species (White et al. 2014), for example, larger pools tend to be more stable in temperature, pH and nutrient levels and are thus more valuable to the widest range of species (White et al. 2014). Furthermore, the mosaic of different

substrate types created by shellfish at larger spatial scales promotes heterogeneity and provides a habitat for a wide range of species (Eklöf et al. 2014). The associated higher biodiversity can be expected to increase ecosystem stability (Tilman et al. 1996). Moreover, retention of resources in pools may contribute to increased system resilience through indirect mechanisms involving trophic interactions (Sanders et al. 2014). Likewise, the presence of pools associated with shellfish reefs allows species more sensitive to emersion (for example, due to desiccation stress) to persist within intertidal communities, both locally within the reefs and at larger spatial scale beyond their physical borders (that is, buffer zone), resulting in more diverse intertidal flats. This implies that biodiversity may be boosted by increasing landscape heterogeneity. This might hold especially for the buffer zone, since the pool volumes are larger, and thus probably more stable, beyond the borders of the reef.

The ability to create pools is not unique to shellfish reefs. In terrestrial systems, many mammals, such as elephants, rhinos, buffalos and warthogs, engage in wallowing, that is, they cover themselves in mud to protect themselves from the sun, parasites and it helps to disinfect wounds (Vanschoenwinkel et al. 2011). The resulting wallows trap rain water, resulting in ephemeral ponds that sometimes retain water for weeks due to compaction of soil (Polley & Collins 1984). Buffalo wallows have an important role in the dynamics and functioning of grassland vegetation (Polley & Collins 1984). Likewise, wallows created by alligators provide environments beneficial to a wide range of organisms (Campbell & Mazzotti 2004). Ponds in elephant footsteps harbor many aquatic insects (Remmers et al. 2016), and finally, peccary wallows have more value for anurans and biodiversity than naturally formed ponds (Beck et al. 2010). These examples underline the generality and importance of pond formation by ecosystem engineering species.

The effect of physical structure on ponding is largely dependent on the large-scale landscape structure. The simulations in this paper provide support for the idea that the effectiveness of structures to retain water depends for an important part on the height of the hummocks (sill), the horizontal scaling parameter (range) and the slope of the surface. The relation between retention and hummock height is positive, while the relation between retention and the range parameter as well as the overall tidal flat slope is negative. Reef depth along with the tidal range are important in determining how much vertical variation can be added to the landscape locally because these factors together determine a growth ceiling for reefs (Rodriguez et al. 2014; Walles et al. 2015). It can be expected that ponding effects are larger in lower locations in the intertidal with large tidal amplitudes, because the potential for vertical accretion of shellfish reefs is largest in these

locations. The tidal cycle is probably less important since the sediments remain saturated with moisture and infiltration is low ensuring the persistence of pools during low tide events. In general, the contribution of ecosystem engineering is likely more relevant on landscapes which naturally exhibit low surface complexity, whereas the contribution is less significant on rough surfaces (like for instance shellfish on rocky shores). Yet, a thorough exploration of the interaction between landscape topography and added surface complexity due to ecosystem engineering is missing in the scientific literature.

Here we approximated the capacity for water retention of a landscape in a very generic way, that is, water is potentially trapped in depressions creating tidal pools during low water, which remains stagnant thereafter. Water flows are not measured or modeled in detail. To more fully comprehend water retention around biogenic structures, we should also distinguish increased residence time of water due to hydrodynamic obstruction, which results in decreased flow rates. The occurrence of engineered structure has important implications for regional hydrodynamics caused by tidal flow (van Leeuwen et al. 2010). Biogenic material, such as shellfish reefs, may slow down flows due to friction, or reroute water entirely due to full obstruction which has consequences for residence time of water in the landscape (Lenihan 1999). The spatial arrangement of geomorphological features on a mudflat such as sandbars, gullies and mud deposits may very well depend on the spatial distribution of biogenic structures such as reefs created by shellfish (van Leeuwen et al. 2010) and vice versa since they are coupled by the prevailing hydrodynamics. Yet, our simple approach is a good first approximation to get general insights into how ecosystem engineering can affect ecosystem functioning by modifying water retention.

In our study, we used near-infrared TLS and airborne LiDAR to assess depression storage capacity. Our assessments of the capacity for water storage were conservative, as these systems could not measure topography under water. LiDAR systems that use green light are better able to penetrate water and can be used to measure topography under water (for example Hannam & Moskal 2015). Further research that assesses actual stagnant water ponding could incorporate LiDAR techniques combined with VNIR (visible and near-infrared) or TIR (thermal infrared) photography from unmanned aerial vehicles to delineate ponds over the tidal cycle.

Our findings highlight that modification of the physical landscape by ecosystem engineering, causing increased water storage capacity, can be significant and should be considered in future research to unravel the implications for ecosystem structure and functioning, as well as biogeomorphological processes. In intertidal systems, this extended engineering might be beneficial to adjacent ecosystem

engineering species resulting in facilitating cascades (Gillis et al. 2014). Such facilitation interactions are especially beneficial for improving the resilience of ecosystem-based coastal defense practices (Temmerman et al. 2013). The importance of spatially extended water impoundment for biodiversity, as well as local and cross-system resilience, should be the focus of future research.

Shellfish reefs increase water storage capacity |







## CHAPTER 5

---

### Satellite remote sensing reveals basin-wide boost of phytobenthos due to shellfish reefs

*To be submitted*

*Sil Nieuwhof, Johan van de Koppel, Britas Klemens Eriksson,  
Jim van Belzen, Han Oloff, Jasper Donker, Peter M.J. Herman  
and Daphne van der Wal*

#### Abstract

Reef building organisms such as mussels and oysters have a profound effect on the primary production fueling important microbial and geochemical processes, both in and beyond the reef itself. Yet, the spatial extent of this effect is unknown, limiting our understanding of the importance of shellfish reefs in estuarine ecosystems. Based on a statistical model of microphytobenthos concentrations across the Dutch Wadden Sea from satellite remote sensing, and information on elevation, currents and waves, we reveal that shellfish reefs may affect the presence of microphytobenthos of up to 40% of the tidal flat surface. Microphytobenthic biomass, as reflected by the Normalized Differential Vegetation Index (NDVI), was found to be increased by 15% in close proximity of the reefs, logarithmically declining within a distance of about 1 kilometer from the reefs. This effectively accumulates to more than an order of magnitude difference between the ecological footprint of shellfish reefs compared to the space directly occupied by reef structure and an increase in microphytobenthos concentrations of 3% across the intertidal of the Dutch Wadden Sea. The largest facilitative effects were observed around mixed reefs, and the smallest in oyster reefs. Our study reveals the keystone importance of shellfish reefs for estuarine food webs, highlighting that human exploitation of shellfish reefs will have large-scale repercussions for estuarine ecosystems.

## Introduction

Keystone species have a disproportionately large effect on the ecosystem despite of their small numbers (Paine 1969). These species have an important role in ecosystems because 1) they form an essential link in trophic webs, 2) they perform vital ecosystem services or 3) because they are able to modify the ecosystem physically (Mills et al. 1993). The ability of organisms to modify the abiotic environment is commonly referred to as ecosystem engineering (Jones et al. 1997; *sensu* Jones et al. 1994). In coastal environments, ecosystem engineers are able to mediate resources and/or alter the physical state of the system locally, but also beyond the borders of the zone that is physically occupied (for an overview see van de Koppel et al. 2015; Donadi, Westra, et al. 2013; van der Zee et al. 2012; Gillis et al. 2014; Engel et al. 2017; Walles et al. 2014; van de Koppel et al. 2006). This is often referred to as spatially extended ecosystem engineering. Ecosystem engineering effects are non-trophic by definition, yet they still can influence food webs indirectly (van der Zee et al. 2015; Sanders et al. 2014) by mediation of resources to plants and animals (Lawton 1994; Wright & Jones 2004).

Although long-distance interactions have apparent consequences for shaping ecosystems, evidence for such interactions is typically acquired from a limited number of localized observations (Kerr & Ostrovsky 2003). As a result, the contribution of these long-distance interactions to the functioning of entire ecosystems at larger scales remains poorly understood. In general, it is difficult to quantitatively estimate the extent of the ecosystem effect of cross-system subsidies, animal migration and physical state change, based on data from the experiments or observational transects by which the presence of the effect was originally established (van de Koppel et al. 2015; Donadi, van der Heide, et al. 2013; Engel et al. 2017). High-resolution synoptic spatial data at the landscape scale are required to establish the scale and extent of the effect of ecosystem engineers. Such data are essential for impact assessments of natural or human-induced losses of such ecosystem-engineering on ecosystem services; both in sustaining natural production and biodiversity, but also for sustained human use and exploitation of natural resources.

On coastal sediments, reef building bivalves are ecosystem engineers that alter hydrodynamic conditions, change sediment properties and the associated community of organisms locally (Bouma et al. 2009; Meadows et al. 2012 and references therein). However, the effect of bivalve reefs is not limited to the physical boundaries of the reef structure, but can transcend to significant distances beyond its local footprint (van der Zee et al. 2012; Donadi, Westra, et al. 2013; Walles et al. 2014; Engel et al. 2017 and Chapter 4), resulting in long-

distance interactions with other species. These effects are caused by 1) a more benign hydrodynamic environment caused by the wave and flow attenuating effects of the rough surfaces created by the shellfish (Borsje et al. 2011; van Leeuwen et al. 2010) and 2) subsidy of nutrient rich fine particulate matter through the production of faeces and pseudo-faeces by the bivalves, which accumulate on adjacent mudflats (Widdows & Brinsley 2002). For example, reefs of blue mussels (*Mytilus edulis*) and Pacific oysters (*Crassostrea gigas*) have been found to increase mud content (Kröncke 1996; van der Zee et al. 2012), sedimentation (Walles et al. 2014), water retention (Chapter 4) and microphytobenthos biomass on adjacent mudflats (Donadi, van der Heide, et al. 2013; Engel et al. 2017). As a result these reefs mediate resource-consumer interactions (van der Zee et al. 2012; Donadi, Westra, et al. 2013) and primary production (Engel et al. 2017) over extended scales. Microphytobenthos is a key component in total primary production of shallow water estuarine systems and is the major contributor of energy to higher trophic levels (Middelburg et al. 2000; Kang et al. 2006; De Jonge & Van Beusekom 1992; Christianen et al. 2017). Although long-distance interactions involving reef building shellfish have been qualitatively demonstrated, the extent has not yet been quantified at the basin scale. This limits the valuation of shellfish reefs as a driver of intertidal community structure, both for fundamental understanding of tidal flat organization as in the assessment of the potential effect of human exploitation of shellfish on primary production and food web structure.

In this study, we aim to quantify the spatial extent and magnitude of microphytobenthos facilitation by mussel-, oyster- and mixed (mussel and oyster) reefs at local and basin scale in the Dutch Wadden Sea. We used *in situ* and satellite data to investigate the spatial distribution of microphytobenthos in relation to a number of shellfish reefs. We also investigated the effect of shellfish reefs on microphytobenthos at the basin scale. We hypothesize that spatially extended ecosystem engineering effects of shellfish beds emerge when corrected for trends of microphytobenthos in response to elevation and hydrodynamics (currents, waves). We further hypothesize that oysters and mussels have different facilitative effects on microphytobenthos, e.g. oyster reefs are typically rougher than mussel beds (Chapter 2) and are thus expected to reduce hydrodynamic forces more and they are also situated deeper in the intertidal (Bouma et al. 2014).

## Materials and Methods

### Study site

The Wadden Sea is a shallow mesotidal basin located in the south east of the North Sea (Appendix B.1), bordered by the Dutch, German and Danish mainland coast and fringed by the Frisian Islands. The Dutch Wadden Sea covers an area

of ca 2550 km<sup>2</sup>, half of which is intertidal area. The unique dynamics in islands, sandflats and gullies and its diversity of life (Lotze 2005; Reise and others 2010) earned the Wadden Sea a place on UNESCO's world heritage list. The mean tidal amplitude ranges between 1.34 m near Den Helder in the west to 2.09 m near the Ems estuary in the east. The area studied here comprised the Dutch Wadden Sea between the islands of Texel and Schiermonnikoog. Mussels disappeared from the Wadden Sea due to intensive shellfish fishery in combination with bad recruitment during the 80s and early 90s (Nehls et al. 2009; Beukema & Cadée 1996). As a result fisheries have been restricted to the subtidal zone since 1991 (Nehls et al. 2009), making the Dutch Wadden Sea ideal to quantify spatial ecosystem engineering effects. Oysters are invasive in the Netherlands, and were first introduced in the Dutch Wadden Sea in the 1970s. Vast oyster reefs established throughout the Wadden Sea in the 1990s (Fey et al. 2009). The ecological implications, especially at spatially extended scales, remain unclear.

## Local effects

### *Field sampling*

Four nearshore shellfish reefs were sampled *in situ* along replicate transects (see Figure 5.1) to investigate the suitability of such methods to investigate spatially extended ecosystem engineering. At Texel, a mussel reef (24<sup>th</sup>-25<sup>th</sup> of June 2013 at 53.158°, 4.891°), an oyster reef (24<sup>th</sup>-25<sup>th</sup> of June 2013 at 53.146°, 4.904°) and a control on bare sand flat (2<sup>nd</sup> of July 2013 at 53.153°, 4.898°) were sampled. Each site contained three transects, sampled at ca. 60 m intervals. Each transect at the mussel reef and control site contained 8 sample stations, while at the oyster reef, transects contained only 6 stations, because of a gully at its seaward side. At Schiermonnikoog, 3 transects were placed over a mussel reef (23<sup>rd</sup>-24<sup>th</sup> of June 2013 and 3<sup>rd</sup>-5<sup>th</sup> of July 2013 at 53.468°, 6.225°) and a bare sand flat (23<sup>rd</sup>-24<sup>th</sup> of June 2013 and 3<sup>rd</sup>-5<sup>th</sup> of July 2013 at 53.468°, 6.231°), with 10 stations (at 50 m to 200 m intervals) each.

In addition, a mixed reef (23<sup>rd</sup>-24<sup>th</sup> of June 2013 and 5<sup>th</sup> of July 2013 at 53.465°, 6.183°) and a second bare sand flat (23<sup>rd</sup>-24<sup>th</sup> of June 2013 and 5<sup>th</sup> of July 2013 at 53.468°, 6.194°) were sampled, with 6 stations at intervals ca. 150m apart. Furthermore, two offshore locations were sampled with 20 samples each placed randomly around the shellfish reefs (see Appendix B.1). One is located between the islands of Texel and Vlieland (6<sup>th</sup> of June 2013 at 53.186°, 4.961°) and the other south of the island (but offshore) of Schiermonnikoog (3<sup>rd</sup> of June 2013 at 53.443°, 6.216°).

## Spatially extended phytobenthos facilitation by shellfish reefs

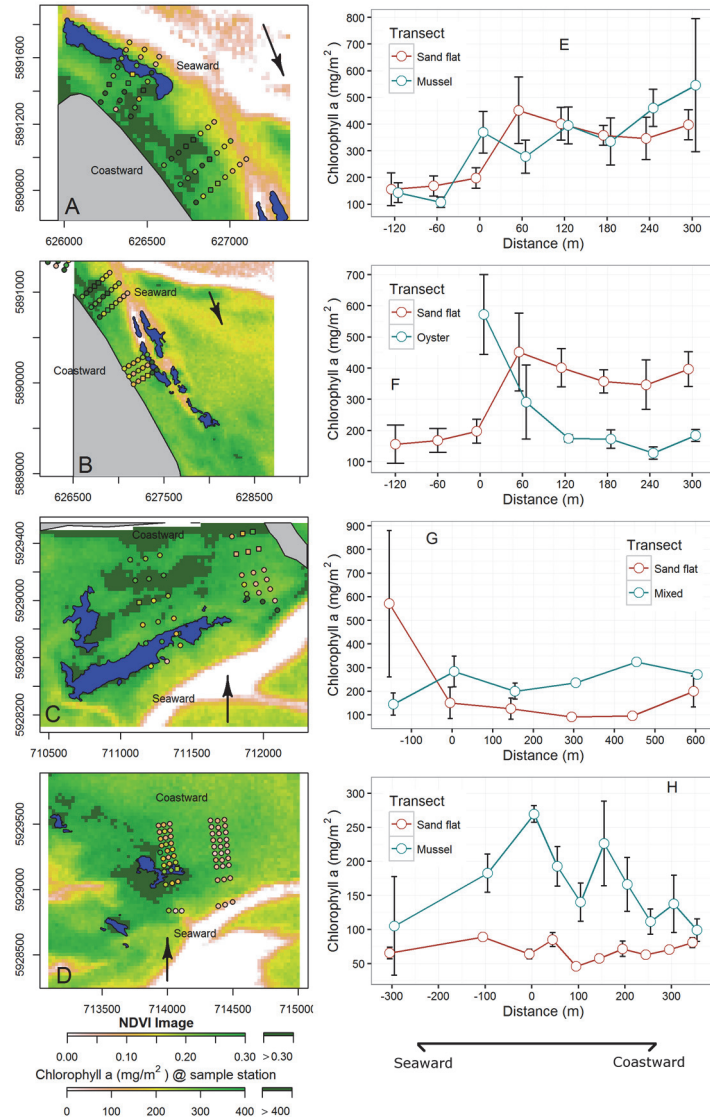


Figure 5.1 Comparison of transect data versus remotely sensed data. NDVI from remote sensing (background colors NDVI > 0.3 is regarded as macro-algae (darkgreen) and NDVI < 0 is regarded as water(white)) and in situ chlorophyll-a (point colors, square indicates > 10% cover macro-algae in the 1 m<sup>2</sup> sampling quadrant) of the shellfish reefs bare sand flats (A) Mussel reef at Texel, B) Oyster reef at Texel, C) Mixed reef at Schiermonnikoog and D) Mussel reef at Schiermonnikoog, the arrows indicate the general direction of the incoming tide). Comparison of chlorophyll-a concentration over shellfish transects (dots in A,B,C and D) and bare sand flat transects, with error bars indicating standard error for the (E) Mussel reef at Texel, F) Oyster reef at Texel, G) Mixed reef at Schiermonnikoog and H) Mussel reef at Schiermonnikoog).

The sample stations were located using Garmin's GPSmap 78 (accuracy of 1.5 m with clear sky conditions). At each sample station a 1m<sup>2</sup> frame was placed. Macroalgae cover (%) was estimated in each plot. Within each plot, 3 samples of the top 1 cm of sediment were pooled to determine chlorophyll-a concentrations (µg/g) of the sediment. In addition, a sediment sample was collected of the top 3 cm at each of the sampling stations to determine bulk density (g/cm<sup>3</sup>). A TRIOS RAMSES spectroradiometer (sensitive within 320-950 nm, spectral resolution of 3.3 nm ± 0.3 nm) was used to measure hyperspectral reflectance spectra of the sediment in triplo. Surface reflectance was measured at nadir as the ratio of upwelling to down-welling radiance. Down-welling radiance was measured using a clean white polystyrene plate. The surface reflectance spectra of each station were calculated by averaging the three replicates. These spectra were used to compute the Normalized Difference Vegetation Index ( $NDVI = (NIR - R)/(NIR + R)$ ), where NIR: 770-900nm and R: 630-690nm to match the bandwidth of the spectra measured by the satellite (see section Satellite image processing). Finally, *in situ* NDVI was related to the chlorophyll-a concentration of the sediment.

#### ***Laboratory analysis***

Chlorophyll-a samples of the sediment were kept cool and dark in the field in a cool box and at -20 °C during the field campaign (max 72 h), and then stored at -80 °C in the laboratory prior to further analysis. For the two offshore locations, chlorophyll-a concentrations of the sediment (µg/g) were determined using both high-performance liquid chromatography (HPLC) and spectrometry. Since both methods performed equally well in determining chlorophyll-a content ( $R^2 > 0.97$ ,  $n=39$ ), chlorophyll-a was measured using the spectrometry method only for all other samples. Sediment chlorophyll-a concentrations (µg/g) were converted to concentrations per unit surface area (mg/m<sup>2</sup>) using dry bulk density of the sediment obtained by dividing the dry weight of the sediment sample by its volume of 19 cm<sup>3</sup>.

### **Large scale effects**

#### ***Satellite image processing***

Air- and space borne remote sensing have been shown to be capable of assessing microphytobenthic biomass at vast spatial scales (e.g., Combe et al. 2005; van der Wal et al. 2008; van der Wal et al. 2010; Benyoucef et al. 2013; Kazemipour et al. 2012). In this study, it was used to quantify the facilitative effect of reef building bivalves on microphytobenthos. Chlorophyll-a (an important pigment) absorbs light mostly in the red part of the electromagnetic spectrum. Using multispectral images, NDVI can be computed by using the surface reflectance in the red (R) and near infrared (NIR) bands. This index correlates well with

microphytobenthic biomass, with higher NDVI values associated with high microphytobenthic biomass, if there is no interference from macroalgae or higher plants (van der Wal et al. 2008); the latter show both absorption in the red and high reflection in the NIR, resulting in higher values for NDVI (van der Wal et al. 2010). Although microphytobenthos mats can be patchy at the cm scale, NDVI is largely insensitive to sensor resolution (Ibrahim et al. 2009).

A single acquisition level L1R UK-DMC-2 image was downloaded from the Dutch Satellite Portal. UK-DMC-2 is a multi-spectral sensor operated by DMC International Imaging (DMCii). The image used was acquired on the 2<sup>nd</sup> of June 2013 at 9:27:39 AM UTC with an incidence angle of 13.89°. It has a nominal resolution of 22 meters and operates in three bands (NIR: 770-900nm, Red: 630-690nm and Green: 520-600nm).

Radiometric calibration was performed following the product manual (Crowley 2010). First, pixel values were converted to radiance levels ( $\text{Wm}^{-2}\text{sr}^{-1}\mu\text{m}^{-1}$ ) using bias and gain values obtained from the metadata. Next, radiance levels were converted to top of atmosphere reflectance using product metadata (Crowley 2010) and the earth-sun distance (NASA n.d.). Atmospheric correction and conversion to surface reflectance values was applied using the 6S radiative transfer model (Vermote et al. 2006), setting solar and sensor geometrical conditions as described in the image metadata. A midlatitude summer maritime aerosol model was used with 30 kilometer visibility (based on a KNMI weather station at Vlieland for both 9 and 10 am UTC) to estimate aerosol optical thickness. A constant filter function was used for all bands. The image was georeferenced to a basemap in ArcGIS 10.1 using 26 well distributed features such as bridges and buildings and resampled using a 2<sup>nd</sup> order polynomial and projected to UTM/WGS84 (zone 31) with a resolution of 25 m using bilinear interpolation. Two spectral indices were calculated, namely the NDVI (see above) to estimate algal biomass, and the Normalized Difference Water Index ( $\text{NDWI} = (\text{G}-\text{NIR})/(\text{G}+\text{NIR})$ , where G is the green band) to locate wet pixels (McFeeters 1996). The image was clipped east of the island of Schiermonnikoog to avoid areas with scattered clouds. Pixels with  $\text{NDWI} > 0$  and  $\text{NDVI} < 0$  were discarded to eliminate areas covered by water. Following Méléder and others (2003), locations with  $\text{NDVI} > 0.3$  were discarded to eliminate areas covered by shellfish and/or macroalgae. Water, shellfish and macroalgae in mixed pixels could not be excluded by these methods. Pixels closer than 25 m from shellfish reefs were disregarded to reduce the chance of including shellfish in pixels. Similarly, pixels within 100 meter from land were excluded to eliminate effects of tarmac or vegetation.



### *Modeling and GIS*

We used shellfish distribution data (TMAP, acquired and compiled by Wageningen Marine Research) from spring 2012 (van den Ende et al. 2012; Folmer et al. 2014). The data was provided as a polygon layer with attributes describing the type of shellfish reef (mussel dominated, mixed reef and oyster dominated). Intertidal elevation was obtained from 5m resolution LiDAR (Light Detection And Ranging) data provided by Rijkswaterstaat. The LiDAR data was acquired by Rijkswaterstaat between 2009 and 2013. Average monthly wind/wave data (based on hourly wind and water level data, provided by KNMI and Rijkswaterstaat, respectively) were compiled using the SWAN (version 40.91AB) model (Donker 2015). Average median near reef orbital velocities ( $\text{ms}^{-1}$ ) were computed for the years 2010 to 2013 from these monthly data. The wave model provided data on a curvilinear grid with a resolution between 70 and 300 meter (Donker 2015). Current velocity ( $\text{ms}^{-1}$ ) were modelled for 2009 to 2010 using GETM (Duran-Matute et al. 2014). The current velocity model uses a regular grid with a resolution of 200 m. Output of the two models was resampled to match imagery resolution using natural neighbor interpolation in ArcGIS 10.1. Effects of shellfish reefs on hydrodynamics were likely not included in wave and current modeling, because the spatial resolution was too coarse to include the effects of such small scale bathymetric changes. Finally, a raster with Euclidean distances to the nearest shellfish reefs was calculated using the Euclidean Allocation tool in ArcGIS 10.1.

### *Statistical analysis*

Boosted Regression Trees (BRT) (Elith et al. 2008) was used to investigate the effect of distance from a shellfish reef (either all reefs, mussel reefs, mixed reefs and oyster reefs, respectively) in combination with elevation, waves and currents on NDVI. The method takes into account any non-linear relationships or interactions between the variables. BRT is an ensemble method in the sense that it combines multiple weak models to do predictions. The method combines decision trees (e.g. De 'ath & Fabricius 2000) with boosting (a method that improves predictive performance by iteratively combining trees and minimizing a loss function) (Elith et al. 2008). The model was fit on a subset of 100,000 observations using 10,000 trees, shrinkage set at 0.0025, tree complexity set at 4, and 10 cross-validation folds and ran using the R package 'gbm' (Ridgeway 2015). The best performance was not achieved using this number of trees, but more trees only included noise on the main trend and changed variable importance estimates just slightly (up to 5%). More importantly, different subsets of observations and more trees in the model showed no significant changes in the main trend and these settings allowed us to explore the partial effects of distance on NDVI exhaustively in a reasonable amount of time. Spatial autocorrelation is

strictly not an issue for BRT modelling, but might still influence the partial dependence estimate of NDVI on distance. To solve this, a residual auto-covariate (RAC) (Crane et al. 2012) was used to remove autocorrelation from the residuals. To compute the RAC, BRT was first fit with all the environmental variables included as predictors. The RAC was subsequently computed on the residuals by calculating the mean of the residuals in a moving window of 3\*3 pixels. Finally, BRT was run with the RAC included as one of the predictor variables.

The partial dependence of NDVI on Distance to shellfish reef can be modelled by a logarithmic relationship in the form  $NDVI = a * \ln(Dist) + b$ , where “Dist” is the distance to shellfish reefs. The logarithmic regression was performed up to 2000 meters, since at larger distances the partial prediction by the BRT becomes unstable due to a low number of observations. The logarithmic relationship was subsequently used to predict the magnitude of NDVI increase in relation to distance from a shellfish reef, and to visualize the effects of shellfish in the Wadden Sea. We considered 1000m from the reefs edges as the influential threshold (the logarithmic relationship is more or less flat from this distance), and assumed reefs had no effect on NDVI beyond this distance. Results were then converted to estimates of the spatial extent of the facilitative effect of shellfish beds on microphytobenthos using the relationship between *in situ* chlorophyll and *in situ* NDVI.

## Results

### Local effects

The ground surveys indicate that within the shellfish beds (i.e., at 0 m along the transect), chlorophyll-a contents are always higher than at the sandflats (Figure 5.1), suggesting local facilitation of microphytobenthos within the beds. Spatially extended facilitation effects are less obvious at this localized scale of the reef. At the Texel site, *in situ* chlorophyll-a increases towards the coast, regardless of the presence of the mussel reef (Figure 5.1A and B). Around the oyster reef at the Texel site, *in situ* chlorophyll-a decreases gradually with distance from the reef, but overall chlorophyll-a contents around the bed are typically lower than on the sandflat. Around the mixed reef (Figure 5.1C & G) and mussel reef (Figure 5.1D and H) on Schiermonnikoog, chlorophyll-a levels were typically higher than compared to the sandflat. The observations are largely supported by the NDVI retrieved from the satellite image. Increased NDVI seems to extend in the direction of the prevalent flow at Texel (Figure 5.1 A & B). Around the reefs at Texel (Figure 5.1A and B) and around the mixed reef at Schiermonnikoog (Figure 5.1C), NDVI seems to be suppressed by flow divergence. Spatially extended facilitation might occur around the mussel reef at Schiermonnikoog (Figure

5.1D), because high NDVI levels are observed around the reef in all directions (Figure 5.1D).

The relationship between area normalized *in situ* chlorophyll-a and *in situ* NDVI (measured with the spectroradiometer) for the NDVI region considered ( $0 < \text{NDVI} < 0.3$ ) was modelled adequately using a linear function:  $\text{chl\_a (mg/m}^2\text{)} = 2025.81 * \text{NDVI} - 50.6$  ( $R^2=0.43$ ,  $F_{1,181}=138.9$ ,  $p<0.05$ ) (see Appendix B.3). This equation is used to estimate the effects of shellfish on area normalized *in situ* chlorophyll-a. *In situ* chlorophyll-a was not modelled as well using satellite NDVI (see Appendix B.3), likely due to a time and spatial scale mismatch in field survey and image acquisition, and due to interference of surface water and macroalgae in the satellite pixels.

### Large scale effects

The basin-wide GIS analysis based on the distance and NDVI data retrieved from the satellite image reveals that NDVI is on average elevated close to shellfish reefs and lower elsewhere (see Figure 5.2). For all reefs together, this NDVI enhancement is approximately 0.04 above the baseline of  $\text{NDVI}=0.18$ , roughly a 17% increase (Figure 5.2A). These effects are strongest close to mussel reefs, lower near mixed reefs and relatively weak close to oyster reefs (Figure 5.2B).

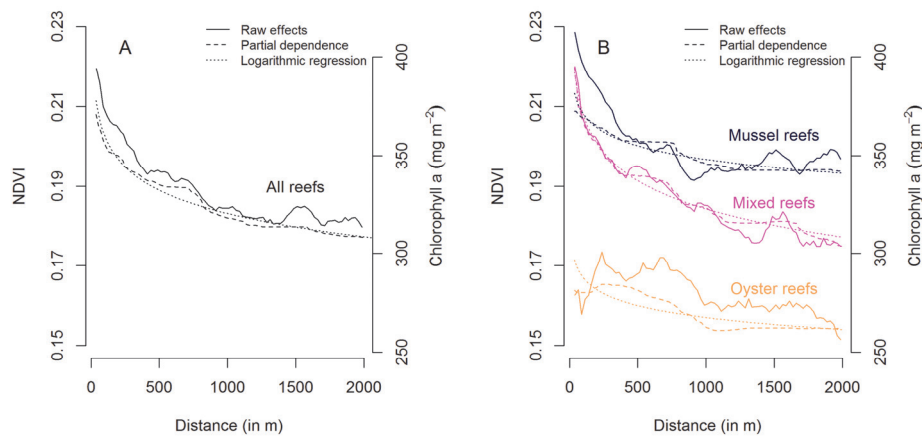


Figure 5.2 Mean NDVI with distance from the nearest shellfish reef, calculated with 25m bins (Raw effects), the partial dependence plots of NDVI on Distance to shellfish reefs as calculated using BRT and the logarithmic regressions on the partial dependence. A) shows the effects of all shellfish reefs, B) distinguishes mussel, mixed and oyster reefs. The right axis shows modelled chlorophyll-a concentration in the sediment based on *in situ* NDVI data. The logarithmic regression equations on the partial dependence of NDVI as a function of Distance from shellfish reef are:  $\text{NDVI (all reefs)} = -0.0085 * \ln(\text{Distance}) + 0.242$ ,  $R^2 = 0.97$ ;  $\text{NDVI (mussel reefs)} = -0.0049 * \ln(\text{Distance}) + 0.231$ ,  $R^2 = 0.93$ ;  $\text{NDVI (mixed reefs)} = -0.0103 * \ln(\text{Distance}) + 0.255$ ,  $R^2 = 0.97$ ;  $\text{NDVI (oyster reefs)} = -0.0043 * \ln(\text{Distance}) + 0.187$ ,  $R^2 = 0.71$ .

The boosted regression tree analysis further reveals that elevation is the most important variable in explaining NDVI (microphytobenthos), followed by currents. Distance to shellfish reefs and waves have comparable importance in explaining NDVI. Shellfish reef types (mussel, mixed and oyster) show different effects: currents explained most variation in NDVI around mussel beds, elevation explained most variation around mixed beds, and distance from shellfish reefs was most important in explaining NDVI around oyster reefs (see Table 1). The partial dependence of NDVI on distance from shellfish reefs based on the BRT, corrected for elevation, current velocity and waves, is similar to the observed raw effects (relationship between NDVI and distance from shellfish reefs not corrected for abiotics) of this relationship, indicating the effect of the shellfish reefs is relatively independent from these other variables. Near mussel reefs there is a co-occurrence based on overlap in preferred habitats as indicated by divergence of the partial dependence and the raw effects (Figure 5.2B), but even here there is facilitation by the reefs. At the scale of the system analyzed, abiotic environmental predictors are more important than shellfish reef presence (Table 5.1). For oyster reefs, the effect of distance to reefs on NDVI is small (Figure 5.2B). However, the BRT indicated that the distance variable is the most important for oyster reefs. The limited range in inundation for the intertidal zone around oysters (all relatively low inundations) compared to intertidal zones allocated to the other reefs (see Appendix B.4) likely contributed to this effect.

Table 5.1. Results from the boosted regression trees. Within the variable importance columns (in terms of %) the most important variable is depicted in bold font.

| Dataset | Model | Explained Deviance | Variable importance (%) |              |       |              |              |
|---------|-------|--------------------|-------------------------|--------------|-------|--------------|--------------|
|         |       |                    | Elevation               | Currents     | Waves | Distance     | RAC          |
| All     | ENV   | 0.39               | <b>40.09</b>            | 31.64        | 14.06 | 14.22        |              |
|         | RAC   | 0.97               | 14.09                   | 13.48        | 4.42  | 3.77         | <b>64.24</b> |
| Mussel  | ENV   | 0.49               | 29.95                   | <b>54.15</b> | 4.54  | 11.36        |              |
|         | RAC   | 0.96               | 14.65                   | 24.33        | 0.80  | 3.68         | <b>56.55</b> |
| Mixed   | ENV   | 0.41               | <b>38.66</b>            | 30.45        | 13.37 | 17.52        |              |
|         | RAC   | 0.96               | 15.33                   | 12.81        | 4.03  | 4.55         | <b>63.28</b> |
| Oyster  | ENV   | 0.35               | 24.08                   | 24.49        | 16.76 | <b>34.67</b> |              |
|         | RAC   | 0.96               | 7.42                    | 6.64         | 4.71  | 8.12         | <b>73.11</b> |

Based on the 1000m influence threshold, the potential ecological footprint is increased over an order of magnitude (~20 times). This maximum extent covers approximately 40% of the intertidal Wadden Sea, compared to the 2% physical footprints of the reefs (Figure 5.3). This translates to an average increase in chlorophyll-a concentration by 3% for the Dutch intertidal Wadden Sea, using the *in situ* relationship between chlorophyll-a and NDVI (see Appendix B.3).

Figure 5.4 visualizes the potential area in which NDVI is boosted by shellfish reefs. The western and eastern part of the Dutch Wadden Sea have different shellfish reef densities (1 and 3% of the intertidal respectively), as a result the influenced zone may be expected to be larger than the average 40% in the eastern Wadden Sea and lower in the western Wadden Sea. This is assuming that the same model relationships based on the total Wadden Sea apply to the western and eastern Wadden Sea separately as well.

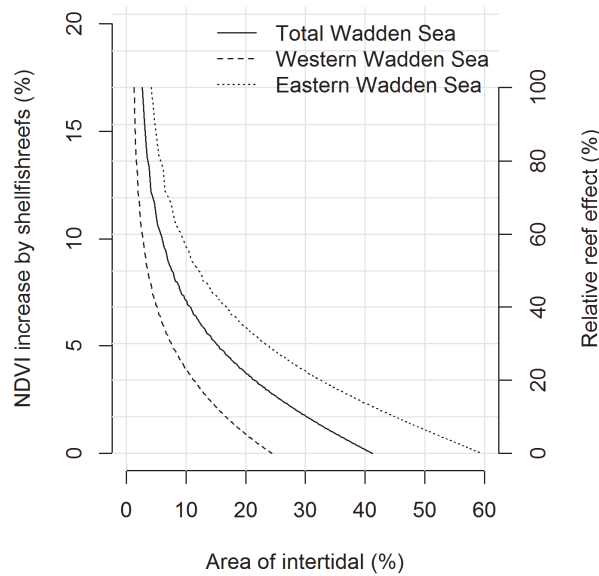


Figure 5.3 The percentage increase in NDVI by shellfish reefs over intertidal area affected is summarized for the total, the western- and the eastern Wadden Sea.

## Discussion

Recent studies established that shellfish reefs facilitate microphytobenthos up to considerable distances beyond the edge of the physical reef (Donadi, Westra, et al. 2013; Engel et al. 2017). However, the number of reefs that is investigated is typically low which might result in idiosyncratic outcomes, and limited understanding of the importance of primary production facilitation by shellfish reefs at landscape scale. In this study, remote sensing reveals that average NDVI levels increase towards shellfish reefs and boosted regression trees analysis shows this is a facilitative engineering effect of shellfish, and not a co-occurrence due to similar habitat preferences. The facilitative effects extend over large areas, influencing NDVI up to significant distances beyond the physical borders of the actual reefs. Shellfish reefs occupy a small portion of the intertidal Dutch Wadden

Sea (ca 2%), but the detected area of facilitation increases their potential ecological footprint by over an order of magnitude. This effectively results in a 3% NDVI increase at basin scale. This study contributes to the growing body of evidence that ecosystem engineers influence ecosystem functioning at large spatial scales (van de Koppel et al. 2015) and, to the authors knowledge, is the first to estimate the contribution of ecosystem engineering shellfish to primary production facilitation at landscape scale.

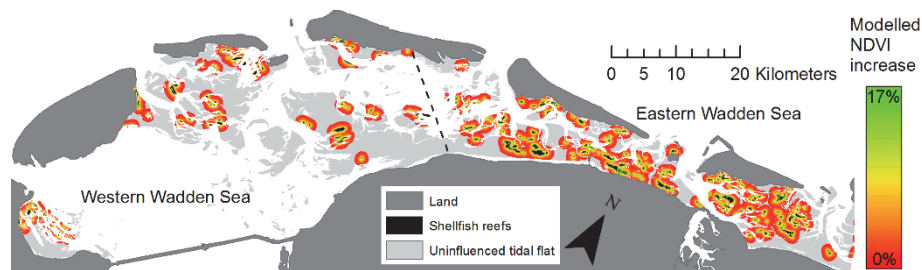


Figure 5.4 Estimate of the magnitude of the positive effect of shellfish reefs on NDVI based on the logarithmic regression. This visualization is based on a buffer analysis up to 1000 m around the shellfish reefs and indicates the potential region in which NDVI is elevated.

Differences in the consequences of ecosystem engineering by mussel- and oyster reefs have been observed in other studies locally (Kochmann et al. 2008; Norling et al. 2015; Hollander & Blomfeldt 2015), but our analysis shows that both the magnitude of NDVI increase, as well as the spatial extent of the NDVI increase are dependent on reef type. While the highest NDVI levels were observed around mussel reefs, the largest facilitative effects were observed around mixed reefs. Typically, the outcome of ecosystem engineering depends on the prevailing environmental conditions (Crain & Bertness 2006; Vaughn et al. 2007; Spooner & Vaughn 2006; Ysebaert et al. 2008). Mussel-, mixed- and oyster reefs are slightly separated in their dispersal along the inundation gradient (see Chapter 3), and this has consequences for the amount of light available for the growth of algae. The tidal flats around the three are also characterized by different hydrodynamic conditions and inundation times. Such differences in environmental conditions might explain the differences in potential for microphytobenthos facilitation. For example, in the low intertidal, high waves and low light levels might pose limitations on microphytobenthos growth and oyster reef roughness, although high, may not be able to alleviate this. In addition, the oyster reef may cause flow divergence due to its structure resulting in local increased erosion and lower NDVI values. At the same time, in the high intertidal microphytobenthos levels are already relatively high and mussel reefs contribute only little to further improve conditions. Moreover, the potential for

microphytobenthos facilitation is largely context dependent, and thus due to niche differentiation (Chapter 3), also species dependent.

The Normalized Difference Vegetation Index does not allow to discriminate between proportions attributed by microphytobenthos, macrophytes and shells, all of which have positive NDVI values. In this study, the contribution of macro-algae at larger scales was resolved by limiting the NDVI of our analysis to 0.3 (Mélédér et al. 2003; Benyoucef et al. 2013). However, at sub-pixel scale there may still be a significant proportion of macro-algae that contribute to the signal observed. In the Wadden Sea, macro-algae, seagrass and salt marsh plants constitute a small portion of the primary producers (Nienhuis 1992). Macro-algae can anchor to shell material (van der Wal et al. 2010) and may therefore have increased density near shellfish reefs (i.e. due to washed out shells or isolated shellfish patches). The one cell buffer around the reefs excluded this partially. At large it should be noted that macro-algae also contribute to primary production and ecosystem functioning. Using the water index, we eliminated the large scale water surfaces, but again cannot rule out contribution of water at sub-pixel scale.

The results obtained from the local scale study emphasize that the effects of shellfish beds on their surroundings are highly anisotropic and spatially complex, interacting strongly with the prevailing hydrodynamics. This highlights the complexity of the interactions of shellfish reefs with their surrounding habitat, which acts by influencing a multitude of processes. It is well known that shellfish reefs can locally reduce hydrodynamic stress imposed by waves (e.g. Widdows and others 2009; van Leeuwen and others 2010; Donker and others 2013) and these benign conditions promote light penetration, prevent resuspension and promote the accumulation of fine material and nutrients. This combination of factors may allow microphytobenthos to thrive at relatively deep locations around shellfish beds. However, physically it is impossible for shellfish reefs to influence waves beyond a certain distance threshold related to reef width (Wallés et al. 2014). Nutrient subsidies might explain facilitative effects over larger distances (Asmus & Asmus 1991), but the precise mechanisms (e.g. sinking and settlement rates of faeces and pseudo-faeces) are not quantified, making precise predictions difficult. Clearly, since both waves and currents are directional in nature, the most pronounced effects are to be expected on the leeward site of the reefs and facilitation is not omni-directional. It should also be noted that the differences in the estimated influenced area between the western and eastern Wadden Sea are due to differences in shellfish reef densities, i.e. the estimates were based on a model that considers the entire Dutch Wadden Sea. The eastern and western Wadden Sea are contrasting systems in terms of environmental forcing (Eriksson et al. 2010) and that should be considered when comparing the different



outcomes. Despite the intrinsic topographic complexity imposed on the spatial distribution of microphytobenthos by external environmental variables, as was also observed in the local scale study, the extent of the influence of reef building shellfish emanates from our data. Our findings underline the importance of integrative tools like remote sensing for the study of system-wide effects. As such, this is the first study that shows the importance of the facilitative effects of shellfish reefs at landscape scale.

Shellfish reefs are ecological hotspots locally, sustaining complex food webs and boosting high biodiversity (Christianen et al. 2016). Moreover, the fact that microphytobenthos is at the very basis of the food web (Christianen et al. 2017) and shellfish reefs partially sustain its production at landscape scale underlines the importance of ecosystem engineers in sustaining food webs (Sanders et al. 2014). The mosaic that is created due to the patchy nature of reefs and their influence zones further structures microbenthic communities (Donadi et al. 2015).

Spatially extended effects of ecosystem engineering are not confined to shellfish reefs, but are observed in other ecosystems as well. For example the beaver modifies the landscape by creating retention dams and boosts plant (Wright et al. 2002) and waterbird (Nummi & Holopainen 2014) diversity at the landscape scale. Spatially extended ecosystem engineering may generate important linkages and interdependencies at the landscape scale such as found in, for example, mangrove, seagrass and coral reef ecosystems (Gillis et al. 2014; van de Koppel et al. 2015). To further our understanding of ecological functioning at the landscape scale it is important to recognize these transboundary influences and study the ecosystem constituents at the appropriate scale.

The importance of shellfish reefs underlined in this study has significant consequences for the management of intertidal ecosystems (van de Koppel et al. 2015). Estuaries and tidal basins serve a multitude of societal functions, often combining nature conservation with the exploitation of natural resources (Lotze et al. 2014). While mussel fisheries do not take place in the intertidal zone of the Dutch Wadden Sea (Dankers and others, 2001), our study puts a clear question mark behind the policy premise to allow local disturbances to shellfish reefs elsewhere. This calls for a paradigm shift in the management of intertidal areas that explicitly considers the interconnectedness of keystone species and their dependent habitats at larger spatial scales.







---

### Synthesis

In temperate tidal systems, aggregates of ecosystem engineering (*sensu* Jones et al. 1994) mussels and oysters increase sedimentation (Walles et al. 2014), organic matter content (van der Zee et al. 2012; Donadi, van der Heide, et al. 2013) and microphytobenthos stocks (Engel et al. 2017) over spatially extended distances. These processes in turn affect the distribution of infaunal organisms (Donadi, van der Heide, et al. 2013) and ultimately organisms from higher trophic levels, such as birds (van der Zee et al. 2012). The ability to structure the environment over large scales might be of importance in sustaining food webs (van der Zee et al. 2015; Sanders et al. 2014). As such, shellfish reefs influence ecosystem functioning and the ecological community at the landscape scale. Yet, the ecosystem effects of reef building shellfish have not been quantified at landscape scale before.

To further the understanding of the relative importance of shellfish reefs for ecological functioning at landscape scale, this thesis focussed on whether we can map shellfish reefs cost-efficiently using remote sensing, and whether mussels and oysters have similar habitat preferences. Furthermore, the consequences of the presence of shellfish reefs for A) structural complexity and the resulting retention of water, as well as B) facilitation of primary production by microphytobenthos, was investigated at landscape scale. Since niche differentiation has consequences for the emergent ecosystem engineering effect, the facilitative ability on microphytobenthos was addressed for mussel-, oyster- and mixed reefs separately. Due to spatial complexity and the large spatial scales, such questions are difficult to address using traditional methodologies like field surveys. Remote sensing was used to ‘get the big picture’; i.e. investigate the effect of ecosystem engineering by shellfish at the scale of estuaries. In this thesis, specifically the combination of satellite Synthetic Aperture Radar (SAR), optical satellite remote sensing, and Light Detection and Ranging (LiDAR) helped to elucidate the importance of shellfish reefs for ecosystem functioning. In this chapter, the main findings of the thesis are summarized and discussed. Table 6.1 summarizes the research questions and corresponding answers.

## Chapter 6

Table 6.1. Research questions and answers addressed in this thesis

| Chapter          | Research questions   | Answers  |
|------------------|--|--|
| <b>Chapter 2</b> | Is it possible to use SAR satellites sensors to map shellfish species and species?   | Using SAR imagery, it is possible to map shellfish reef distribution, however, it so far remains impossible to distinguish species or estimate shellfish densities.  |
| <b>Chapter 3</b> | Are mussel-, oyster- and mixed reefs spatially separated along the inundation gradient?  | Although there is overlap, mussel-, mixed- and oyster reefs are spatially slightly separated along the intertidal inundation gradient. Mussel reefs occur relatively shallow, oyster reefs in the deep intertidal and the mixed reefs in between.  |
|                  | Is the spatial separation driven by differences in adaptation to inundation time at individual level?  | Oysters have the highest condition index in the low intertidal, while mussels have the highest condition index at intermediate inundation values.  |
|                  | Is there competition or facilitation at the local scale between oysters and mussels?   | Shell size is negatively affected in presence of the other species, but not condition index. Oysters may facilitate mussels slightly in growth.  |
| <b>Chapter 4</b> | Does physical landscape modification by shellfish induce tidal pool formation and does that occur over spatially extended distances?                             | Shellfish induce landscape roughness, which allows for the formation of tidal pools. The sediment surrounding shellfish reefs potentially retains more water beyond ca 100 m away from the reefs borders.  |
| <b>Chapter 5</b> | What is the importance of (micro)phytobenthos facilitation by shellfish reefs at basin scales and how does this facilitation differ between mussels and oysters? | In the Dutch Wadden Sea, shellfish increase (micro)phytobenthos stocks by up to 15% near the reef borders. Stocks decrease, on average, logarithmically with distance and stocks are, on average, still elevated up to 5% at 340m distance. This means that at landscape scale, (micro)phytobenthos may be increased by up to 3%.<br>The strongest facilitative effect is observed around mixed reefs and mussel reefs, while relatively weak effects on (micro)phytobenthos are observed around oyster reefs. |

## Mapping intertidal zones using remote sensing

A prerequisite to assess large scale effects of shellfish reefs is to be able to map shellfish reefs. Using traditional optical remote sensing, it is challenging to detect shellfish due to cryptic reflectance spectra, i.e. shellfish reefs resemble mud and microphytobenthos (Le Bris et al. 2016b). Synthetic Aperture Radar (SAR) satellites are sensitive to surface roughness and the topography induced by shellfish reefs was expected to be in the right order of magnitude to generate a significant increase in microwave backscatter when compared to backscatter from intertidal sand flat (Choe et al. 2012; Dehouck et al. 2011). In Chapter 2 it was hypothesized that using data from two SAR satellites (TerraSAR-X and Radarsat 2), it is possible (1) to map the presence of shellfish beds on intertidal mudflats, (2) to distinguish between shellfish species (i.e., mussels versus oysters) and (3) to determine the density of shellfish, by comparing remotely sensed data with an extensive in situ data set. Based on field data, we found that shellfish beds exhibit high vertical surface roughness compared to surrounding sand flat. As a result, shellfish cause strong backscatter in X-band (TerraSAR-X) and C-Band (Radarsat 2) imagery, as well as strong depolarization of the microwaves. Shellfish maps were constructed, using a multivariate classification algorithm based on a logistic regression on dual-polarized satellite data. Although significant surface roughness was observed in the field between substrate types, it was found that radar backscatter in both C- and X-band saturates in shellfish beds with only moderate surface cover, making it impossible to distinguish species, and thereby limiting the potential to discriminate between shellfish densities. Based on that, we conclude that using this method, spaceborne (dual-polarised) SAR only allows for monitoring of presence and absence of shellfish-beds without species differentiation (Chapter 2). It is worth exploring the use of multitemporal SAR data (Gade and Melchionna 2016), texture analysis (Jung et al. 2015), multi-sensor fusion (Van Beijma et al. 2014) and very high resolution SAR images to further improve shellfish classification and characterization. However, the method to detect shellfish reefs proposed here is a cost effective solution to the traditional surveys. Weather and light do not restrict the window for data acquisition and the cryptic appearance of mussels and oysters is no problem for SAR data. The ability to acquire data with high temporal resolution allows this method to track changes in reef distribution and follow the development and stability of shellfish reefs at large spatial scales. This is useful in both ecosystem management as well as ecosystem studies.

As shown in this thesis, remote sensing can also be used effectively to investigate the ecosystem engineering effects of shellfish reefs at landscape scales. In Chapter 3, we used a tidal inundation map from Rijkswaterstaat that was based on LiDAR data and a tidal model to investigate the occurrence of the different

shellfish reef types along the inundation gradient. In Chapter 4, the potential of shellfish reefs to increase the water storage capacity of the landscape was investigated. SAR was used to map shellfish on the intertidal flats south of the island Schiermonnikoog in the Netherlands. Terrestrial LiDAR was used to investigate reef morphology and to test the potential of intertidal pools to form during low tide at reef scale. Airborne LiDAR data was used to see what the effect of shellfish reefs on water storage capacity is on landscape scale. Using these methods, we were able to establish that water storage capacity was increased to spatially extended distances. In Chapter 6, we investigated the species-dependent ecosystem engineering effects of shellfish reefs on benthic algae. Ideally, we would have used the SAR method to map shellfish reefs. However, since the SAR method remained unable to discriminate between species, we relied on ground surveys of shellfish reefs instead. Multispectral optical satellite data were used to investigate concentrations of benthic algae in the intertidal zone of the entire Wadden Sea. This allowed us to establish that shellfish reefs facilitate benthic algae over spatially extended distances.

Remote sensing provides more perspective, beyond the findings presented so far in this thesis, in elucidating what the role of ecosystem engineering shellfish is in shaping the intertidal landscape and in determining ecological function. The structure of shellfish reefs causes flow and wave divergence on large scales (van Leeuwen et al. 2010), which likely results in changed erosion and sedimentation patterns, which may be investigated using remote sensing as well (Ryu et al. 2008). Comparable to saltmarsh ecosystems, such processes may result in channel formation (Temmerman et al. 2007). In the intertidal zone, water line detection algorithms based on remote sensing (e.g. Ryu et al. 2002) can be used to investigate the spatial relation of water channels with regard to shellfish reefs. The opportunities for the use of remote sensing for ecosystem assessment have further increased by recent new satellite missions, like Sentinel 1 and 2, which allow to further study intertidal processes at vast scales. In addition, new earth observation satellites, like the hyperspectral EnMap, with improved spectral resolution, will be able to facilitate research to reveal the role and importance of ecosystem engineering species in the intertidal.

### **Ecosystem engineering beyond the physical reef structures**

In the dynamic realm of estuarine and coastal systems, some organisms can influence their environment beyond their local footprint. Cordgrass reduces wave action that can facilitate the community in its wake (e.g., forb on a cobble beach) (Bruno 2000; van de Koppel et al. 2006). Likewise mussels and oyster reefs, as described earlier, promote sedimentation by reducing the hydrodynamic regime (Wallace et al. 2014; Widdows et al. 2009). In time the sediment in close proximity

to shellfish reefs become muddy environments enriched with faeces and pseudofaeces which enables microphytobenthos growth and facilitates infauna and their associated predators (van der Zee et al. 2012; Donadi, Westra, et al. 2013; Donadi, van der Heide, et al. 2013). In tropical systems, spatially extended effects can eventually evolve into different systems that become increasingly dependent on one another. Such dependencies are for example observed between coral, mangrove and seagrass systems (Gillis et al. 2014). Additionally, the role of ecosystem engineers has been found to be of key importance to food web structure by modifying intrinsic network properties (link density and connectance), even though this is strictly mediated through non-trophic interactions (van der Zee et al. 2016). This thesis aimed to quantify how large effects beyond the local footprint may be.

Chapter 4 revealed that the effects of increased landscape complexity and consequent increase in water storage capacity extends to significant distances beyond the physical borders of the shellfish reefs, probably because there are more complex mud hummocks in the immediate surroundings of shellfish reefs. SAR satellite data in combination with airborne LiDAR revealed that these effects potentially extend up to approximately 100 meters away from the edge of the shellfish beds. The implications are that although only about 2% of the intertidal area is directly influenced by the local footprint, the extended effects increase the influenced area up to about 11% of the total intertidal. Since many organisms depend on tidal pools to take refuge during low tide, tidal pool creation has important consequences for ecosystem structuring and functioning (White et al. 2014; Firth et al. 2013), also beyond the local reef edges.

Furthermore, Chapter 6 revealed that shellfish reefs have a facilitative effect on the growth of (micro)phytobenthos, key primary producers in the intertidal zone. Even though the abiotic environment is crucial in explaining the spatial distribution of the vegetation index NDVI (a proxy for the biomass of intertidal (micro)phytobenthos as derived from a satellite image), the statistical modelling suggests that the relation between the observed pattern of NDVI and the distance from a shellfish reef is causal. When we statistically account for elevation, waves and currents, shellfish reefs still increase (micro)phytobenthos stocks by up to 15% near the reef borders. This spatially extended engineering extends the reefs' footprints by an order of magnitude. This means that at landscape scale microphytobenthos biomass may be increased by up to 3%. The facilitation of a key benthic primary producer across up to 40% of tidal flat in the Dutch Wadden Sea underlines the impact of ecosystem engineering bivalves and these species should be considered as vital in the functioning of the system in ecosystem management. Microphytobenthos has been shown to be the most important



primary producer in these ecosystems and as such it forms the foundation of the entire food web (Christianen et al. 2017). In addition, microphytobenthos produced on intertidal flats may be resuspended and transferred to the subtidal zone where it may subsidize production (Yoshino et al. 2012). Apart from its role as key primary producer, microphytobenthos, like reef building shellfish, is able to stabilize sediments (Miller et al. 1996). In the absence of consumers, this stabilisation may result in regular patterns with small hummocks covered by microphytobenthos alternated with water filled hollows (Weerman et al. 2011). This structure with high microphytobenthos levels might be beneficial for settlement of other benthic invertebrates (Weerman et al. 2011). Further investigation of this effect on sediment stability might reveal additional extended indirect effects of shellfish reefs on their surroundings.

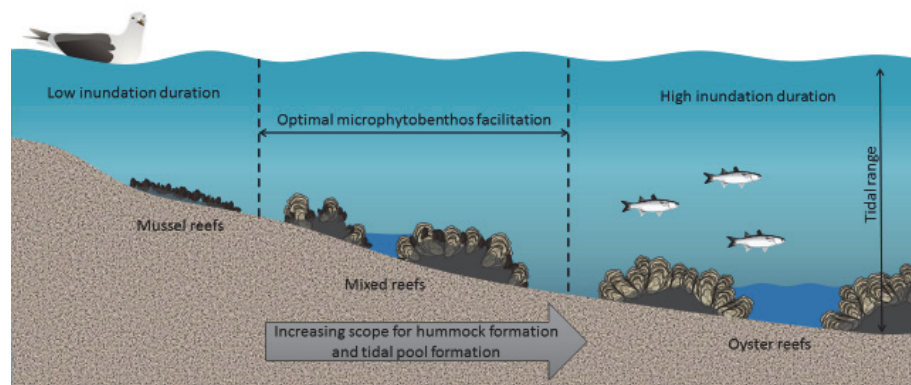


Figure 6.1 Differences in reef species composition and emergent ecosystem engineering effects along the inundation gradient. Pure mussel reefs occur in shallow zones and there is little scope for the formation of high hummocks and for facilitation of benthic microalgae. In the deepest zone, shellfish reefs are dominated by oysters and the largest potential for sedimentation is found (Wallis et al. 2015). This has important consequences for potential intertidal pool formation. Finally, at intermediate inundations mixed reefs occur and there is a moderate scope for ponding, but the largest scope for microphytobenthos facilitation over spatially extended distances.

### Differential niche occupation of mussels and oysters and consequences for the ecosystem

The Pacific oyster is native to the Pacific coast of Asia; however, it has become invasive to coasts around the world (see Chapter 1). The introduction of the oyster to these systems is likely not without consequences for the native community. For example, oyster reefs increase landscape heterogeneity (Gutiérrez et al. 2003), replace soft-bottom communities with hard-substrate epifaunal communities (Gutiérrez et al. 2003), deplete suspended phytoplankton and modify food availability (Diederich 2006; Smaal et al. 2005). While native mussel reefs partly

have the same effects, they are not fully identical in the way they influence, for example, the local ecological community (Kochmann et al. 2008). Invasive species are often considered a nuisance and a threat to ecological diversity and ecosystem functioning (Sousa et al. 2009). However, it should be noted that species extinctions due to biological invasions are rare and anecdotal (Gurevitch & Padilla 2004). As indicated in Chapter 3 and earlier suggested by Fey et al. (2009), mussels and oysters can co-exist within the same system, and even within the same reef. However, Chapter 3 shows that there is a slight but distinct difference in the preference of inundation time between shellfish species in the intertidal zone, i.e. oysters occur most in the deep zones of the intertidal and mussels occur most in slightly shallower zones. Physiological differences (see Chapter 1) might explain these differences in niche space.

Although small, differences in niche space with regard to inundation may have implications for the emergent effects of ecosystem engineering. For example, given that the maximum reef accretion is dictated by the relative position in the intertidal frame (Rodriguez et al. 2014; Walles et al. 2015), the potential for pools to form may be expected to be greater at deeper locations (Chapter 4). Differences in pool characteristics, in turn, influence the function they have for the residing inhabitants (White et al. 2014). Intertidal pools are an ideal refuge for animals during low tide and thus allow organisms to expand their distribution to higher parts of the intertidal zone. At the same time the water buffers extreme temperatures and desiccation. The presence of organisms associated to shellfish reefs alters the local ecological community and this may scale up to determine species richness at landscape scales. Dependence of the emergent effect of ecosystem engineering on position in the intertidal frame and species composition (mussels versus oysters) might also be true for the structure modification at spatially extended distances.

Chapter 5 revealed that there is a profound difference in ecosystem engineering between mussel, mixed and oyster reefs. It turned out that the highest microphytobenthos stocks (as indicated by the normalized difference vegetation index) are found around mussel reefs, the strongest facilitation is observed around mixed reefs and there is hardly facilitation around oyster reefs (see Figure 6.1, for a summary). Such differences might be explained in context of the environment and especially by inundation. Mussel reefs occur in the relative shallow regions of the intertidal zone and therefore microphytobenthos stocks may be high because light availability is high (Underwood & Kromkamp 1999) and resuspension is low. Near mixed reefs at intermediate elevations, light conditions may become limiting. The reefs may, however, increase light penetration by filter feeding and reducing the hydrodynamic stress and thus have

a large beneficial effect. Next to light limitation, strong currents around the reef hummocks may cause strong erosion that causes low microphytobenthos levels directly near oyster reefs deeper in the intertidal.

It should be noted that initially oysters invaded the Wadden Sea by occupying the lower regions in the intertidal and started slowly invading mussel reefs afterwards, while mussels also invade oyster reefs (Chapter 3). As a result, with time progressing most reefs are becoming mixed reefs and pure mussel reefs are mostly restricted to the high intertidal zone. So far, only a few reefs remain as pure oyster reef in the low intertidal zone.

### Management implications

Since the introduction of the concept, ecosystem engineering has been recognized as an important feature in ecosystem management to achieve conservation, restoration and amelioration (Wright & Jones 2006). While traditional ecosystem conservation often focusses on conserving flagship species with a certain charisma (Crain & Bertness 2006), it is unclear what charisma really means or what it is supposed to represent in ecological sense (Ducarme et al. 2013). Instead, the conservation of keystone species, such as ecosystem engineers, focusses on conservation of species that guarantee the well-being of whole communities (Simberloff 1998). Such species (e.g. insects, worms, shellfish, coral and algae) are hardly charismatic (Ducarme et al. 2013), but still define major ecological processes within an environmental background (Crain & Bertness 2006). As such, ecosystem engineers determine ecological diversity (van der Zee et al. 2015; Christianen et al. 2016) and resilience (Eriksson et al. 2010; Christianen et al. 2016). Chapters 4 and 5 and other recent literature reveal that these ecological driving processes are not limited to the physical borders of the created habitat, but extend to influence significant areas beyond the borders of ecosystem engineering species. Both mussels and oysters are valued consumption species and targeted by shellfish fisheries. While mussel fishery is restricted to the subtidal regions of the Dutch Wadden Sea (Dankers et al. 2001), conservation of intertidal habitats elsewhere is often managed by localizing the anthropogenic disturbance to the targeted species, under the assumption that the ecological disturbances are also localized (van de Koppel et al. 2015). This assertion is clearly challenged by the findings in this thesis. Furthermore, spatially extended effects of different species may get entangled, which may result in interdependencies such that demise of one species results in the collapse of entire systems (Gillis et al. 2014; van de Koppel et al. 2015). Systems, such as intertidal flats, where spatially extended ecosystem engineering is a predominant determinant of ecosystem functioning for the system at large, call for holistic conservation and management approaches. Because of this, the construction of

marine protected areas at the scale of tidal flats or tidal basin might be needed to ensure successful conservation (van de Koppel et al. 2015). At the same time, our understanding of ecosystem processes that take effect at such vast spatial scales is still in its infancy. As shown in this thesis, remote sensing provides tools that allow to investigate the status of species that have especially large effects on the ecosystem (Chapter 2) as well as their influenced footprint (Chapter 4 and 5). In light of ecosystem management remote sensing tools provide solutions to cost-effectively assess the current state of ecosystem (engineering) health and it allows to estimate the efficacy of mitigation effort (Dahdouh-Guebas 2002; Kerr & Ostrovsky 2003). Using such modern technologies like remote sensing in combination with the right conservation policies we may be able to maximize the beneficial effects that engineering species have on ecosystems. That way we can sustainably use marine resources and guarantee maximal ecological integrity.





---

## References



## References

- De 'ath, G. & Fabricius, K.E., 2000. Classification and regression trees: a powerful yet simple technique for ecological data analysis. *Ecology*, 81(11), pp.3178–3192.
- Agüera, A. et al., 2012. Winter feeding activity of the common starfish (*Asterias rubens* L.): The role of temperature and shading. *Journal of Sea Research*, 72, pp.106–112.
- AIRBUS Defence and Space, 2008. Radiometric calibration of TerraSAR-X Data., pp.1–16.
- Albrecht, A., 1998. Soft bottom versus hard rock: Community ecology of macroalgae on intertidal mussel beds in the Wadden Sea. *Journal of Experimental Marine Biology and Ecology*, 229, pp.85–109.
- Altse, E. & Bolognani, O., 1996. Retrieving soil moisture over bare soil from ERS 1 synthetic aperture radar data: Sensitivity analysis based on a theoretical surface scattering model and field data. *Water Resources Research*, 32(3), pp.653–661.
- Arkema, K.K. et al., 2013. Coastal habitats shield people and property from sea-level rise and storms. *Nature Climate Change*, 3(10), pp.913–918.
- Asmus, R. & Asmus, H., 1991. Mussel beds: Limiting or promoting phytoplankton? *Journal of Experimental Marine Biology and Ecology*, 148(2), pp.215–232.
- Balke, T. et al., 2012. Conditional outcome of ecosystem engineering: A case study on tussocks of the salt marsh pioneer *Spartina anglica*. *Geomorphology*, 153–154, pp.232–238.
- Beck, H., Thebpanya, P. & Filiaggi, M., 2010. Do Neotropical peccary species (Tayassuidae) function as ecosystem engineers for anurans? *Journal of Tropical Ecology*, 26(4), pp.407–414.
- Beck, M.W. et al., 2011. Oyster Reefs at Risk and Recommendations for Conservation, Restoration, and Management. *BioScience*, 61(2), pp.107–116.
- Beck, M.W. et al., 2009. *Shellfish reefs at risk: a global analysis of problems and solutions*, Arlington VA.
- Benyoucef, I. et al., 2013. Microphytobenthos interannual variations in a north-European estuary (Loire estuary, France) detected by visible-infrared multispectral remote sensing. *Estuarine, Coastal and Shelf Science*, 136, pp.43–52.
- Bertness, M.D., 1991. Zonation of *Spartina Patens* and *Spartina Alterniflora* in New England Salt Marsh. *Ecology*, 72(1), pp.138–148.
- Bertness, M.D. & Grosholz, E., 1985. Population-Dynamics of the Ribbed Mussel, *Geukensia-Demissa* - the Costs and Benefits of an Aggregated Distribution. *Oecologia*, 67(2), pp.192–204.
- Beukema, J.J. et al., 2015. Large-scale synchronization of annual recruitment success and stock size in Wadden Sea populations of the mussel *Mytilus edulis* L. *Helgoland Marine Research*, 69(4), pp.327–333.
- Beukema, J.J. & Cadée, G.C., 1996. Consequences of the sudden removal of nearly all mussels and cockles from the Dutch Wadden Sea. *Marine Ecology*, 17((1-3)), pp.279–289.
- Beukema, J.J. & Dekker, R., 2015. Density dependence of growth and production in a Wadden Sea population of the cockle *Cerastoderma edule*. *Marine Ecology Progress Series*, 538, pp.157–167.
- Bishop, M.J. & Peterson, C.H., 2006. Direct effects of physical stress can be counteracted by indirect benefits: oyster growth on a tidal elevation gradient. *Oecologia*, 147(3), pp.426–433.
- Borsje, B.W. et al., 2011. How ecological engineering can serve in coastal protection. *Ecological Engineering*, 37(2), pp.113–122.
- Bos, A.R. et al., 2007. Ecosystem engineering by annual intertidal seagrass beds: Sediment accretion and modification. *Estuarine, Coastal and Shelf Science*, 74(1–2), pp.344–348.
- Bouma, T.J. et al., 2009. Ecosystem engineering and biodiversity in coastal sediments: posing hypotheses. *Helgoland Marine Research*, 63(1), pp.95–106.
- Bouma, T.J. et al., 2014. Identifying knowledge gaps hampering application of intertidal habitats in coastal protection: Opportunities & steps to take. *Coastal Engineering*, 87, pp.147–157.
- Bretar, F. et al., 2013. An advanced photogrammetric method to measure surface roughness: Application to volcanic terrains in the Piton de la Fournaise, Reunion Island. *Remote Sensing of Environment*, 135, pp.1–11.
- ten Brinke, W.B.M., Augustinus, P.G.E.F. & Berger, G.W., 1995. Fine-grained sediment deposition on mussel beds in the Oosterschelde (The Netherlands), determined from echosoundings, radio-isotopes and biodeposition field experiments. *Estuarine, Coastal and Shelf Science*, 40(2), pp.195–217.
- Brinkman, A.G., Danker, N. & van Stralen, M., 2002. An analysis of mussel bed habitats in the Dutch Wadden Sea. *Helgoland Marine Research*, 56(1), pp.59–75.
- Le Bris, A. et al., 2016a. Hyperspectral remote sensing of wild oyster reefs. *Estuarine, Coastal and Shelf Science*, 172, pp.1–12.
- Le Bris, A. et al., 2016b. Hyperspectral remote sensing of wild oyster reefs. *Estuarine, Coastal and Shelf Science*, 172, pp.1–12.
- Bruno, J., 2000. Facilitation of cobble beach plant communities through habitat modification by *Spartina alterniflora*. *Ecology*, 81(5), pp.1179–1192.



## References

- Bruno, J.F., Stachowicz, J.J. & Bertness, M.D., 2003. Inclusion of facilitation into ecological theory. *Trends in Ecology & Evolution*, 18(3), pp.119–125.
- Buschbaum, C., Cornelius, A. & Goedknegt, M.A., 2016. Deeply hidden inside introduced biogenic structures – Pacific oyster reefs reduce detrimental barnacle overgrowth on native blue mussels. *Journal of Sea Research*, 117, pp.20–26.
- Buschbaum, C. & Saier, B., 2001. Growth of the mussel *Mytilus edulis* L. in the Wadden Sea affected by tidal emergence and barnacle epibionts. *Journal of Sea Research*, 45(1), pp.27–36.
- Byers, J.E. et al., 2015. Geographic variation in intertidal oyster reef properties and the influence of tidal prism. *Limnology and Oceanography*, 60(3), pp.1051–1063.
- Campbell, M.R. & Mazzotti, F.J., 2004. Characterization of natural and artificial alligator holes. *Southeastern Naturalist*, 3(4), pp.583–594.
- Cardoso, J.F.M.F. et al., 2007. Spatial variability in growth and reproduction of the Pacific oyster *Crassostrea gigas* (Thunberg, 1793) along the west European coast. *Journal of Sea Research*, 57(4), pp.303–315.
- Carrère, V., Spilmont, N. & Davoult, D., 2004. Comparison of simple techniques for estimating chlorophyll a concentration in the intertidal zone using high spectral-resolution field-spectrometer data. *Marine Ecology Progress Series*, 274, pp.31–40.
- Chappuis, E. et al., 2014. Vertical zonation is the main distribution pattern of littoral assemblages on rocky shores at a regional scale. *Estuarine, Coastal and Shelf Science*, 147, pp.113–122.
- Chargulaf, C.A., Townsend, K.A. & Tibbetts, I.R., 2011. Community structure of soft sediment pool fishes in Moreton Bay, Australia. *Journal of Fish Biology*, 78, pp.479–494.
- Choe, B.-H. et al., 2012. Detection of oyster habitat in tidal flats using multi-frequency polarimetric SAR data. *Estuarine, Coastal and Shelf Science*, 97, pp.28–37.
- Christianen, M. et al., 2016. Biodiversity and food web indicators of community recovery in intertidal shellfish reefs. *Biological Conservation*.
- Christianen, M.J.A. et al., 2017. Benthic primary producers are key to sustain the Wadden Sea food web: stable carbon. *Ecology*, 38(1), pp.42–49.
- Combe, J.P. et al., 2005. Mapping microphytobenthos biomass by non-linear inversion of visible-infrared hyperspectral images. *Remote Sensing of Environment*, 98(4), pp.371–387.
- Commito, J. & Rusignuolo, B., 2000. Structural complexity in mussel beds: the fractal geometry of surface topography. *Journal of experimental marine biology and ecology*, 255(2), pp.133–152.
- Compton, T.J. et al., 2013. Distinctly variable mudscapes: Distribution gradients of intertidal macrofauna across the Dutch Wadden Sea. *Journal of Sea Research*, 82, pp.103–116.
- Connell, J.H., 1972. Interactions on Marine Rocky Intertidal Shores. *Annual Review of Ecology and Systematics*, 3(Connell 22), pp.169–192.
- Correll, D.L., Jordan, T.E. & Weller, D.E., 2000. Beaver pond biogeochemical effects in the Maryland Coastal Plain. *Biogeochemistry*, 49, pp.217–239.
- Crain, C.M. & Bertness, M.D., 2006. Ecosystem engineering across environmental gradients: implications for conservation and management. *BioScience*, 56(3), pp.211–218.
- Crase, B., Liedloff, A.C. & Wintle, B.A., 2012. A new method for dealing with residual spatial autocorrelation in species distribution models. *Ecography*, 35(10), pp.879–888.
- Cressman, K. a et al., 2003. Effects of oyster reefs on water quality in a tidal creek estuary. *Journal of Shellfish Research*, 22(3), pp.753–762.
- Crowley, G., 2010. *Dmc Data Product Manual*, Guildford.
- Dahdouh-Guebas, F., 2002. The use of remote sensing and GIS in the sustainable management of tropical coastal ecosystems. *Environment, Development and Sustainability*, 4, pp.93–112.
- Dankers, N. et al., 2004. *Het ontstaan en verdwijnen van droogvallende mosselbanken in de Nederlandse Waddenzee*. Alterra-rapport 921, Alterra, Wageningen.
- Dankers, N. et al., 2003. *Historische ontwikkeling van droogvallende mosselbanken in de Nederlandse Waddenzee*, Wageningen.
- Dankers, N. et al., 2001. Recovery of intertidal mussel beds in the Waddensea: Use of habitat maps in the management of the fishery. *Hydrobiologia*, 465, pp.21–30.
- Daubenmire, R.F., 1943. Vegetational zonation in the Rocky Mountains. *Botanical Review*, 9(6), pp.325–393.
- Davidson, M.W.J. et al., 2000. On the characterization of agricultural soil roughness for radar remote sensing studies. *IEEE Transactions on Geoscience and Remote Sensing*, 38, pp.630–640.
- Davis, B., Baker, R. & Sheaves, M., 2014. Seascape and metacommunity processes regulate fish assemblage structure in coastal wetlands. *Marine Ecology Progress Series*, 500, pp.187–202.
- Dehouck, A. et al., 2011. Potential of TerraSAR-X imagery for mapping intertidal coastal wetlands. In *Proceedings of the 4th TerraSAR-X Science Team Meeting*. Oberpfaffenhofen, pp. 1–8.

## References

- Diederich, S., 2005. Differential recruitment of introduced Pacific oysters and native mussels at the North Sea coast: coexistence possible? *Journal of Sea Research*, 53(4), pp.269–281.
- Diederich, S., 2006. High survival and growth rates of introduced Pacific oysters may cause restrictions on habitat use by native mussels in the Wadden Sea. *Journal of Experimental Marine Biology and Ecology*, 328(2), pp.211–227.
- Donadi, S., van der Heide, T., et al., 2013. Cross-habitat interactions among bivalve species control community structure on intertidal flats. *Ecology*, 94(2), pp.489–498.
- Donadi, S. et al., 2015. Multi-scale habitat modification by coexisting ecosystem engineers drives spatial separation of macrobenthic functional groups. *Oikos*, 124(11), pp.1502–1510.
- Donadi, S., Westra, J., et al., 2013. Non-trophic Interactions Control Benthic Producers on Intertidal Flats. *Ecosystems*, 16(7), pp.1325–1335.
- Donker, J.J.A., 2015. Wave forcing in the Dutch Wadden Sea and the effects on mussel habitats. In *Hydrodynamic processes and the stability of intertidal mussel beds in the Dutch Wadden Sea*. p. 134.
- Donker, J.J.A., van der Vegt, M. & Hoekstra, P., 2013. Wave forcing over an intertidal mussel bed. *Journal of Sea Research*, 82, pp.54–66.
- Drinkwaard, A.C., 1999. Introductions and developments of oysters in the North Sea area: a review. *Helgolander Meeresuntersuchungen*, 52(3–4), pp.301–308.
- Dubois, P.C., van Zyl, J. & Engman, T., 1995. Measuring soil moisture with imaging radars. *IEEE Transactions on Geoscience and Remote Sensing*, 33(4), pp.915–926.
- Ducarme, F., Luque, G.M. & Courchamp, F., 2013. What are “charismatic species” for conservation biologists? *BioSciences Master Reviews*, 1(July), pp.1–8.
- Duran-Matute, M. et al., 2014. Residual circulation and freshwater transport in the Dutch Wadden Sea: A numerical modelling study. *Ocean Science*, 10(4), pp.611–632.
- Eklöf, J.S. et al., 2014. Effects of antagonistic ecosystem engineers on macrofauna communities in a patchy, intertidal mudflat landscape. *Journal of Sea Research*, 97, pp.56–65.
- Elith, J., Leathwick, J.R. & Hastie, T., 2008. A working guide to boosted regression trees. *Journal of Animal Ecology*, 77(4), pp.802–813.
- van den Ende, D. et al., 2012. *Het mosselbestand en het areaal aan mosselbanken op de droogvallende platen van de Waddenzee in het voorjaar van 2012. Wageningen IMARES Rapport, C149/12, Yerseke*.
- Engel, F.G. et al., 2017. Mussel beds are biological power stations on intertidal flats. *Estuarine, Coastal and Shelf Science*, 191, pp.21–27.
- Ens, B.J. et al., 2009. Changes in the abundance of intertidal birds in the Dutch Wadden Sea in 1990–2008: differences between East and West. *Limosa*, 82, pp.100–112.
- Eriksson, B.K. et al., 2010. Major Changes in the Ecology of the Wadden Sea: Human Impacts, Ecosystem Engineering and Sediment Dynamics. *Ecosystems*, 13(5), pp.752–764.
- Eschweiler, N. & Christensen, H.T., 2011. Trade-off between increased survival and reduced growth for blue mussels living on Pacific oyster reefs. *Journal of Experimental Marine Biology and Ecology*, 403(1–2), pp.90–95.
- Fawcett, T., 2006. An introduction to ROC analysis. *Pattern Recognition Letters*, 27(8), pp.861–874.
- Fey, F. et al., 2009. Development and distribution of the non-indigenous Pacific oyster (*Crassostrea gigas*) in the Dutch Wadden Sea. *Aquaculture International*, 18(1), pp.45–59.
- Firth, L.B. et al., 2014. Biodiversity in intertidal rock pools: Informing engineering criteria for artificial habitat enhancement in the built environment. *Marine Environmental Research*, 102, pp.122–130.
- Firth, L.B. et al., 2013. The importance of water-retaining features for biodiversity on artificial intertidal coastal defence structures. *Diversity and Distributions*, 19(10), pp.1275–1283.
- Fodrie, F.J. et al., 2014. Classic paradigms in a novel environment: Inserting food web and productivity lessons from rocky shores and saltmarshes into biogenic reef restoration S. Arnott, ed. *Journal of Applied Ecology*, 51(5), pp.1314–1325.
- Folmer, E.O. et al., 2014. Large-Scale Spatial Dynamics of Intertidal Mussel (*Mytilus edulis* L.) Bed Coverage in the German and Dutch Wadden Sea. *Ecosystems*, 17(3), pp.550–566.
- Fung, A.K. et al., 2002. An improved IEM model for bistatic scattering from rough surfaces. *Journal of Electromagnetic Waves and Applications*, 16(5), pp.689–702.
- Fung, A.K. & Chen, K.-S., 2010. *Microwave Scattering and Emission Models for Users*, Norwood: Artech House.
- Fung, A.K., Li, Z. & Chen, K.S., 1992. Backscattering from a randomly rough dielectric surface. *IEEE Transactions on Geoscience and Remote Sensing*, 30(2), pp.356–369.
- Gade, M. et al., 2008. Classification of sediments on exposed tidal flats in the German Bight using multi-frequency radar data. *Remote Sensing of Environment*, 112(4), pp.1603–1613.

## References

- Gade, M. et al., 2014. Multi-frequency SAR data help improving the monitoring of intertidal flats on the German North Sea coast. *Estuarine, Coastal and Shelf Science*, 140, pp.32–42.
- Gillis, L.G. et al., 2014. Potential for landscape-scale positive interactions among tropical marine ecosystems. *Marine Ecology Progress Series*, 503, pp.289–303.
- Gaitán-Espitia, J.D., Quintero-Galvis, J.F., Mesas, A. & D'Elia, G., 2016. Mitogenomics of southern hemisphere blue mussels (Bivalvia: Pteriomorpha): Insights into the evolutionary characteristics of the *Mytilus edulis* complex. *Scientific reports* 6:26853
- Grace, J.B. & Wetzel, R.G., 1981. Habitat partitioning and competitive displacement in cattails (Typha): Experimental field studies. *The American Naturalist*, 118(4), pp.463–474.
- Green, D.S., Boots, B. & Crowe, T.P., 2012. Effects of Non-Indigenous Oysters on Microbial Diversity and Ecosystem Functioning. *PLoS ONE*, 7(10), pp.1–10.
- Green, D.S., Rocha, C. & Crowe, T.P., 2013. Effects of Non-indigenous Oysters on Ecosystem Processes Vary with Abundance and Context. *Ecosystems*, 16(5), pp.881–893.
- Grime, J.P., 1977. Evidence for the Existence of Three Primary Strategies in Plants and Its Relevance to Ecological and Evolutionary Theory. *The American Naturalist*, 111(982), pp.1169–1194.
- Gurevitch, J. & Padilla, D.K., 2004. Are invasive species a major cause of extinctions? *Trends in Ecology and Evolution*, 19(9), pp.470–474.
- Gurney, W.S.C. & Lawton, J.H., 1996. The population dynamics of ecosystem engineers. *Oikos*, 76(2), pp.273–283.
- Gutiérrez, J.L. et al., 2003. Mollusks as ecosystem engineers: the role of shell production in aquatic habitats. *Oikos*, 101(2003), pp.79–90.
- Gutiérrez, J.L. et al., 2011. Physical ecosystem engineers and the functioning of estuaries and coasts. In C. H. R. Heip, C. J. . Philippart, & J. . Middelburg, eds. *Treatise on Estuarine and Coastal Science*. Elsevier, pp. 1–99.
- Hallikainen, M. et al., 1985. Microwave Dielectric Behavior of Wet Soil-Part 1: Empirical Models and Experimental Observations. *IEEE Transactions on Geoscience and Remote Sensing*, GE-23(1), pp.25–34.
- Hannam, M. & Moskal, L.M., 2015. Terrestrial Laser Scanning Reveals Seagrass Microhabitat Structure on a Tideflat. *Remote Sensing*, 7, pp.3037–3055.
- Hansen, B., Schjønning, P. & Sibbesen, E., 1999. Roughness indices for estimation of depression storage capacity of tilled soil surfaces. *Soil and Tillage Research*, 52(1–2), pp.103–111.
- Haralick, R.M., Shanmugam, K. & Dinstein, I., 1973. Textural features for image classification. *IEEE Transactions on Systems, Man and Cybernetics*, SMC-3(6), pp.610–621.
- Harding, J. & Mann, R., 2006. Age and growth of wild Suminoe (*Crassostrea ariakensis*, Fugita 1913) and Pacific (*C. gigas*, Thunberg 1793) oysters from Laizhou Bay, China. *Journal of Shellfish Research*, 25(1), pp.73–82.
- Harvey, J.W., Germann, P.F. & Odum, W.E., 1987. Geomorphological control of subsurface hydrology in the creekbank zone of tidal marshes. *Estuarine, Coastal and Shelf Science*, 25(6), pp.677–691.
- Hastings, A. et al., 2007. Ecosystem engineering in space and time. *Ecology letters*, 10(2), pp.153–64.
- Heip, C.H.R. et al., 1995. Production and consumption of biological particles in temperate tidal estuaries. *Oceanography and Marine Biology*, 33, pp.1–149.
- Helm, M.M., Bourne, N. & Lovatelli, A., 2004. *Hatchery culture of bivalves: a practical manual*, Food and agriculture organization of the United Nations.
- Herman, P. & Scholten, H., 1990. Can suspension-feeders stabilise estuarine ecosystems? *Trophic relationships in the marine environment.*, pp.104–116.
- Hijmans, R.J., 2015. raster: Geographic Data Analysis and Modeling. R package version 2.3-40.
- Hollander, J. & Blomfeldt, J., 2015. Effects of the alien Pacific oyster (*Crassostrea gigas*) on subtidal macrozoobenthos communities. *Marine Biology*, pp.547–555.
- Holm, M.W. et al., 2016. Coexistence of Pacific oyster *Crassostrea gigas* (Thunberg, 1793) and blue mussels *Mytilus edulis* Linnaeus, 1758 on a sheltered intertidal bivalve bed? *Aquatic Invasions*, 11(2), pp.155–165.
- Hughes, C.E., Binning, P. & Willgoose, G.R., 1998. Characterisation of the hydrology of an estuarine wetland. *Journal of Hydrology*, 211(1–4), pp.34–49.
- Ibrahim, E. et al., 2009. Effect of Spatial Resolution on Intertidal Sediment Characterization. In I. Manakos & C. Kalaitzidis, eds. *Proceedings 29th EARSeL Symposium, Imaging Europe*. Crete: IOS Press, NL, pp. 15–18.
- Johnson, K.D. & Smee, D.L., 2014. Predators influence the tidal distribution of oysters (*Crassostrea virginica*). *Marine Biology*, 161(7), pp.1557–1564.
- Johnston, C.A. & Naiman, R.J., 1987. Boundary dynamics at the aquatic-terrestrial interface: The influence of beaver and geomorphology. *Landscape Ecology*, 1(1), pp.47–57.
- Jones, C.G. et al., 2010. A framework for understanding

## References

- physical ecosystem engineering by organisms. *Oikos*, 119(12), pp.1862–1869.
- Jones, C.G., Lawton, J.H. & Shachak, M., 1997. Positive and negative effects of organisms as physical ecosystem engineers. *Ecology*, 78(7), pp.1946–1957.
- Jones, C.G., Lawton, J.H. & Shachak, M., 1994. Organisms as Ecosystem Engineers. *Oikos*, 69(3), pp.373–386.
- De Jonge, V.N. & Van Beusekom, J.E.E., 1992. Contribution of resuspended microphytobenthos to total phytoplankton in the EMS estuary and its possible role for grazers. *Netherlands Journal of Sea Research*, 30(1992), pp.91–105.
- Kang, C. et al., 2006. Microphytobenthos seasonality determines growth and reproduction in intertidal bivalves. *Marine Ecology Progress Series*, 315, pp.113–127.
- Katsanevakis, S. et al., 2014. Impacts of invasive alien marine species on ecosystem services and biodiversity: a pan-European review. *Aquatic Invasions*, 9(4), pp.391–423.
- van Katwijk, M.M. et al., 2010. Sediment modification by seagrass beds: Muddification and sandification induced by plant cover and environmental conditions. *Estuarine, Coastal and Shelf Science*, 89(2), pp.175–181.
- Kazempour, F., Launeau, P. & Méléder, V., 2012. Microphytobenthos biomass mapping using the optical model of diatom biofilms: Application to hyperspectral images of Bourgneuf Bay. *Remote Sensing of Environment*, 127, pp.1–13.
- Kemp, P.S. et al., 2012. Qualitative and quantitative effects of reintroduced beavers on stream fish. *Fish and Fisheries*, 13(2), pp.158–181.
- Kerr, J.T. & Ostrovsky, M., 2003. From space to species: Ecological applications for remote sensing. *Trends in Ecology and Evolution*, 18(6), pp.299–305.
- Kim, D. et al., 2011. Submarine groundwater discharge in tidal flats revealed by space-borne synthetic aperture radar. *Remote Sensing of Environment*, 115(2), pp.793–800.
- Knecht, C.L. et al., 2012. Retention capacity of random surfaces. *Physical review letters*, 108(4), p.45703.
- Kochmann, J. et al., 2008. Shift from native mussels to alien oysters: Differential effects of ecosystem engineers. *Journal of Experimental Marine Biology and Ecology*, 364(1), pp.1–10.
- van de Koppel, J. et al., 2015. Long-distance interactions regulate the structure and resilience of coastal ecosystems. *Annual review of marine science*, 7, pp.139–58.
- van de Koppel, J. et al., 2005. Scale-dependent feedback and regular spatial patterns in young mussel beds. *The American naturalist*, 165(3), pp.E66–77.
- van de Koppel, J. et al., 2006. Scale-dependent interactions and community structure on cobble beaches. *Ecology letters*, 9(1), pp.45–50.
- Kovalenko, K.E., Thomaz, S.M. & Warfe, D.M., 2012. Habitat complexity: Approaches and future directions. *Hydrobiologia*, 685(1), pp.1–17.
- Kröncke, I., 1996. Impact of biodeposition on macrofaunal communities in intertidal sandflats. *Marine Ecology*, 17, pp.159–174.
- Krylov, V.A. et al., 2011. Supervised High-Resolution Dual-Polarization SAR Image Classification by Finite Mixtures and Copulas. *IEEE Journal of Selected Topics in Signal Processing*, 5(3), pp.554–566.
- Landis, J. & Koch, G., 1977. The measurement of observer agreement for categorical data. *biometrics*, 33(1), pp.159–174.
- Lawton, H.J., 1994. What do species do in ecosystems. *Oikos*, 71, pp.367–374.
- Lee, H., Chae, H. & Cho, S.-J., 2011. Radar Backscattering of Intertidal Mudflats Observed by Radarsat-1 SAR Images and Ground-Based Scatterometer Experiments. *IEEE Transactions on Geoscience and Remote Sensing*, 49(5), pp.1701–1711.
- Lee, J.-S., 1981. Refined filtering of image noise using local statistics. *Computer Graphics and Image Processing*, 15(4), pp.380–389.
- van Leeuwen, B. et al., 2010. Modeling the influence of a young mussel bed on fine sediment dynamics on an intertidal flat in the Wadden Sea. *Ecological Engineering*, 36(2), pp.145–153.
- Legendre, P. & Legendre, L.F.J., 2012. *Numerical ecology* 24th ed., Elsevier.
- Lenihan, H.S., 1999. Physical-biological coupling on oyster reefs: how habitat structure influences individual performance. *Ecological Monographs*, 69(3), pp.251–275.
- Lillesand, T., Kiefer, R.W. & Chipman, J., 2014. *Remote sensing and image interpretation*, John Wiley & Sons.
- Lin, N. et al., 2012. Physically-based Assessment of Hurricane Surge Threat under Climate Change Accessed. *Nature Climate Change*, 2, pp.462–467.
- Lindeboom, H., 2002. The coastal zone: an ecosystem under pressure. In *Oceans*. pp. 49–84.
- Liu, Q.-X. et al., 2012. Alternative mechanisms alter the emergent properties of self-organization in mussel beds. *Proceedings of the Royal Society B: Biological Sciences*, 279(March), pp.2744–2753.
- Lotze, H.K. et al., 2014. Depletion, Degredation, and

## References

- Recovery Potential of Estuaries and Coastal Seas. *Science*, 312(5781), pp.1806–1809.
- Lotze, H.K., 2005. Radical changes in the Wadden Sea fauna and flora over the last 2,000 years. *Helgoland Marine Research*, 59(1), pp.71–83.
- Malkin, S.Y. et al., 2017. Electrogenic Sulfur Oxidation by Cable Bacteria in Bivalve Reef Sediments. *Frontiers in Marine Science*, 4(February).
- Markert, A. et al., 2013. Habitat change by the formation of alien *Crassostrea*-reefs in the Wadden Sea and its role as feeding sites for waterbirds. *Estuarine, Coastal and Shelf Science*, 131, pp.41–51.
- Markert, A., Wehrmann, A. & Kröncke, I., 2010. Recently established *Crassostrea*-reefs versus native *Mytilus*-beds: differences in ecosystem engineering affects the macrofaunal communities (Wadden Sea of Lower Saxony, southern German Bight). *Biological Invasions*, 12(1), pp.15–32.
- McFeeters, S.K., 1996. The use of the Normalized Difference Water Index (NDWI) in the delineation of open water features. *International journal of remote sensing*, 17(7), pp.1425–1432.
- McGrorty, S. & Goss-Custard, J.D., 1993. Population dynamics of the mussel *Mytilus edulis* along environmental gradients: spatial variations in density-dependent mortalities. *Journal of Animal Ecology*, 62(3), pp.415–427.
- McGrorty, S., Goss-Custard, J.D. & Clarke, R.T., 1993. Mussel *Mytilus edulis* (Mytilacea) dynamics in relation to environmental gradients and intraspecific interactions. *Netherlands Journal of Aquatic Ecology*, 27, pp.163–171.
- Meadows, P.S., Meadows, A. & Murray, J.M.H., 2012. Biological modifiers of marine benthic seascapes: Their role as ecosystem engineers. *Geomorphology*, 157–158, pp.31–48.
- Mélédér, V. et al., 2003. Cartographie des peuplements du microphytobenthos par télédétection spatiale visible-infrarouge dans un écosystème conchylicole. *Comptes Rendus Biologies*, 326(4), pp.377–389.
- Metaxas, A. & Scheibling, R.E., 1993. Community structure and organization of tidepools. *Marine Ecology Progress Series*, 98, pp.187–198.
- Middelburg, J.J. et al., 2000. The fate of intertidal microphytobenthos carbon: An in situ <sup>13</sup>C-labeling study. *Limnology and Oceanography*, 45(6), pp.1224–1234.
- Miller, D.C., Geider, R.J. & MacIntyre, H.L., 1996. Microphytobenthos: The Ecological Role of the “Secret Garden” of Unvegetated, Shallow-Water Marine Habitats. II. Role in Sediment Stability and Shallow-Water Food Webs. *Estuaries*, 19(2), p.202.
- Mills, L.S., Soulé, M.E. & Doak, D.F., 1993. The keystone-species concept in ecology and conservation. *BioScience*, 43(4), pp.219–224.
- Mitchell, J. & Jones, B., 1978. Micro-Relief Surface Depression Storage: Changes During Rainfall Events And Their Application To Rainfall-Runoff Models. *JAWRA Journal of the American Water Resources Association*, 14(4), pp.777–802.
- Miossec, L., Le Deuff, R.M. & Goulletquer, P., 2009. Alien Species Alert: *Crassostrea gigas* (Pacific oyster). *ICES Cooperative Research Report*, Copenhagen.
- Molnar, J.L. et al., 2008. Assessing the global threat of invasive species to marine biodiversity. *Frontiers in Ecology and the Environment*, 6(9), pp.485–492.
- NASA, Landsat 7 Science Data Users Handbook. Available at: [https://landsat.gsfc.nasa.gov/wp-content/uploads/2016/08/Landsat7\\_Handbook.pdf](https://landsat.gsfc.nasa.gov/wp-content/uploads/2016/08/Landsat7_Handbook.pdf) [Accessed June 4, 2017].
- Nehls, G. et al., 2009. Beds of blue mussels and Pacific oysters. Thematic Report No. 11. In H. Marencic & J. de Vlas, eds. *Wadden sea ecosystem No. 25*. Wilhelmshaven, Germany: Common Wadden Sea Secretariat, Trilateral Monitoring and Assessment Group, p. 30.
- Nehls, G. et al., 2006. Wadden Sea mussel beds invaded by oysters and slipper limpets: competition or climate control? *Helgoland Marine Research*, 60(2), pp.135–143.
- Nehls, G., Hertzler, I. & Scheiffarth, G., 1997. Stable mussel *Mytilus edulis* beds in the Wadden Sea—They’re just for the birds. *Helgoländer Meeresuntersuchungen*, 51, pp.361–372.
- Nehls, G. & Thiel, M., 1993. Large-scale distribution patterns of the mussel *Mytilus edulis* in the Wadden Sea of Schleswig-Holstein: Do storms structure the ecosystem? *Netherlands Journal of Sea Research*, 31(2), pp.181–187.
- Newell, R.I.E., Cornwell, J.C. & Owens, M.S., 2002. Influence of simulated bivalve biodeposition and microphytobenthos on sediment nitrogen dynamics: A laboratory study. *Limnology and Oceanography*, 47(5), pp.1367–1379.
- Nicholls, R.J. & Cazenave, A., 2010. Sea Level Rise and Its Impact on Coastal Zones. *Science*, 328(2010), pp.1517–1520.
- Nienhuis, P. & Smaal, A., 1994. The Oosterschelde estuary, a case-study of a changing ecosystem: an introduction. *Hydrobiologia*, 282/283, pp.1–14.
- Nienhuis, P.H., 1992. Eutrophication, Water Management, and the Functioning of Dutch Estuaries and Coastal Lagoons. *Estuaries*, 15(4), pp.538–548.
- Norling, P. et al., 2015. Effects of live and post-mortem shell structures of invasive Pacific oysters and native blue mussels on macrofauna and fish. *Marine Ecology*

## References

- Progress Series*, 518, pp.123–138.
- Nummi, P. & Holopainen, S., 2014. Whole-community facilitation by beaver: Ecosystem engineer increases waterbird diversity. *Aquatic Conservation: Marine and Freshwater Ecosystems*, 24(5), pp.623–633.
- Nuttle, W.K. & Harvey, J.W., 1995. Fluxes of water and solute in a coastal wetland sediment. I. The contribution of regional groundwater discharge. *Journal of Hydrology*, 164, pp.89–107.
- Oh, Y., 2004. Quantitative retrieval of soil moisture content and surface roughness from multipolarized radar observations of bare soil surfaces. *IEEE Transactions on Geoscience and Remote Sensing*, 42(3), pp.596–601.
- Oh, Y., Sarabandi, K. & Ulaby, F., 1992. An empirical model and an inversion technique for radar scattering from bare soil surfaces. *IEEE Transactions on Geoscience and Remote Sensing*, 30(2), pp.370–381.
- Okamura, B., 1986. Group living and the effects of spatial position in aggregations of *Mytilus edulis*. *Oecologia*, 69(3), pp.341–347.
- Oliver, L.R., Seed, R. & Reynolds, B., 2008. The effect of high flow events on mussels (*Mytilus edulis*) in the Conwy estuary, North Wales, UK. *Hydrobiologia*, 606, pp.117–127.
- Page, E.S., 1954. Continuous inspection schemes. *Biometrika*, 41(1), pp.100–115.
- Paine, R.T., 1969. A note on trophic complexity and community stability. *The American Naturalist*, 103(929), pp.91–93.
- Park, S. et al., 2010. Tidal Wetland monitoring using polarimetric synthetic aperture radar. XXXVIII(2004), pp.187–191.
- Park, S.-E., Moon, W.M. & Kim, D., 2009. Estimation of Surface Roughness Parameter in Intertidal Mudflat Using Airborne Polarimetric SAR Data. *IEEE Transactions on Geoscience and Remote Sensing*, 47(4), pp.1022–1031.
- Pearson, T.H. & Rosenberg, R., 1978. Macrobenthic succession in relation to organic enrichment and pollution of the marine environment. *Oceanogr. Mar. Biol. Ann. Rev.*, 16(June 2015), pp.229–3011.
- Pebesma, E.J., 2004. Multivariable geostatistics in S: The gstat package. *Computers and Geosciences*, 30(7), pp.683–691.
- Pennings, S.C. & Callaway, R.M., 1992. Salt marsh plant zonation: the relative importance of competition and physical factors. *Ecology*, 73(2), pp.681–690.
- Pennings, S.C., Grant, M.B. & Bertness, M.D., 2005. Plant zonation in low-latitude salt marshes: Disentangling the roles of flooding, salinity and competition. *Journal of Ecology*, 93(1), pp.159–167.
- Peterson, C.H., 1991. Intertidal Zonation of Marine Invertebrates in Sand and Mud. *American Scientist*, 79(3), pp.236–249.
- Petitpas, B. et al., 2010. Roughness measurement from multi-stereo reconstruction. In N. Paparoditis et al., eds. *ISPRS Technical Commission III Symposium, PCV 2010*. Saint-Mandé, France, pp. 104–109.
- Petraitis, P.S., 1990. Direct and indirect effects of predation, herbivory and surface rugosity on mussel recruitment. *Oecologia*, 83(3), pp.405–413.
- Polis, G. a., Anderson, W.B. & Holt, R.D., 1997. Toward an Integration of Landscape and Food Web Ecology: The Dynamics of Spatially Subsidized Food Webs. *Annual Review of Ecology and Systematics*, 28(1), pp.289–316.
- Polley, H.W. & Collins, S.L., 1984. Relationships of vegetation and environment in buffalo wallows. *American Midland Naturalist*, 112(1), pp.178–186.
- Pollock, M.M., Heim, M. & Werner, D., 2003. Hydrologic and Geomorphic Effects of Beaver Dams and Their Influence on Fishes. In *American Fisheries Society Symposium*. pp. 213–233.
- Porter, E.T., Cornwell, J.C. & Sanford, L.P., 2004. Effect of oysters *Crassostrea virginica* and bottom shear velocity on benthic-pelagic coupling and estuarine water quality. *Marine Ecology Progress Series*, 271, pp.61–75.
- R Development Core Team, 2015. R: A language and environment for statistical computing.
- Ragnarsson, S.Á. & Raffaelli, D., 1999. Effects of the mussel *Mytilus edulis* L. on the invertebrate fauna of sediments. *Journal of Experimental Marine Biology and Ecology*, 241(1), pp.31–43.
- Reise, K., 1998. Pacific oysters invade mussel beds in the European Wadden Sea. *Senckenbergiana maritima*, 28(4–6), pp.167–175.
- Reise, K. et al., 2010. *The Wadden Sea - A outstanding tidal wetland. Wadden Sea Ecosystem No. 29*, Wilhelmshaven, Germany.
- Remmers, W. et al., 2016. Elephant (*Loxodonta africana*) footprints as habitat for aquatic macroinvertebrate communities in Kibale National Park, south-west Uganda. *African journal of ecology*.
- Ridgeway, G., 2015. gbm: Generalized Boosted Regression Models.
- Rodriguez, A.B. et al., 2014. Oyster reefs can outpace sea-level rise. *Nature Climate Change*, 4(June), pp.493–497.
- Rosenberg, R., 2001. Marine benthic faunal successional stages and related sedimentary activity. *Scientia Marina*, 65, pp.107–119.



## References

- Ruesink, J.L. et al., 2005. INTRODUCTION OF NON-NATIVE OYSTERS: Ecosystem Effects and Restoration Implications. *Annual Review of Ecology, Evolution, and Systematics*, 36(1), pp.643–689.
- Ryu, J. et al., 2008. Detecting the intertidal morphologic change using satellite data. *Estuarine, Coastal and Shelf Science*, 78, pp.623–632.
- Ryu, J., Won, J. & Min, K.D., 2002. Waterline extraction from Landsat TM data in a tidal flat A case study in Gomso Bay, Korea. , 83, pp.442–456.
- Saier, B., 2001. Direct and indirect effects of seastars *Asterias rubens* on mussel beds (*Mytilus edulis*) in the Wadden Sea. *Journal of Sea Research*, 46(1), pp.29–42.
- Sanders, D. et al., 2014. Integrating ecosystem engineering and food webs. *Oikos*, 123(5), pp.513–524.
- Saurel, C., Gascoigne, J. & Kaiser, M.J., 2004. *The Ecology of Seed Mussel Beds: Literature Review*, Menai Bridge.
- Schindelin, J. et al., 2012. Fiji: an open-source platform for biological-image analysis. *Nature methods*, 9(7), pp.676–82.
- Schrenk, K.J. et al., 2014. Retention capacity of correlated surfaces. *Physical Review E*, 89(6), p.62141.
- Seed, R., 1976. Ecology of marine mussels. In B. L. Bayne, ed. *Marine mussels: their ecology and physiology*. London: Cambridge University Press, pp. 13–65.
- Seed, R. & Suchanek, T.H., 1992. Population and community ecology of *Mytilus*. *The mussel Mytilus: ecology, physiology, genetics and culture*, 25, pp.87–170.
- Simberloff, D., 1998. Flagships, umbrellas, and keystones: Is single-species management passe in the landscape era? *Biological Conservation*, 83(3), pp.247–257.
- Smaal, A., Stralen, M. & Craeymeersch, J., 2005. Does the introduction of the pacific oyster *Crassostrea gigas* lead to species shifts in the Wadden Sea? *The Comparative Roles of ...*, 47, pp.277–289.
- Smaal, A.C. et al., 2013. Decrease of the carrying capacity of the Oosterschelde estuary (SW Delta, NL) for bivalve filter feeders due to overgrazing? *Aquaculture*, 404–405, pp.28–34.
- Somero, G.N., 2002. Thermal physiology and vertical zonation of intertidal animals: Optima, limits, and costs of living. *Integrative and Comparative Biology*, 42(4), pp.780–789.
- Sousa, R., Gutiérrez, J.L. & Aldridge, D.C., 2009. Non-indigenous invasive bivalves as ecosystem engineers. *Biological Invasions*, 11(10), pp.2367–2385.
- Spooner, D.E. & Vaughn, C.C., 2006. Context-dependent effects of freshwater mussels on stream benthic communities. *Freshwater Biology*, 51(6), pp.1016–1024.
- Stachowicz, J.J., 2001. Mutualism, Facilitation, and the Structure of Ecological Communities. *BioScience*, 51(3), p.235.
- Syvitski, J.P.M. et al., 2009. Sinking deltas due to human activities. *Nature Geoscience*, 2(10), pp.681–686.
- Tanck, G., Alpers, W. & Gade, M., 1999. Determination of surface roughness parameters of tidal flats from SIR-C/X-SAR 3-frequency SAR data. In *IEEE 1999 International Geoscience and Remote Sensing Symposium IGARSS99 Cat No99CH36293*. pp. 8–10.
- Temmerman, S. et al., 2013. Ecosystem-based coastal defence in the face of global change. *Nature*, 504(7478), pp.79–83.
- Temmerman, S. et al., 2007. Vegetation causes channel erosion in a tidal landscape. *Geology*, 35(7), p.631.
- Thomas, Y. et al., 2016. Global change and climate-driven invasion of the Pacific oyster (*Crassostrea gigas*) along European coasts: A bioenergetics modelling approach. *Journal of Biogeography*, 43(3), pp.568–579.
- Tilman, D., Wedin, D. & Knops, J., 1996. Productivity and sustainability influenced by biodiversity in grassland ecosystems. *Nature*, 379(6567), pp.718–720.
- TMAG—Trilateral Monitoring and Assessment Group, 1997. *TMAP manual. The Trilateral Monitoring and Assessment Program (TMAP)*, Wilhelmshaven, Germany.
- Trenberth, K.E., 1997. The Definition of El Niño. *Bulletin of the American Meteorological Society*, 78(12), pp.2771–2777.
- Troost, K., 2010. Causes and effects of a highly successful marine invasion: Case-study of the introduced Pacific oyster *Crassostrea gigas* in continental NW European estuaries. *Journal of Sea Research*, 64(3), pp.145–165.
- Troost, K. et al., 2012. Ontwikkeling van schelpdierbestanden op de droogvallende platen van de Waddenzee. *De Levende Natuur*, pp.83–88.
- Troost, K., 2009. *Pacific oysters in Dutch estuaries: causes of success and consequences for native bivalves*. University of Groningen.
- Troost, K., Kamermans, P. & Wolff, W.J., 2008. Larviphagy in native bivalves and an introduced oyster. *Journal of Sea Research*, 60(3), pp.157–163.
- Ulaby, F.T., Moore, R.K. & Fung, A.K., 1986. *Microwave remote sensing, active and passive, volume III: From theory to applications*. Dedham: Artech House.
- Underwood, G.J.C. & Kromkamp, J., 1999. Primary

## References

- Production by Phytoplankton and Microphytobenthos in Estuaries. *Advances in Ecological Research*, 29(C), pp.93–153.
- Vanschoenwinkel, B. et al., 2011. Passive external transport of freshwater invertebrates by elephant and other mud-wallowing mammals in an African savannah habitat. *Freshwater Biology*, 56(8), pp.1606–1619.
- Vaughn, C.C., Spooner, D.E. & Galbraith, H.S., 2007. Context-dependent species identity effects within a functional group of filter-feeding bivalves. *Ecology*, 88(7), pp.1654–62.
- Van Der Veer, H.W. et al., 1998. Importance of predation by crustaceans upon bivalve spat in the intertidal zone of the Dutch Wadden Sea as revealed by immunological assays of gut contents. *Journal of Experimental Marine Biology and Ecology*, 231(1), pp.139–157.
- Verhoest, N.E.C. et al., 2008. On the Soil Roughness Parameterization Problem in Soil Moisture Retrieval of Bare Surfaces from Synthetic Aperture Radar. *Sensors*, 8, pp.4213–4248.
- Vermote, E. et al., 2006. *Second Simulation of a Satellite Signal in the Solar Spectrum - Vector (6SV)*.
- Vismann, B. et al., 2016. Field clearance of an intertidal bivalve bed: Relative significance of the co-occurring blue mussel *Mytilus edulis* and pacific oyster *Crassostrea gigas*. *Aquatic Biology*, 25, pp.107–119.
- de Vlas, J. et al., 2005. Intertidal blue mussel beds. In K. Essink et al., eds. *Wadden Sea Quality Status Report 2004. Wadden Sea Ecosystem No. 19*. Wilhelmshaven, Germany, pp. 190–200.
- Wa Kangeri, A.K. et al., 2014. Perturbation induced changes in substrate use by the blue mussel, *Mytilus edulis*, in sedimentary systems. *Journal of Sea Research*, 85, pp.233–240.
- van der Wal, D. et al., 2008. Distribution and dynamics of intertidal macrobenthos predicted from remote sensing: response to microphytobenthos and environment. *Marine Ecology Progress Series*, 367, pp.57–72.
- van der Wal, D., Herman, P. & Ysebaert, T., 2004. Spaceborne synthetic aperture radar of intertidal flat surfaces as a basis for predicting benthic macrofauna distribution. *EARSeL eProceedings*, pp.69–80.
- van der Wal, D., Herman, P.M.J. & Wielemaker-van den Dool, A., 2005. Characterisation of surface roughness and sediment texture of intertidal flats using ERS SAR imagery. *Remote Sensing of Environment*, 98(1), pp.96–109.
- van der Wal, D., Wielemaker-van den Dool, A. & Herman, P.M.J., 2010. Spatial Synchrony in Intertidal Benthic Algal Biomass in Temperate Coastal and Estuarine Ecosystems. *Ecosystems*, 13(2), pp.338–351.
- Waldbusser, G.G., Powell, E.N. & Mann, R., 2013. Ecosystem effects of shell aggregations and cycling in coastal waters: An example of Chesapeake Bay oyster reefs. *Ecology*, 94(4), pp.895–903.
- Wallès, B. et al., 2015. Demography of the ecosystem engineer *Crassostrea gigas*, related to vertical reef accretion and reef persistence. *Estuarine, Coastal and Shelf Science*, 154(January), pp.224–233.
- Wallès, B., Troost, K., et al., 2016. From artificial structures to self-sustaining oyster reefs. *Journal of Sea Research*, 108(January), pp.1–9.
- Wallès, B., Fodrie, F.J., et al., 2016. Guidelines for evaluating performance of oyster habitat restoration should include tidal emersion: reply to Baggett et al. *Restoration Ecology*, 24(1), pp.4–7.
- Wallès, B., Smaal, A.C., et al., 2016. Niche dimension differs among life-history stages of Pacific oysters in intertidal environments. *Marine Ecology Progress Series*, 562, pp.113–122.
- Wallès, B. et al., 2014. The ecosystem engineer *Crassostrea gigas* affects tidal flat morphology beyond the boundary of their reef structures. *Estuaries and Coasts*, 38(3), pp.941–950.
- Waser, A.M. et al., 2016. Impact on bird fauna of a non-native oyster expanding into blue mussel beds in the Dutch Wadden Sea. *Biological Conservation*, 202, pp.39–49.
- Weerman, E.J. et al., 2014. Predation by native brown shrimp on invasive Pacific oyster spat. *Journal of Sea Research*, 85, pp.126–130.
- Weerman, E.J., Herman, P.M.J. & Van De Koppel, J., 2011. Top-down control inhibits spatial self-organization of a patterned landscape. *Ecology*, 92(2), pp.487–95.
- White, G.E., Hose, G.C. & Brown, C., 2014. Influence of rock-pool characteristics on the distribution and abundance of inter-tidal fishes. *Marine Ecology*, 36, pp.1332–44.
- Whitehouse, R.J.S. et al., 2000. The influence of bedforms on flow and sediment transport over intertidal mudflats. *Continental Shelf Research*, 20(10–11), pp.1099–1124.
- Widdows, J. et al., 2009. Influence of self-organised structures on near-bed hydrodynamics and sediment dynamics within a mussel (*Mytilus edulis*) bed in the Menai Strait. *Journal of Experimental Marine Biology and Ecology*, 379(1–2), pp.92–100.
- Widdows, J. & Brinsley, M., 2002. Impact of biotic and abiotic processes on sediment dynamics and the consequences to the structure and functioning of the intertidal zone. *Journal of Sea Research*, 48(2), pp.143–156.
- Wing, M., 2011. Consumer-Grade GPS Receiver Measurement Accuracy in Varying Forest

## References

- Conditions. *Research Journal of Forestry*, 5(2), pp.78–88.
- Wright, J.P., Flecker, A.S. & Jones, C.G., 2003. Local vs. landscape controls on plant species richness in beaver meadows. *Ecology*, 84(12), pp.3162–3173.
- Wright, J.P. & Jones, C.G., 2004. Predicting effects of ecosystem engineers on patch-scale species richness from primary productivity. *Ecology*, 85(8), pp.2071–2081.
- Wright, J.P. & Jones, C.G., 2006. The Concept of Organisms as Ecosystem Engineers Ten Years On: Progress, Limitations, and Challenges. *BioScience*, 56(3), p.203.
- Wright, J.P., Jones, C.G. & Flecker, A.S., 2002. An ecosystem engineer, the beaver, increases species richness at the landscape scale. *Oecologia*, 132(1), pp.96–101.
- Wu, C., 2011. VisualSFM: A Visual Structure from Motion System. Available at: <http://ccwu.me/vsfm/> [Accessed September 3, 2012].
- Yamaguchi, K., 1994. Shell structure and behaviour related to cementation in oysters. *Marine Biology*, 118(1), pp.89–100.
- Yang, S.L. et al., 2008. Spatial and temporal variations in sediment grain size in tidal wetlands, Yangtze Delta: On the role of physical and biotic controls. *Estuarine, Coastal and Shelf Science*, 77(4), pp.657–671.
- Yoshino, K. et al., 2012. Intertidal bare mudflats subsidize subtidal production through outwelling of benthic microalgae. *Estuarine, Coastal and Shelf Science*, 109, pp.138–143.
- Ysebaert, T., Hart, M. & Herman, P.M.J., 2008. Impacts of bottom and suspended cultures of mussels *Mytilus* spp. on the surrounding sedimentary environment and macrobenthic biodiversity. *Helgoland Marine Research*, 63(1), pp.59–74.
- van Zanten, E. & Adriaanse, L., 2008. *Verminderd getij. Verkenning van mogelijke maatregelen om de erosie van platen, slikken en schorren van de Oosterschelde te beperken; Rapport RWS/2008*, Middelburg, Zeeland.
- van der Zee, E.M. et al., 2015. Habitat modification drives benthic trophic diversity in an intertidal soft-bottom ecosystem. *Journal of Experimental Marine Biology and Ecology*, 465, pp.41–48.
- van der Zee, E.M. et al., 2016. How habitat-modifying organisms structure the food web of two coastal ecosystems. *Proceedings of the Royal Society B: Biological Sciences*, 283, p.20152326.
- van der Zee, E.M. et al., 2012. Spatially Extended Habitat Modification by Intertidal Reef-Building Bivalves has Implications for Consumer-Resource Interactions. *Ecosystems*, 15(4), pp.664–673.
- Zribi, M. & Dechambre, M., 2002. A new empirical model to retrieve soil moisture and roughness from C-band radar data. *Remote Sensing of Environment*, 84, pp.42–52.



---

## Appendix

### A.1 Pool water depth development during low tide

To verify that pools within shellfish reefs contain surface water while the shellfish reefs are emerged during the low water period, water levels were measured using a simple ruler and using pressure loggers in five pools in the oyster reef and seven locations (not necessarily pools) outside of the reef at Neeltje Jans (see Figure A.1 A). The development of the water depth was recorded using two water pressure loggers at each of these locations (Sensus Ultra by ReefNet Inc, resolution = 1 mbar). To prevent interference of the pressure measurements due to bed load transport and accretion of sediments, the pressure loggers were placed 5 cm above the sediment surface. The pressure loggers were deployed on March the 15<sup>th</sup> 2017 and retrieved on March the 17<sup>th</sup>. Water height above the pressure loggers was measured using a ruler during deployment just before the tide came in. After deployment, the loggers were placed in a bucket with water with 0, 5, 10, 16.5 and 20 cm of water on top, to allow calibrations of each sensor and to convert pressure in mbar to water height in cm (1 mbar roughly corresponds to 1 cm water height). At each point in time, the average pressure recorded by two pressure loggers on land was subtracted from the pressure of each submersed loggers to compensate for atmospheric effects. To minimize the effect of logger-specific deviations during the deployment, we only interpreted the water levels of the last low tide period, which was closest to the sensor calibration. We calculated the average water depth at low tide for each location obtained from the two sensors just before they were removed from the field. The results (Figure A.1 B-D) reveal restricted drainage from the pools particularly at the beginning of the low tide period, whereas two hours prior to the incoming tide the water is virtually stagnant in the pools within the reef and location 2 and 4 outside the reef; i.e. here water remains in the pool during the entire low tide period (see Figure A.1 C and D). At the other locations, water depths drain to or below 5cm above the sediment surface, which is below sensor height (see Figure A.1 D). Hence, these measurements reveal that water is retained in the pools and remains relatively stagnant during the emergence of the reef.



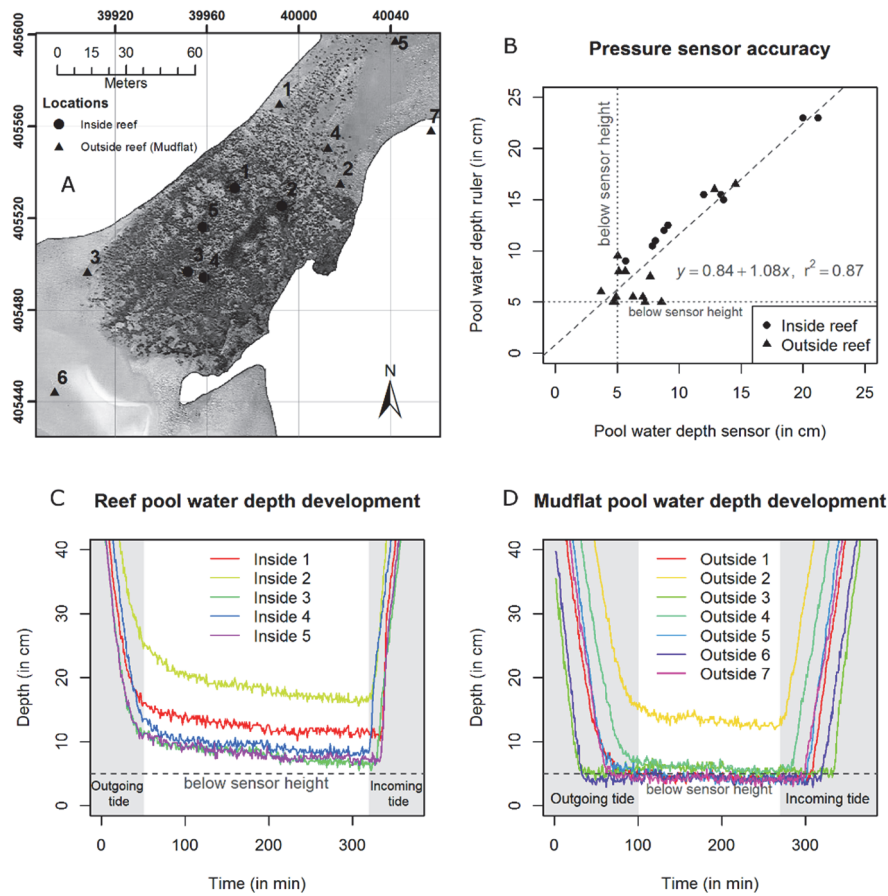
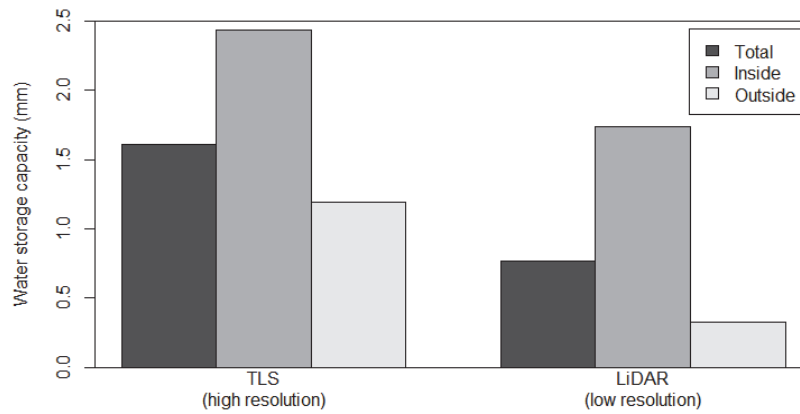


Figure A.1 A) The locations which were measured using a ruler and logged using the Sensus pressure loggers. B) The comparison between water depth obtained with a ruler and water depth obtained with the pressure loggers. Note that water depths under 5 cm cannot be detected, as the sensors were placed 5 cm above the sediment surface. The  $R^2$  value of 0.87 indicates the pressure loggers measure water depth reasonably accurate. C) Water depth development of the 5 pools in the oyster reef. D) Water depth development of the locations outside of the oyster reef.

## A.2 Comparison TLS data and LIDAR data



*Figure A.2 The effect of investigating water storage capacity at various resolutions obtained by decreasing the resolution of the high resolution TLS data (pixel size = 25\*25 cm) of the mussel reef at Schiermonnikoog to match the low resolution LiDAR data (pixel size = 5\*5 m). Although differences can be observed in average water storage capacity per pixel, total water storage capacity is hardly affected by the resolution at investigation. In addition, the differences between the classes are maintained at different resolutions.*

### A.3 Landscape characterization procedure

40\*40 m<sup>2</sup> sub selections were taken from the terrestrial laser scan data of both reef and bare mudflat classes for surface characterization (see Fig. 1). Since the characterization of the landscape by semivariograms requires our data to be stationary, the measured landscapes were detrended using a 5<sup>th</sup> degree polynomial surface. This detrending procedure did not remove surface features at the scale of the reef structures, however it does increase ponding by removing slopes, which means that detrended landscapes will overestimate retention (see results main text). 2D semivariance was calculated from the detrended surfaces in all directions. The minor and major axis of anisotropy were found by finding the angles of the smallest and largest distance respectively, where the 2d semivariogram equals half the variance of the total surface. The distances of these axes were also used to calculate the anisotropy ratio (minor/major). In order to fit a correlation structure, the data were transformed in the direction of the major axis (longest correlation structures) to obtain isotropic data. Next, data were binned in 0.25m classes to fit a spherical, a Gaussian and an exponential correlation structure to the semivariogram to obtain range and sill parameters (Legendre & Legendre 2012) (see Figure A.3). We used the Akaike Information Criterion (AIC) to decide which correlation structure best described the topography of our surfaces. Results for the individual reefs and their surrounding mudflat are given in Table A.3.

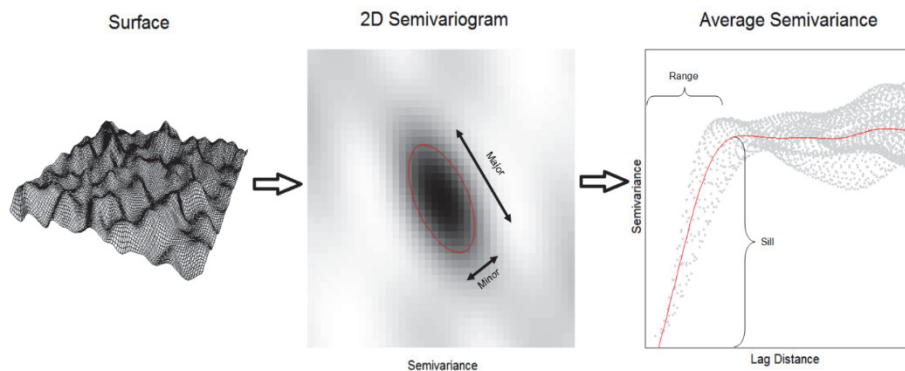


Figure A.3 A schematic of the landscape characterization procedure. A surface (rasterized from the pointcloud of the laser scanner) was used to compute a 2D semivariogram. The red line contour indicates where the semivariogram equals half the variance of the input surface. From the ellipse the major and minor axes, their ratio and the angle are derived. Finally range and sill parameters are derived from the average semivariogram; depending on the autocorrelation function (ACF), which showed the best fit according to the Aikaike Information Criterion (AIC).

## Appendix

Table A.3. Surface parameters of the different investigated locations, ACF with asterisk indicates model with lowest AIC value.

| Location                       | Name                                | Ratio<br>(minor/major) | Angle <sup>1</sup><br>(°) | ACF  | AIC       | Nugget<br>(mm) | Sill<br>(mm) | Major<br>Range<br>(m) |
|--------------------------------|-------------------------------------|------------------------|---------------------------|------|-----------|----------------|--------------|-----------------------|
| Schiermonnikoog,<br>Wadden Sea | Mussel<br>reef                      | 0.51                   | -5                        | Sph* | -46743.70 | -2.26E-02      | 3.00         | 3.52                  |
|                                |                                     |                        |                           | Gau  | -46729.67 | 2.36E-01       | 2.74         | 1.63                  |
|                                |                                     |                        |                           | Exp  | -46703.57 | -3.48E-01      | 3.35         | 1.26                  |
|                                | Mudflat<br>around<br>musel reef     | 0.50                   | -164                      | Sph  | -55337.56 | 1.96E-02       | 0.07         | 6.10                  |
|                                |                                     |                        |                           | Gau  | -55298.89 | 2.65E-02       | 0.06         | 2.85                  |
|                                |                                     |                        |                           | Exp* | -55356.41 | 9.66E-03       | 0.08         | 2.11                  |
|                                | Oyster<br>reef                      | 0.92                   | -106                      | Sph  | -67129.58 | 4.91E-02       | 0.31         | 5.64                  |
|                                |                                     |                        |                           | Gau  | -67097.24 | 7.59E-02       | 0.28         | 2.54                  |
|                                |                                     |                        |                           | Exp* | -67183.18 | 6.83E-03       | 0.36         | 2.07                  |
|                                | Mudflat<br>around<br>Oyster<br>reef | 0.50                   | -63                       | Sph  | -27061.68 | 4.20E-03       | 0.01         | 3.91                  |
|                                |                                     |                        |                           | Gau  | -27050.16 | 4.75E-03       | 0.01         | 1.59                  |
|                                |                                     |                        |                           | Exp* | -27088.31 | 3.23E-03       | 0.01         | 1.67                  |
| Neeltje Jans,<br>Oosterschelde | Oyster<br>reef                      | 0.11                   | -42                       | Sph  | -63756.26 | 3.65E+00       | 3.21         | 12.68                 |
|                                |                                     |                        |                           | Gau  | -63732.22 | 4.03E+00       | 2.83         | 6.13                  |
|                                |                                     |                        |                           | Exp* | -63771.19 | 3.22E+00       | 3.77         | 4.77                  |
|                                | Mudflat<br>around<br>oyster reef    | 0.27                   | -45                       | Sph  | -66705.90 | -2.82E-02      | 0.75         | 3.70                  |
|                                |                                     |                        |                           | Gau* | -66716.34 | 4.19E-02       | 0.69         | 1.76                  |
|                                |                                     |                        |                           | Exp  | -66667.90 | -6.94E-02      | 0.81         | 1.52                  |

<sup>1</sup> Angle of the major axis, 0° indicates a south-north direction, ACF is the auto correlation function (Spherical, Gaussian or Exponential), AIC is the Akaike Information Criterion, \* indicates the best fit ACF based on the lowest AIC

## B.1 Locations of field sampling

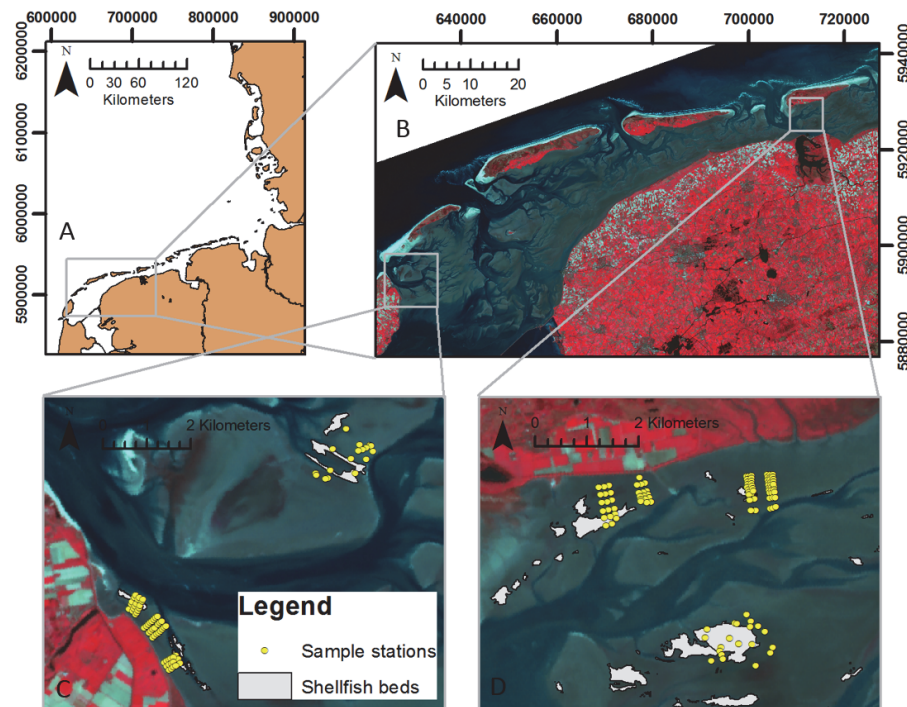


Figure B.1 Locations of field sampling. A) The location of the Dutch Wadden Sea. B) UKDMC-ii image with study areas. C) Sampling stations near the island of Texel in the western part of the Wadden Sea. D) Sampling stations south of the island of Schiermonnikoog in the eastern part of the Wadden Sea.

## B.2 Macro-algae cover in ground surveys

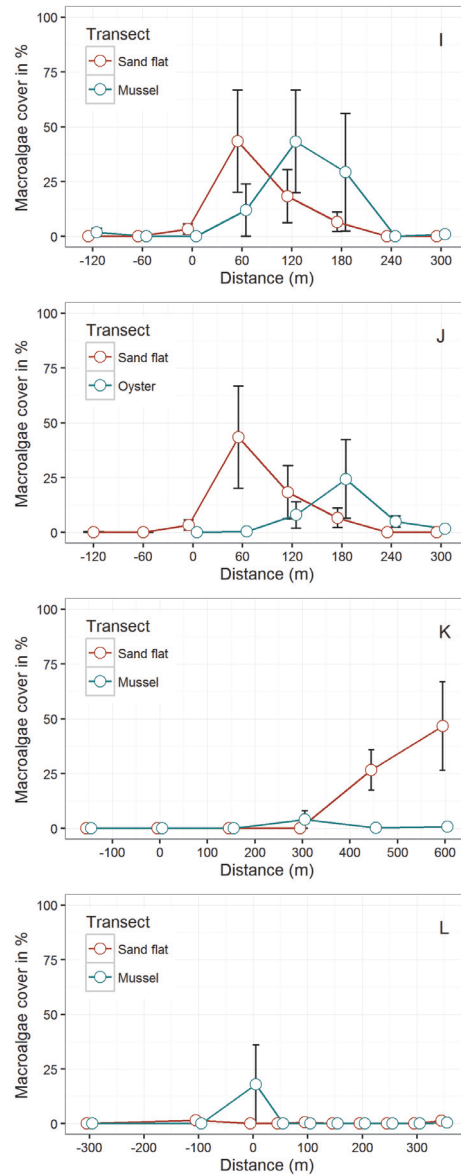


Figure B.2 Macro algae cover (in %) from ground surveys, averaged per set of three mussel/oyster and sand flat transects, respectively. A) at the Texel mussel reef; B) at the Texel oyster reef; C) at the Schiermonnikoog mixed reef and D) at the Schiermonnikoog mussel reef. See Fig. S1 for location of the transects. Distance of 0 is within the reef, positive distances are in seaward direction.



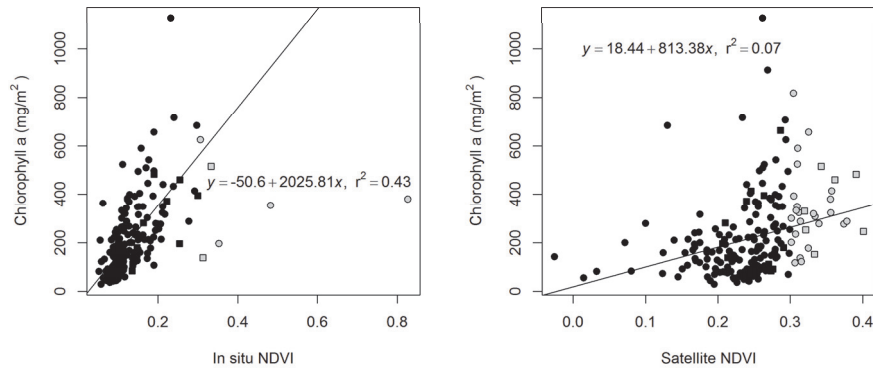
B.3 Satellite NDVI vs *in situ* NDVI

Figure B.3. Relation between *in situ* NDVI and chlorophyll a concentration ( $\text{mg}/\text{m}^2$ ) ( $F_{1,181}=138.9$ ,  $p < 0.05$ ) and satellite NDVI and chlorophyll a concentration ( $\text{mg}/\text{m}^2$ ) ( $F_{1,186}=11.75$ ,  $p < 0.05$ ), at the sample stations (see Figure B.1). Samples in frames with macroalgae cover <10% are displayed with dots, samples with macroalgae cover >10% are displayed as squares. Samples with NDVI < 0.3 are displayed in black, NDVI > 0.3 are displayed in light grey. Regression lines are fitted on samples with NDVI < 0.3 only.

## B.4 Abiotic circumstances at reef types

Table B.4 Mean and standard deviations (SD) of the abiotic variables (elevation, currents and waves) as well as distance to shellfish reef and NDVI for the tidal flats allocated to the three different reef types in the different regions of the Wadden Sea.

| Reef type     | Region<br>Wadden Sea | Mean<br>Elevation (cm) |        | Mean Currents<br>(ms <sup>-1</sup> ) |       | Mean Waves<br>(ms <sup>-1</sup> ) |        | Mean<br>Distance (m) |      | Mean<br>NDVI |       | N       |
|---------------|----------------------|------------------------|--------|--------------------------------------|-------|-----------------------------------|--------|----------------------|------|--------------|-------|---------|
|               |                      | Mean                   | SD     | Mean                                 | SD    | Mean                              | SD     | Mean                 | SD   | Mean         | SD    |         |
| <b>All</b>    | Within reef, All     | -39.845                | 27.470 | 0.179                                | 0.042 | 0.0213                            | 0.0101 | N.A.                 | N.A. | 0.263        | 0.085 | 27242   |
|               | All                  | -32.393                | 46.280 | 0.189                                | 0.066 | 0.0212                            | 0.0146 | 1850                 | 1841 | 0.184        | 0.056 | 1302914 |
|               | West                 | -36.929                | 39.796 | 0.187                                | 0.055 | 0.0269                            | 0.0157 | 2532                 | 2157 | 0.174        | 0.053 | 698486  |
|               | East                 | -27.152                | 52.303 | 0.192                                | 0.077 | 0.0145                            | 0.0098 | 1063                 | 879  | 0.197        | 0.058 | 604428  |
| <b>Mussel</b> | Within reef, All     | -25.291                | 20.318 | 0.161                                | 0.037 | 0.0172                            | 0.0080 | N.A.                 | N.A. | 0.253        | 0.059 | 12770   |
|               | All                  | -25.844                | 50.437 | 0.187                                | 0.071 | 0.0177                            | 0.0134 | 1821                 | 1725 | 0.194        | 0.057 | 573657  |
|               | West                 | -31.512                | 43.244 | 0.185                                | 0.050 | 0.0258                            | 0.0163 | 3318                 | 2098 | 0.189        | 0.052 | 181619  |
|               | East                 | -23.217                | 53.238 | 0.188                                | 0.079 | 0.0139                            | 0.0098 | 1128                 | 894  | 0.197        | 0.059 | 392038  |
| <b>Mixed</b>  | Within reef, All     | -49.517                | 25.203 | 0.194                                | 0.040 | 0.0235                            | 0.0093 | N.A.                 | N.A. | 0.285        | 0.082 | 12328   |
|               | All                  | -33.477                | 43.808 | 0.188                                | 0.062 | 0.0206                            | 0.0128 | 1573                 | 1376 | 0.186        | 0.056 | 472611  |
|               | West                 | -30.619                | 40.388 | 0.182                                | 0.057 | 0.0229                            | 0.0141 | 1997                 | 1478 | 0.179        | 0.054 | 296311  |
|               | East                 | -38.281                | 48.645 | 0.200                                | 0.067 | 0.0168                            | 0.0091 | 861                  | 772  | 0.198        | 0.057 | 176300  |
| <b>Oyster</b> | Within reef, All     | -70.914                | 26.689 | 0.199                                | 0.034 | 0.0332                            | 0.0120 | N.A.                 | N.A. | 0.197        | 0.161 | 2144    |
|               | All                  | -45.037                | 37.355 | 0.195                                | 0.062 | 0.0299                            | 0.0167 | 2426                 | 2569 | 0.159        | 0.050 | 256646  |
|               | West                 | -49.867                | 32.236 | 0.195                                | 0.054 | 0.0330                            | 0.0153 | 2604                 | 2698 | 0.154        | 0.048 | 220556  |
|               | East                 | -15.520                | 50.581 | 0.195                                | 0.096 | 0.0107                            | 0.0105 | 1335                 | 1021 | 0.192        | 0.048 | 36090   |









---

## Summary

### Ecosystem engineering shellfish

Blue mussels (*Mytilus edulis*) and Pacific oysters (*Crassostrea gigas*) are bivalves that occur on temperate intertidal coasts and estuaries. Typically, these shellfish attach to hard substrates like rocks and dike embankments. However, in the absence of suitable hard substrate they create reefs on soft sandy bottoms using both living and dead shell material as attachment substrate. Shellfish reefs can become large enough to significantly change the environment in several ways. The physical structure of the reefs influences flow patterns and dampens wave action. The shellfish filter the water, allowing more sunlight to reach the bottom. The physical structure of the shellfish reefs provides a habitat to organisms that seek shelter from predation and desiccation during low tide. Species that exert such a pronounced influence on the functioning of the ecosystem by modifying physical properties of the ecosystem are called ecosystem engineers.

Despite the value of mussel and oyster reefs, they are under pressure due to fisheries and global change. Moreover, species invasions related to aquaculture and transport are rapidly changing the composition and structure of shellfish reefs worldwide. As an example, the Pacific oyster is invasive in large parts of Europe and is still expanding its distribution range. It is still unclear what the consequences of this invasion are for the functioning of ecosystems.

Recent qualitative assessments have demonstrated that the spatial extent of ecosystem engineering by shellfish reefs largely exceeds the area of occurrence of the reefs. However, using traditional monitoring techniques (field surveys), it is virtually impossible to assess the spatial effects of shellfish reefs cost-efficiently. In this thesis, remote sensing tools are applied to identify the presence of shellfish reefs (Chapter 2) and to quantitatively assess the extended range of influence and its consequences for the surrounding ecosystem (Chapter 4 and 5). Chapter 2 describes how shellfish reefs can be monitored using radar satellite data. Chapter 3 examines where mussel-, oyster- and mixed reefs (consisting of both species) manifest themselves in relation to the tidal gradient within the Dutch Wadden Sea. Chapters 4 and 5 quantify two different types of spatially extended ecosystem engineering in a spatial context.

## Using satellite and airborne remote sensing to detect shellfish reefs and their long-distance effects

In this thesis, remote sensing techniques, such as satellite Synthetic Aperture Radar (SAR)-, optical satellite remote sensing and airborne Light Detection and Ranging (LiDAR), were used extensively to elucidate the importance of shellfish reefs for ecosystem functioning. Synthetic Aperture Radar (SAR) sensors send microwaves to the earth and measure the backscatter of these microwaves. Using SAR it is possible to distinguish rough surfaces, such as the rough surface of shellfish reefs compared to flat mud. In addition, shellfish reefs depolarize the microwave signal and as a result the cross-polarized channel discriminates well between mud flat and shellfish reefs. Unlike optical sensors, SAR sensors do not depend on the sun and are largely insensitive to clouds, increasing the window of opportunity for successful data acquisitions. In this thesis the potential of two dual polarized SAR satellite sensors (Radarsat and TerraSAR-X) was explored for shellfish mapping. SAR satellite sensors were found unsuitable to discriminate species and densities, but, using dual polarized data, they allowed mapping presence and absence of shellfish reefs over vast areas of intertidal flat (Chapter 2)

The niche of the different types of shellfish reefs (mussel-, oyster- and mixed reefs) along the tidal gradient was studied using LiDAR-based inundation time maps in combination with shellfish field surveys (Chapter 3). Long-distance effects of the presence of the reefs were also investigated using remote sensing. Laser altimetry data was used to obtain information on potential water retention (tidal pools) within and around shellfish reefs (Chapter 4). Finally, satellite optical remote sensing was used to retrieve information on the biomass of (micro)phytobenthos around shellfish reefs (Chapter 5).

## Mussel versus oysters in the Dutch Wadden Sea

While mussels are native in the Wadden Sea, Japanese oysters invaded the area from the 1990s onwards. Initially, it was feared that the invasive oyster might outcompete the native mussels, but now it has become clear that mussels and oysters can co-exist in a stable situation in a single reef. To understand how the extent of the spatial effects depends on shellfish reef type (mussel, oyster and mixed reefs) it was investigated whether and how the three different reef types partition themselves along the tidal gradient and whether this distribution is linked to the species' physiological performance (Chapter 3). Oysters initially colonized the deeper parts of the intertidal, but used pre-existing mussel reefs to expand to shallower areas. In the same manner, mussels have made use of stable oyster reefs to occur deeper in the intertidal. Because of this, mixed reefs are becoming more prominent at the expense of pure mussel and oyster reefs which



have become restricted to the shallow intertidal and deep intertidal zone respectively. Oysters perform better (as indicated by condition index) with increasing depth, while mussels have a preference for intermediate inundation times. This partitioning indicates that both species can co-exist in the Wadden Sea, without one species outcompeting the other. However, the modified distribution patterns caused by the introduction of the oysters might still have consequences for the spatially extended ecosystem engineering effects.

### Long-distance effects of mussel and oyster presence

In this thesis two different kinds of ecosystem engineering have been examined: A) the formation of tidal pools by modifying the topography of the mudflats (Chapter 4) and B) the facilitation of benthic microalgae (Chapter 5).

The roughness of shellfish reefs in combination with the production of (pseudo-) faeces by the shellfish promotes sedimentation of fine particulate matter in and around the reefs. The spatial differences in fine sediment accumulation around shellfish reefs creates a landscape where at some locations water may be trapped which hardly drains during low tide. Such pools provide refuge from tidal desiccation and predation to many species. The shellfish reefs do not only promote such pools locally. Using a combination of SAR satellite remote sensing and airborne laser altimetry, it was established that south of the island of Schiermonnikoog in the Wadden Sea shellfish reefs promote pool formation up to 115 meter beyond the local footprint of the shellfish reefs. Given that the local footprint of shellfish reefs only occupies about 2% of the intertidal zone in that area, the extended footprint occupies up to 11% of the intertidal zone (a five-fold increase).

Multiple processes cause the facilitation of benthic microalgae on the mudflats. The shellfish reefs reduce flow and waves preventing erosion of algae. Light can better penetrate water because it is less turbid. Faeces accumulate on the leeward side of the bed. These circumstances in the wake of shellfish reefs are ideal for the growth of benthic algae. Concentrations of benthic algae are retrieved from optical satellite remote sensing (i.e., an UK DMC-2 image) (Chapter 5). A statistical model was developed that predicts these benthic algae concentrations from height information and information from models that describe waves and currents in the Wadden Sea. Results show that although abiotics are most important in predicting the biomass of benthic algae, shellfish reefs play a significant role as well. Allowing for height, waves and flow, the model predicts that, on average, benthic algal biomass is elevated by 15% in the vicinity of shellfish reefs, and that this facilitating effect declines logarithmically up to a distance of 1000 meters. A statistical model shows that at 340 meters, the (micro)algae stocks are still elevated by 5%. A spatially extended effect of up to

1000 meters implies that 40% of the entire intertidal Dutch Wadden Sea is potentially influenced by shellfish reefs. The highest concentrations of (micro)algae are observed around mussel reefs, but the strongest facilitation is observed around mixed reefs. The facilitation by shellfish reefs implies that at the scale of the Dutch Wadden Sea total benthic (micro)algae concentrations are 3% higher with shellfish reefs compared to a situation where the reefs would be absent. This underlines the importance of shellfish reefs for the functioning of the ecosystem at large spatial scales and their fundamental role in sustaining shellfish, fishes (and thus fisheries), birds and mammals.

### Management implications

This thesis shows that shellfish reefs drive key processes at much larger spatial scales than their area of occurrence. The large scale spatial effects of ecosystem engineers described in this thesis show that it is important for management to consider the ecosystem at large as a linked dynamic network of systems rather than a collection of independent systems.







---

## Samenvatting

### Biobouwende schelpdieren

Mosselen (*Mytilus edulis*) en Japanse oesters (*Crassostrea gigas*) zijn tweekleppige schelpdieren die voorkomen in droogvallende kustgebieden met een gematigd klimaat. Normaliter vestigen deze schelpdieren zich op hard substraat zoals rotsen en dijkverstevingen, maar bij gebrek hieraan kunnen ze ook banken vormen op zachte zandbodems. Levende en dode schelpen doen dan dienst als verankeringsubstraat. De schelpdierbanken kunnen dusdanig groot worden dat ze de directe omgeving op een aantal manieren sterk beïnvloeden. Eén van die invloeden is dat door de structuur van de banken stromingspatronen veranderen en golven worden gedempt. Verder filteren de schelpdieren het water, waardoor meer zonlicht de wadbodem kan bereiken. Bij de filtratie produceren ze (pseudo-) faeces die het omliggende wad verrijken met nutriënten en slib. De schelpdierbanken zelf fungeren als een belangrijk habitat voor allerlei dieren die daar beschutting zoeken tegen predatie en uitdroging tijdens eb. Soorten die een sterke invloed hebben op het functioneren van de lokale ecologie doordat ze de fysieke eigenschappen van de omgeving veranderen, worden biobouwers genoemd.

Mossel- en oesterbanken zijn ecologisch uiterst waardevolle systemen, maar staan desondanks in veel gebieden onder druk. In grote delen van Europa, ook in Nederland, is de oorspronkelijke platte oester bijna verdwenen, en breidt de niet-inheemse Japanse oester zich sterk uit. Het is niet duidelijk wat de gevolgen zijn van de aanwezigheid van deze biobouwers voor het functioneren van de ecosystemen.

Recent werk heeft aangetoond dat de biobouwer-effecten invloed hebben op een ruimtelijke schaal die groter is dan de schelpdierbanken zelf. Het is belangrijk om goed te begrijpen hoe groot de rol is van biobouwende schelpdieren voor het functioneren van het ecosysteem en op welke ruimtelijke schaal en onder welke condities die effecten zich manifesteren. Dat maakt het uiteindelijk mogelijk om een inschatting te maken van de gevolgen voor het ecosysteem wanneer schelpdierbanken verdwijnen, of wanneer ze juist geïntroduceerd worden. In dit proefschrift worden remote sensing technieken gebruikt om de schelpdierbedden te karteren (Hoofdstuk 2) en om de ruimtelijke invloed van schelpdierbanken te kwantificeren (Hoofdstuk 4 en 5). Hoofdstuk 2 beschrijft hoe schelpdierbedden



gekarteed en gemonitord kunnen worden met behulp van radar satelliet remote sensing. Hoofdstuk 3 beschrijft waar mossel-, oester- en gemengde banken zich ruimtelijk manifesteren ten opzichte van de getijdegradiënt in de Nederlandse Waddenzee. In hoofdstukken 4 en 5 worden twee biobouwende effecten van de verschillende typen schelpdierbedden in ruimtelijke zin gekwantificeerd.

### Remote Sensing van schelpdierbanken en hun ruimtelijke effecten

In dit proefschrift worden verschillende remote sensing technieken, zoals imaging SAR (Synthetic Aperture Radar), waarneming met optische satelliet-sensoren en vliegtuig LiDAR (Light Detection and Ranging), gebruikt om het belang van schelpdierbanken voor het functioneren van het ecosysteem te onderzoeken. SAR sensoren zenden microgolven naar de aarde en meten de hoeveelheid microgolven die teruggekaatst worden door het aardoppervlak. Met behulp van SAR is het goed mogelijk om ruwe oppervlakten, zoals schelpdierbanken, te onderscheiden van vlakke oppervlakten, zoals slik. Daarnaast depolariseren schelpdierbedden de microgolven en kan gebruik worden gemaakt van het cross-polarized kanaal van de SAR satelliet-sensor voor extra onderscheidend vermogen. Anders dan bij optische satelliet-sensoren, is detectie met een SAR instrument niet afhankelijk van de zon en nauwelijks gevoelig voor wolken. Dit vergroot het aantal beelden dat ingewonnen kan worden in de tijd. In dit proefschrift is onderzocht of twee ‘dual polarized’ SAR satellieten (Radarsat-2 en TerraSAR-X) gebruikt kunnen worden om schelpdierbanken in kaart te brengen. Alhoewel deze sensoren niet in staat bleken onderscheid te maken tussen soorten en dichtheden van schelpen binnen een bank, konden ze wel de aan- of afwezigheid van schelpdierbanken over grote oppervlakten getijgebied succesvol karteren (Hoofdstuk 2).

De niche van de verschillende type schelpdierbanken (mossel-, oester- en gemengde banken) over de inundatie-gradiënt is afgeleid van inundatietijdkaarten (gebaseerd op LiDAR data), in combinatie met veldonderzoek van schelpdierbanken (Hoofdstuk 3). Lange afstandseffecten van de schelpdierbanken zijn ook in kaart gebracht met behulp van remote sensing. Laser altimetrie data zijn gebruikt om te bepalen waar potentiële getijde-poeltjes worden gevormd binnen en buiten de schelpdierbanken (Hoofdstuk 4). Uit optische satellietbeelden is een schatting gemaakt van de biomassa van benthische (micro-)algen rond de banken (Hoofdstuk 5).

### Mosselen versus oesters in de Nederlandse Waddenzee

Terwijl mosselen van nature in de Waddenzee voorkomen, hebben de invasieve Japanse oesters zich hier pas echt succesvol gevestigd sinds de jaren ‘90.



Aanvankelijk bestond de vrees dat Japanse oesters de inheemse mosselen zouden verdrijven, maar inmiddels blijkt dat mosselen en oesters samen in een schelpdierbank kunnen voorkomen. Met het oog op het inschatten van ecosysteemeffecten, is in hoofdstuk 3 onderzocht waar mossel-, oester- en gemengde banken voorkomen ten opzichte van de inundatie-gradiënt en waar mosselen en oesters de beste conditie hebben. Oesters hebben zich aanvankelijk op de diepere plekken van droogvallend gebied gevestigd, maar kunnen mosselbanken gebruiken om zich in beperkte mate naar de ondiepere delen uit te breiden. Op dezelfde manier kunnen mosselen de bescherming binnen oesterbanken gebruiken om wat dieper voor te komen dan ze zonder de aanwezigheid van oesters zouden kunnen. Gemengde bedden zijn op die manier het meest voorkomende type schelpdierbank aan het worden. Pure mosselbanken komen enkel nog voor op de meest ondiepe plekken en er zijn alleen pure oesterbanken op plekken die nauwelijks droogvallen. Oesters hebben over het algemeen een hogere conditie in de lagere delen van het intergetijdengebied, terwijl dat optimum voor mosselen hoger ligt. Deze verdeling betekent dat de kans vrij groot is dat beide soorten stabiel samen voor kunnen komen in de Waddenzee zonder elkaar weg te concurreren. Wel kan dit samen voorkomen van beide soorten gevolgen hebben voor de ruimtelijke effecten van het biobouwen.

### Lange afstandseffecten van schelpdierbanken

In dit proefschrift zijn twee verschillende vormen van biobouwen nader onderzocht: A) het vormen van potentiële getijdepoelen door het aanpassen van de structuur (topografie) van het wad (hoofdstuk 4) en B) het faciliteren van microalgen op het sediment (hoofdstuk 5).

De ruwheid van schelpdierbedden in combinatie met de productie van (pseudo-) faeces door de schelpdieren zorgt voor verhoogde sedimentatie van fijne bodemdeeltjes. De afwisselende ophoping van bodemdeeltjes zorgt ervoor dat er een landschap ontstaat waarin op bepaalde plekken water kan blijven staan. Deze poeltjes lopen nauwelijks leeg tijdens eb en bieden vele organismen een plek om bijvoorbeeld de tijd tussen eb en vloed te overbruggen en om beschutting te zoeken tegen predatoren. De schelpdierbanken faciliteren de vorming van potentiële getijdepoelen niet alleen lokaal. Met behulp van remote sensing is bepaald dat het potentieel om water vast te houden op het wad ten zuiden van het eiland Schiermonnikoog verhoogd is tot op ongeveer honderd meter buiten de schelpdierbanken. De schelpdierbanken nemen slechts 2% van de oppervlakte van het getijdengebied in, maar de oppervlakte waarop deze biobouwers invloed uitoefenen buiten de fysieke grenzen van de schelpdierbanken om, is tot meer dan 5 keer groter (tot 11%).

Het faciliteren van microalgen op het wad wordt veroorzaakt door verschillende processen. De schelpdierbanken dempen de stroomsnelheid en golfwerking, wat voorkomt dat de algen wegspoelen. Licht kan beter doordringen in het water doordat er minder materiaal in het water zweeft. Ontlasting vanuit de schelpdierbanken hoopt op in de luwte van de bedden. Deze omstandigheden die door de biobouwers in de luwte van de banken worden gecreëerd, zijn ideaal voor de groei van algen. De concentraties van benthische algen om de schelpdierbanken heen is bepaald aan de hand van optische beelden van de satelliet UK-DMC 2. Een statistisch model gebaseerd op informatie van de algenconcentraties van de bodem uit remote sensing in combinatie met hoogte-informatie en informatie uit golf- en stromingsmodellen, laat zien dat in de Waddenzee het voorkomen van de algen met name wordt verklaard door de stroming en golven, maar ook door de nabijheid van schelpdierbanken. Gecorrigeerd voor hoogteligging, stroming en golven, zijn nabij schelpdierbanken de algenconcentraties 15% hoger dan op niet door schelpdierbanken beïnvloede plekken en dit faciliteren van algen loopt met logaritmisch afnemende sterkte door tot ongeveer een kilometer buiten de schelpdierbanken. Zo is de NDVI (de Normalized Difference Vegetation index, een vegetatie-index voor de hoeveelheid benthische algen op het wad) op 340 m afstand van schelpdierbedden gemiddeld nog zo'n 5% verhoogd. In totaal laat het statistisch model zien dat binnen een straal van een kilometer rond de bedden facilitatie van algen kan plaatsvinden. Dit beïnvloede gebied beslaat tot 40% van de hele Nederlandse Waddenzee. De concentraties van microalgen op het sediment zijn het hoogst nabij mosselbanken, maar de facilitatie van microalgen is het sterkst rondom gemengde banken. De facilitatie door schelpdierbanken betekent op de schaal van de hele Waddenzee een toename van 3% in de hoeveelheid microalgen op de bodem en onderstreept het belang van schelpdierbanken voor het functioneren van het ecosysteem op veel grotere schaal. Schelpdierbanken vormen een fundament van het ecosysteem, en ondersteunen andere schelpdieren, vissen, vogels en zoogdieren.

### De implicaties

De resultaten in dit proefschrift laten zien dat schelpdierbanken niet alleen lokale processen beïnvloeden, maar dat ze ecologische processen op veel grotere schalen aandrijven. Toch staan schelpdierbanken, en biobouwers in het algemeen, wereldwijd onder druk. Het verdwijnen van deze sleutelorganismen heeft niet alleen grote ecologische gevolgen maar ook economische. Machinale schelpdiervisserij is inmiddels niet meer toegestaan op alle droogvallende delen van de Nederlandse Waddenzee, maar andere vormen van beheer en beleid zijn vaak gericht op veel lokalere beperkingen van antropogene verstoringen. De grootschalige ruimtelijke effecten van biobouwers op het ecosysteem die worden

beschreven in dit proefschrift, laten zien dat het belangrijk is om voorbij het strikt lokale te kijken en systemen op een grote schaal te beheren en te beschermen.



---

## Acknowledgements

This thesis marks the end of a scientific adventure that was at times tedious while at other times it was absolutely fascinating and exciting. However, above all this, it has been incredibly educational to me. The work and the people I worked with have taught me things that will be meaningful for the rest of my life, both professionally and personally. There are many people I should thank for their support during these years and my appreciation is certainly not restricted to the people I list in this section.

I owe the first word of thanks to my supervisors Daphne and Peter. Daphne you got funding from this project from NSO and trusted me to work on this project. Thanks for all the time you made available for discussions and manuscript revisions. A common complaint among PhD students is that their supervisors take ages before returning comments on manuscripts, but I often had a reply the next day! Peter, in retrospect I regret that I did not try to discuss the work more often with you, especially during the early stages of my PhD. You have been very insightful and was able to get the train going when it got totally stuck more than once. Especially towards the end the road was sometimes bumpy, but I am glad that I had you as supervisors during these years.

My interest in science was not sparked if it was not for Bart Nieuwenhuis who supervised my minor MSc thesis and with whom I co-authored my first academic paper. Ronald Osinga and Tim Wijgerde allowed me to work in the coral lab and further fueled my interest for science. It was Brenda Walles who supervised me during my internship at IMARES and introduced me to ecological fieldwork with oysters.

A word of thanks also goes to Johan van de Koppel. Your enthusiasm and discussions really helped the two manuscripts on extended effects of ecosystem engineering. For this, I would also like to acknowledge Britas Klemens and Han Olff. I would like to thank Henko de Stigter for co-supervising a student with me. Sadly, I did not find the time to write a manuscript for the oyster cores, but maybe in the future still? I am thankful for the discussions I had with Norbert Dankers, Tjisse van der Heide and Karline Soetaert. Your ideas also helped shape the manuscripts in this thesis. I would like to acknowledge my students Berber Heerschop, Siep Busink and Kristof Peene for their work. I had many people helping out in the field, and this work can be tough! You get stuck in the mud and

## Acknowledgements

have to be careful not to cut yourself on the razor sharp oyster shells. First of all my acknowledgements go to the technical assistants Lennart IJzerloo, Jeroen van Dalen and Aniek van de Berg. Furthermore, I thank Jeremy Charnier, Zhenchang Zhu, Siti Yaakub, Gerna Groeneveld, Ellen Besseling, Laurine Burdorf, Silvia Hidalgo, Sairah Malkin and Tijmen Nieuwhof for their assistance and company during field trips. Annette Wielemaker-van den Dool was invaluable in supporting GIS and remote sensing analyses.

A special thanks goes to all the people of the spatial ecology department, which has now been merged into the estuarine and delta systems department. More specifically, I want to thank my French officemates Laura Soissons and Hélène de Paoli for nice discussions and mental support. Wouter Suykerbuyk, that Snarky Puppy concert was a really nice idea! The people at the guesthouse (de Keete) are acknowledged for the many nice evenings they organized. Kris, thank you for taking me out for some running from time to time. Sven, the bass jams were awesome (I still have your bass by the way!). Tadao, thank you for your company during the EGU in Vienna, and of course for taking care of our chickens when we were out of town!

Jim van Belzen, your contributions to my work have been invaluable. It was really nice working together and hopefully we can continue to do so in the future. Bas Oteman, I am really happy that I found someone who was not a nerd amongst all those nerds. It was nice talking code (literally!), butterflies, games, etc. Also the hackatons were a lot of fun. Let's do more of those!

Vincent and Eric, I know I was not always there but so were you guys. I hope that we can meet more often in the future. ooooOOOORRMUS!

Arvid, I don't think we will ever manage to change the way the (scientific) method works. However, it was nice to know there is someone who shares the same ideology. Sadly, due to both our PhD's we did not see each other much; but this will change soon when we start our new band!

I want to thank my family for their support and interest in my work. I appreciate your believe in me and your trust that eventually everything will work out just fine.

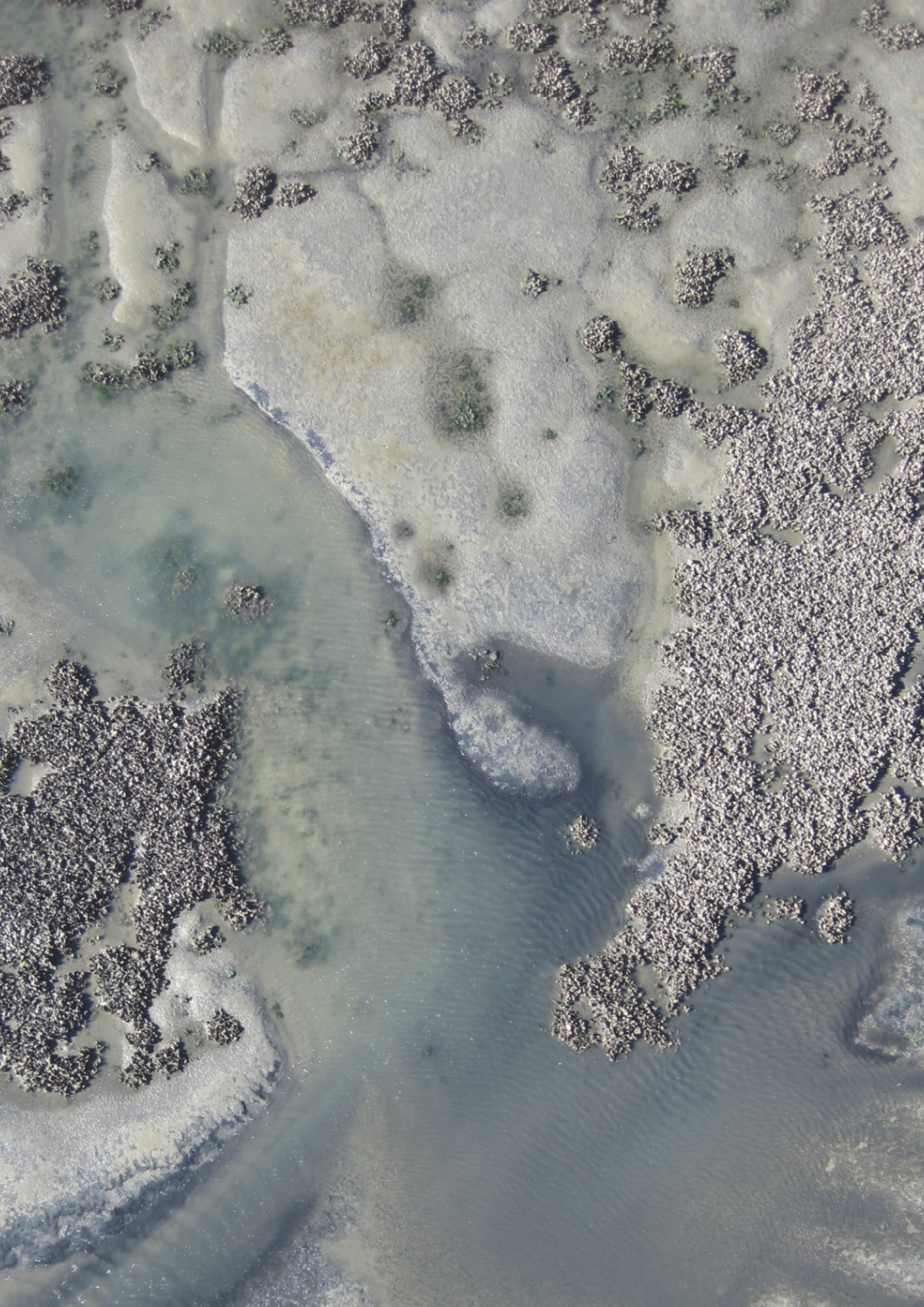
Ellen, if it were not for you none of this would have happened. You supported my decision to pursue a PhD in Zeeland. Somehow, we would make that work. Soon after you also got a PhD position at the WUR and arranged a working place at the neighbors. I am very grateful for your support and patience. There were quite some challenges along the way during the past years, but we faced them all together. I am also very grateful for our little 'Potjappel', which now makes us a



## Acknowledgements |

small family. Thank you for being there for me; I love you. Tijl, it is unbelievable how you get to love someone in such a small period of time and with so little words. Thank you for the welcome distraction in the finishing stage of my thesis.







---

## Curriculum Vitae

### The author

Sil Nieuwhof was born on September 21, 1987 in Bennekom, The Netherlands. As a young child he was always fascinated by nature, and, sparked by the frequent holidays to the province of Zeeland, quickly developed a keen interest in the marine environment. He attended VWO at the Marnix College in Ede from 1999 to 2005. He earned his BSc and Msc in Biology with a specialization in ecology at Wageningen University from 2005 to 2011. He did a minor focusing on fungal mating genetics, but the major thesis and internship were focused on marine topics. His major thesis was titled “Growth and photosynthesis in the scleractinian coral *Stylophora pistillata* under a constant and variable light regime” and during this work Sil was motivated to further explore marine science. For his internship he first came to Yerseke to work at IMARES on a building with nature project involving artificial oyster reefs. After obtaining his MSc degree he shortly worked as a research assistant at Wageningen University before returning to Yerseke to pursue a PhD degree at the spatial ecology department of the Royal Netherlands Institute for Sea Research (NIOZ). The project focused on understanding spatially extended ecosystem engineering by shellfish reefs by means of remote sensing. In 2017 Sil continued to work on ecology, remote sensing and data analysis in his current position at the engineering consultancy firm Witteveen+Bos.

### Publications

- Nieuwhof S**, Belzen J van, Oteman B, Koppel J van de, Herman PMJ, Wal D van der (2018) Shellfish Reefs Increase Water Storage Capacity on Intertidal Flats Over Extensive Spatial Scales. *Ecosystems*.
- Malkin SY, Seitaj D, Burdorf LDW, **Nieuwhof S**, Hidalgo-Martinez S, Tramper A, Geeraert N, Stigter H De, Meysman FJR (2017) Electrogenic Sulfur Oxidation by Cable Bacteria in Bivalve Reef Sediments. *Frontiers in Marine Science*
- Walles B, Troost K, Ende D van den, **Nieuwhof S**, Smaal AC, Ysebaert T (2016) From artificial structures to self-sustaining oyster reefs. *Journal of Sea Research*

- Walles B, Fodrie FJ, **Nieuwhof S**, Jewell OJD, Herman PMJ, Ysebaert T (2016) Guidelines for evaluating performance of oyster habitat restoration should include tidal emersion: reply to Baggett et al. *Restoration Ecology*
- Nieuwhof S**, Herman PMJ, Dankers N, Troost K, Wal D van der (2015) Remote Sensing of Epibenthic Shellfish Using Synthetic Aperture Radar Satellite Imagery. *Remote Sensing*
- Nieuwenhuis BPS, **Nieuwhof S**, Aanen DK (2013) On the asymmetry of mating in natural populations of the mushroom fungus *Schizophyllum commune*. *Fungal Genetics and Biology*

### Courses

- Sampling in space and time for survey and monitoring of natural resources, PE&RC, Wageningen, April 2012.
- Biogeochemical modelling in aquatic environments: Using R as a simulation environment, NIOZ, Yerseke, October 2012.
- How to write a scientific paper, NIOZ, Yerseke, October 2012.
- How to give a good talk, presenting science, NIOZ, Yerseke, January 2013.
- Scientific Image Processing and Analysis, BioVoxxel, Yerseke October 2013.
- Spatial Ecology, PE&RC, RSEE and SENSE, Oosterbeek, March 2014

### Student supervision

- BSc thesis, Berber Heerschop, Utrecht University, 2013; Berber assisted in the field and investigated ecosystem engineering using spectra over shellfish reefs.
- MSc traineeship, Siep Busink, Wageningen University, 2013; Siep worked on collecting and analysing data for the radionucleides study.
- MBO traineeship, Kristof Peene, Scalda Vlissingen, 2015; Kristof assisted in the field and measured shellfish samples in the laboratory related to the niche separation of mussels and oysters.

### Lectures and presentations

- Nieuwhof, S. Remote sensing of shellfish reefs and their extended spatial effects, Lecture: University College Roosevelt, Yerseke, March 2016.
- Nieuwhof, S., Herman P.M.J., Dankers, N., van de Koppel, J., van Belzen, J., van der Wal, D., Mapping reef building mussels and oysters, and their effects on the ecosystem using remote sensing, Earth Observation for Science and Society Symposium (EO3S), NSO, The Hague, October 2015.

- Nieuwhof, S., Herman, P.M.J., Dankers, N., Troost, K., van der Wal, D., Synthetic aperture radar satellite remote sensing of shellfish beds, Symposium Remote Sensing of the Wadden Sea, Delmenhorst (Germany), March 2015.
- Nieuwhof, S. van Belzen, J. Oteman, B. Van de Koppel, J. Herman, P.M.J., van der Wal, D. Biogenic structure enhances water retention on intertidal flats at extensive spatial scales, EGU General Assembly, Vienna (Austria), April 2015.
- Nieuwhof, S. van Belzen, J. Oteman, B. Van de Koppel, J. Herman, , P.M.J., van der Wal, D. Biogenic structure enhances water retention on intertidal flats at extensive spatial scales, NCK Days (Netherlands Centre for Coastal Research), Schoorl, March 2015.
- Nieuwhof, S. van Belzen, J. Oteman, B. Van de Koppel, J. Herman, , P.M.J., van der Wal, D. Added biogenic structure enhances landscape retention in a context-dependent way, Presentation. NAEM Meeting, Lunteren, February 2015.
- Nieuwhof, S., van Belzen, J., van de Koppel, J., Herman, P.M.J., van der Wal, D. Flashtalk: Spatially extended ecosystem engineering by shellfish, NIOZ Science Days, Texel, The Netherlands, 2014, June 2014.
- Nieuwhof, S., van Belzen, J., van de Koppel, J., Herman, P.M.J., van der Wal, D. Spatially extended ecosystem engineering by shellfish. Presentation Marine Master Course, NIOZ, Texel, July 2014.
- Nieuwhof, S., van der Wal, D., van de Koppel, J., Dankers, N., Olff, H., Eriksson, B.K., Donadi, S. van der Heide, T., Herman, P. Spatially extended ecosystem engineering by epibenthic shellfish. Young Wadden Sea Meeting, Utrecht, Netherlands, January 2013.
- Nieuwhof, S., van der Wal, D., van de Koppel, J., Dankers, N., Olff, H., Eriksson, B.K., Donadi, S. van der Heide, T., Herman, P. Spatially extended ecosystem engineering by epibenthic shellfish. Young Wadden Sea Meeting, Utrecht, Netherlands, November 2013.
- Nieuwhof, S., van der Wal, D., Herman, P. Snapshot: Ecosystem engineering by epibenthic shellfish. Theme day Remote Sensing of the Coastal Zone–NCK, Utrecht, Netherlands, January 2013.
- van der Zee, E.M., van der Wal, D., Donadi, S., Nieuwhof, S., Lui, Q-Xi, van der Heide, T., Weerman E.J., Eklöf, J.S. van der Veer, H.W., van de Koppel,

J., Eriksson, B.K., Dankers, N., Fey, N., Herman, P.M.J., Piersma, T., Olf, H. Influence of mussel beds on their environment: results of in situ and satellite observations. International workshop on mussel-related research in the Wadden Sea, Leeuwarden, November 2013 (joint presentation E.M. van der Zee and D. van der Wal).

## Posters

Nieuwhof, S. de Stigter, H, Busink, S., Herman, P.M.J., van der Wal, D. Bioturbators vs Biostabilizers; Opposite Worlds? Poster Netherlands Annual Ecology Meeting, Lunten, February 2014.

Nieuwhof, S. de Stigter, H, Busink, S., Herman, P.M.J., van der Wal, D. Bioturbators vs Biostabilizers; Opposite Worlds? Poster NIOZ Science Days, Texel, June 2014.

Nieuwhof, S., van de Koppel, J., Dankers, N., Olf, Herman, P., van der Wal, D. Beyond space boundaries – Ecosystem engineering by epibenthic shellfish. Poster Netherlands annual ecology meeting, Lunten, Netherlands, February 2013.

Nieuwhof, S., van de Koppel, J., Dankers, N., Olf, Herman, P., van der Wal, D. Beyond space boundaries – Ecosystem engineering by epibenthic shellfish. Poster NIOZ science days, Noordwijkerhout, Netherlands, April 2013. Awarded best poster prize.